PHYSICAL REVIEW
LETTERS

VOLUME 6 MAY 15, 1961 NUMBER 10

ELECTROSTATIC POTENTIAL GRADIENTS IN A PENNING DISCHARGE

F. Salz, R. G. Meyerand, Jr., E. C. Lary, and A. P. Walch
Research Laboratories, United Aircraft Corporation, East Hartford, Connecticut
(Received April 10, 1961)

It is well known that electrostatic voltage gradients over dimensions appreciably greater than a Debye length do not exist in a plasma in thermal equilibrium.[1,2] However, it has been shown that self-consistent potential gradients may be calculated for appropriate nonthermal velocity distributions of ions and electrons.[3] The purpose of this Letter is to show that the Penning or oscillating-electron discharge produces such distributions together with potential gradients in the discharge. The mechanism by which the gradients are generated and maintained is the net volume production of ion-electron pairs.

The existence of a potential gradient can be justified by the following physical argument. The density n of particles of a given type is

$$n = \int \frac{d\phi}{v} = \phi/\bar{v}, \qquad (1)$$

where ϕ is the scalar particle flux and $\bar{v}$ the magnitude of the average velocity. If a potential gradient is assumed to exist initially (such as the vacuum electric field), then ions will be accelerated in the direction of the electric field and electrons will be decelerated. Consequently, if the flux remains constant for both, the density of ions will decrease and the density of electrons will increase. However, if a fraction of the electron flux is electrostatically reflected by the potential gradient, then the flux of electrons can decrease sufficiently to maintain the charge density equality between ion and electrons,[4] and the appropriate potential gradient may exist over arbitrary length scales. (A mathematical treatment of this situation in one dimension is given in reference 3.)

This argument may be generalized to show that a potential gradient not only can exist but may be self-generated and maintained in the presence of ion-electron pair production. To show that potential gradients can exist, the following physical argument may be made. Starting with an assumed potential gradient (or the vacuum electric field), the volume production of charged particles results in an increase of the total ion flux in the direction of the field, and a decrease in the electron flux. Charge density equality[4] requires that

$$\phi_e/\bar{v}_e = Z\phi_i/\bar{v}_i, \qquad (2)$$

so that the average velocity of the ions has to increase and the average velocity of the electrons decrease, consistent with the potential distribution assumed. The potential distribution required to maintain equilibrium by satisfying the density equality may then be computed using Eq. (2) and the appropriate boundary conditions. This method of solution will be illustrated for a specific case.

The electrode configuration of the Penning discharge is such that the vacuum electric field traps electrons and ejects ions which are produced in the discharge (see Fig. 1). For simplicity it may be assumed that: (1) ions and electrons are essentially constrained to motion in one dimension (due in this example to the magnetic field); (2) the potential $V(x)$ is symmetric; (3) the electrons produced in the electrostatic well are trapped longitudinally and lost only by lateral

diffusion across the magnetic field; (4) ions and electrons have mean free paths that are large compared to the length scale of the discharge; (5) electrons born at x make $R(x)$ electrostatic reflections before being lost by diffusion. The equality of electron and ion density, based on Eq. (1), takes the form

$$n_{ec}(x)+\left(\frac{m_e}{2e}\right)^{1/2}\int_x^L \frac{d\phi_e(x')}{[V(x)-V(x')]^{1/2}}=n(x)=\left(\frac{M_i}{2Ze}\right)^{1/2}\int_0^x \frac{d\phi_i(x')}{[V(x')-V(x)]^{1/2}}, \tag{3}$$

where $n_{ec}(x)$ is the density of electrons emitted from the cathode and the ion flux produced in dx is

$$d\phi_i(x)=[\phi_e+n_{ec}(x)\bar{v}_{ec}(x)]N(x)\sigma_i(x)dx. \tag{4}$$

N is the neutral gas density, σ_i the ionization cross section appropriate to the local velocity distribution, v_{ec} the average speed of the cathode electrons, and ϕ_e the trapped-electron flux, given by

$$\phi_e(x)=2\int_x^L R(x')[\phi_e(x')+n_{ec}(x')v_{ec}(x')]$$

$$\times\ N(x')\sigma_i(x')dx'. \tag{5}$$

The factor 2 takes into account the electrons produced between $-x$ and $-L$. A self-consistent potential distribution $V(x)$ is in principle determined by the above equations but the solution is difficult to obtain analytically. Recourse is, therefore, made to numerical solutions obtained by an iterative procedure using finite differences.

The actual procedure is as follows: The region of interest is divided into a number of cells. Since the mean free path of particles is large compared to the dimensions of the plasma, the flux of trapped electrons characteristic of a given cell (i.e., those electrons that electrostatically reflect in that cell) is essentially constant throughout the discharge between the points of reflection. Moreover, the local potential determines the speed of these electrons and hence their density may be deduced. The production, the number of reflections, and the density of ions and electrons may then be computed for each cell. The production in the center cell is computed first. The potential required to balance the ion and electron charge density at the cell interface is determined. On the basis of the computed interface potential, the electrostatic attenuation of the electron flux is computed. This procedure is repeated for each subsequent cell. The trapped-electron flux may then be redetermined from the computed production rates in each cell and the number of reflections each group of electrons makes by the evaluation of the appropriate loss rates. This provides the input for the next iteration which can then be carried out in the same manner. A stable, self-consistent solution is obtained when the results of two succeeding iterations agree within established tolerances.

This method has been used to calculate the potential gradient in a Penning discharge. The resulting voltage distribution for a particular case (assuming only a given value of cathode current I_c, anode voltage V_0, and neutral gas density N_0, together with known collision and ionization cross sections) is shown in Fig. 2. The potential distribution measured experimentally with both emitting and conventional Langmuir probes (and verified by a momentum analysis of the ejected ions) is also plotted in Fig. 2.

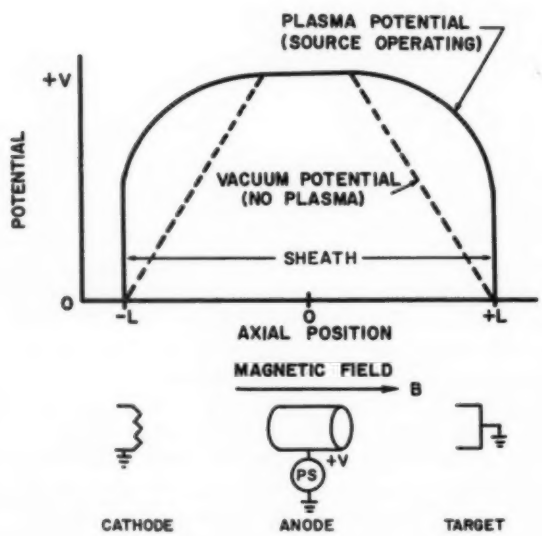

FIG. 1. Penning source electrode configuration and potential distribution.

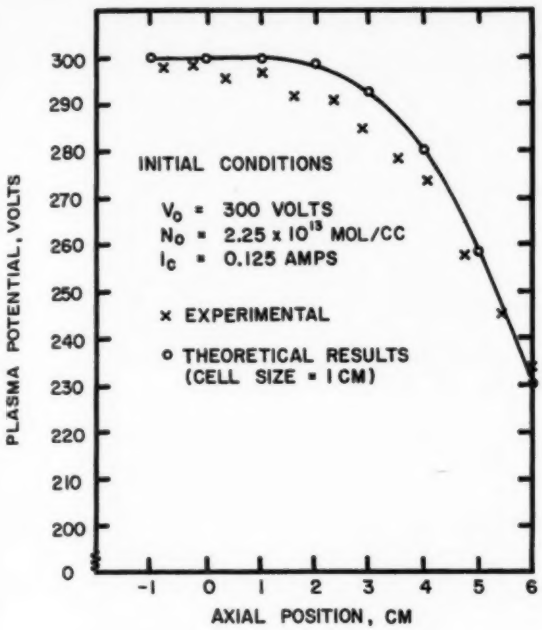

FIG. 2. Comparison of experimental and theoretical plasma potentials in the Penning discharge.

As can be seen, there is satisfactory agreement between theory and experiment.

In conclusion, it may be said that stable electrostatic potential gradients may exist in a plasma over a length scale, determined by the production mechanism, which for most cases of interest is large compared to the Debye length. These gradients are established by the nonthermal velocity distributions generated by the volume production of ion-electron pairs. The potential gradient may be determined, in general, by a simultaneous solution of Poisson's equation and the appropriate equations of motion. However, in most cases of interest, the assumption of equal ion and electron densities leads to a considerable simplification and allows the determination of the potential gradient from the flux-velocity quotient.

---

[1]L. Spitzer, The Physics of Fully Ionized Gases (Interscience Publishers, Inc., New York, 1956), p. 16.

[2]L. Tonks and Irving Langmuir, Phys. Rev. 34, 876 (1929).

[3]D. J. Rose, Massachusetts Institute of Technology Quarterly Progress Report, No. 53, April, 1959 (unpublished).

[4]In general Poisson's equation must be satisfied (i.e., the difference in the densities of ions and electrons is the source of the electric field), but for most plasmas of laboratory interest the approximation of equal ion and electron densities is sufficiently accurate and leads to a considerable simplification.

EXPERIMENTS ON THE ENERGY BALANCE AND CONFINEMENT OF A MAGNETIZED PLASMA

J. Bergström, S. Holmberg, and B. Lehnert

Royal Institute of Technology, Stockholm, Sweden

(Received April 20, 1961)

The possibility to confine a plasma in the magnetic field of a current loop has been discussed in a number of earlier reports.[1-4] It has been suggested[2] to supply energy and to heat the plasma in crossed electric and magnetic fields by a method used earlier in rotating plasma devices.[5,6] In a mirror machine with a rotating plasma the confinement is improved by the centrifugal force.[5,6] The large radial extensions of the current loop configuration are of special advantage when a strong centrifugal confinement has to be realized. This is indicated both by a theory on particle motion[3] and by a macroscopic approach including the energy balance.[4]

The purpose of the present experiments is to study how the energy balance and the confinement of a rotating plasma are influenced by particle losses along the magnetic field lines to a nonconducting wall. Figure 1 demonstrates the experimental arrangement which consists of a cylindrical vacuum vessel with an interior, ring-shaped magnetic coil (main coil) and two external auxiliary coils. The lines of the magnetic field $\vec{B}$ are sketched in the figure. A discharge is produced by a transverse electric field $\vec{E}$ arising from the voltage applied between the shield surrounding the main coil and the walls of the vacuum chamber. The energy is supplied from a condenser bank by means of a timed ignitron switch. A second ignitron can be used to study

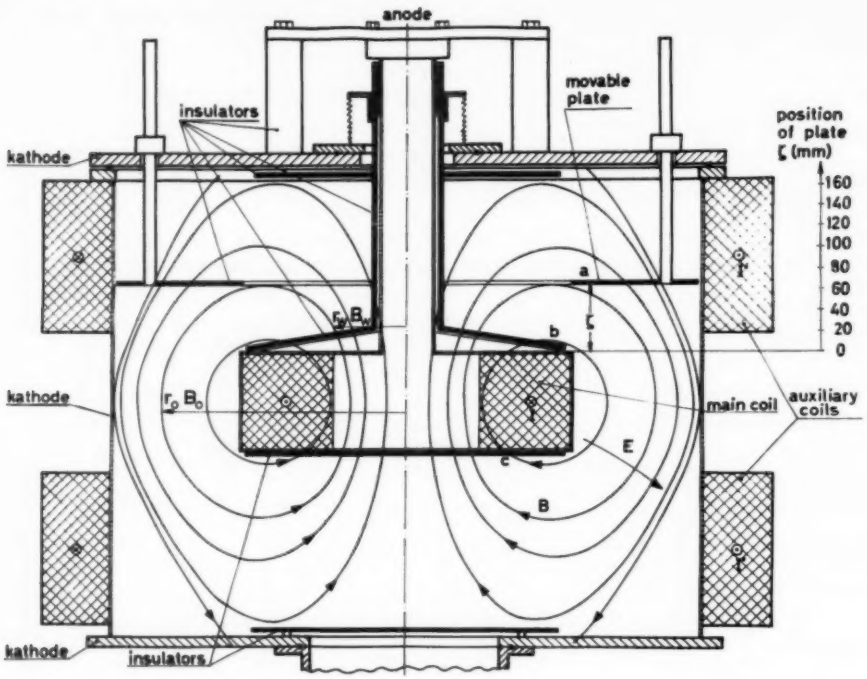

FIG. 1. The experimental device.

back-pulses by applying a short circuit ("crowbar") across the device.

As shown in the figure, a wall consisting of a movable, ring-shaped plate (a) can be placed across the field of the magnetic bottle at different distances from the equatorial plane. The mean field strength in this plane is about $B = 0.44$ weber/m^2. When the plate is in its upper position ($\zeta = 165$ mm) the mean values of the radial ratio r_0/r_w and the mirror ratio B_w/B_0 become about 3.4 and 7.6, respectively. Consequently, by a variation of the plate position conditions can be obtained which closely correspond to the homopolar,[5] Ixion,[6] and current loop configurations within the same experimental device.

The experimental results can be summarized as follows:

1. Voltage and current characteristics. When the plate is in its upper position [Fig. 2(a)], the discharge starts with a large current pulse during which ionization and acceleration mainly take place and the voltage reaches a maximum about 0.2 millisecond from the start. Then, a period follows during which the voltage is decaying slowly and the current remains at a low level. A short circuit of the device at 0.5 millisecond from the start shows a large back-pulse, indicating that a considerable amount of energy is still present in the plasma at this time. The back-pulses increase rapidly with the strength of the applied magnetic field. The kinetic energy of the rotating plasma was found to decay from about 135 joules at 0.1 millisecond from the start to about 15 joules at 0.7 millisecond later. The equivalent capacity of the rotating plasma seems to be nearly constant at the same time.

With the plate in lower position [Fig. 2(b)] the acceleration period requires a somewhat larger current which slowly returns to zero at the same time as the energy of the plasma is dissipated. At 0.5 millisecond from the start, Fig. 2(b) shows no trace of any remaining energy in the form of a back-pulse; only a discharge of low ionization degree is still burning at this time.

The voltage level of the decay period is much lower in Fig. 2(b) than in Fig. 2(a) and reaches a constant value after 0.2 millisecond which agrees well with the values observed earlier by Fahleson.[7] The same levels are also observed in a low-current discharge with the plate in its upper position.

If the series resistor R_s is reduced to very low values, the discharge breaks down across

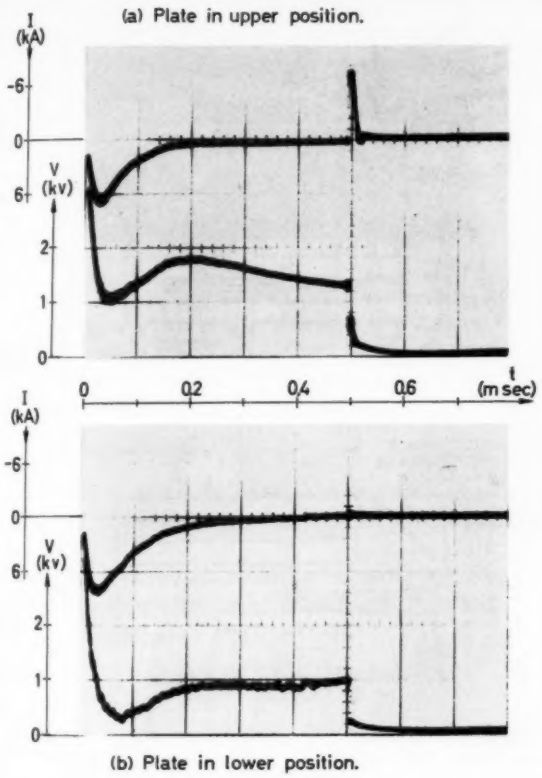

FIG. 2. Discharge current I and voltage V as functions of time t for hydrogen at an initial density corresponding to 45×10^{-3} mm Hg. The condenser bank, which has a capacity of 330 microfarads and an initial voltage of 4.5 kilovolts, supplies the energy to the discharge through a series resistor, $R_s = 0.4$ ohm. (a) Plate in upper position. Back-pulse of current is obtained at 0.5 millisecond from start. (b) Plate in lower position. No back-pulse is observed.

the plate when it is in the lower position and the current starts to oscillate violently. However, with the plate in the upper position the voltage still remains at a high level and the current drops to a low value after the acceleration period has been finished.

When the plate was placed in an intermediate position, electrical characteristics were obtained about halfway between those corresponding to the upper and lower positions.

2. Light intensity. Photometric measurements on a hydrogen discharge indicate a strong pulse of light during the early stages of the discharge when the plate is in its lower position. When the plate is in the upper position, the light intensity decreases considerably and its duration is extended at the same time.

3. Gas production and wall constitution. For a nitrogen discharge with a density corresponding to 9×10^{-3} mm Hg at the start, the relative gas production was found to decrease gradually from 190% to about 3% when the plate was moved from the lower to the upper position.

After having been exposed to more than 1000 discharges the insulator surfaces (b) and (c) of Fig. 1 showed very small signs of contamination but plate (a) in the same figure was heavily damaged by the discharge.

The present results indicate that the interaction between a rotating plasma and the surrounding walls of its container can be reduced considerably by using a magnetic field with large radial ratios and mirror ratios. Further, there are apparently no severe losses of energy due to instabilities since the plasma contains a considerable amount of energy for more than 0.7 millisecond.

A detailed report is under preparation.

[1]B. Lehnert, Nature 181, 331 (1958).
[2]B. Lehnert, J. Nuclear Energy, Sec. C 1, 40 (1959).
[3]B. Bonnevier and B. Lehnert, Arkiv Fysik 16, 231 (1960).
[4]B. Lehnert, Arkiv Fysik 18, 251 (1960); Revs. Modern Phys. 32, 1012 (1960).
[5]O. A. Anderson, W. R. Baker, A. Bratenahl, H. P. Furth, H. P. Ise, W. B. Kunkel, and J. M. Stone, Proceedings of the Second International Conference on the Peaceful Uses of Atomic Energy, Geneva, 1958 (United Nations, Geneva, 1958), Vol. 32, p. 155.
[6]K. Boyer, J. E. Hammel, C. L. Longmire, D. Nagle, F. L. Ribe, and W. B. Riesenfeld, Proceedings of the Second International Conference on the Peaceful Uses of Atomic Energy, Geneva, 1958 (United Nations, Geneva, 1958), Vol. 31, p. 319.
[7]U. V. Fahleson, Phys. Fluids 4, 123 (1961); see also H. Alfvén, Revs. Modern Phys. 32, 710 (1960).

MICROWAVE MODULATION OF THE ELECTRO-OPTIC EFFECT IN KH_2PO_4

I. P. Kaminow
Bell Telephone Laboratories, Holmdel, New Jersey
(Received April 17, 1961)

KH_2PO_4 (KDP) is a colorless transparent crystal that belongs to the tetragonal group $\bar{4}2m$ (V_d), which lacks a center of inversion, and exhibits a linear electro-optic effect. It undergoes a ferroelectric phase transition at 120°K.[1] According to a model of KDP and isomorphous compounds, the dielectric polarization depends upon the motion of the protons in a double minimum potential.[1,2] These protonic motions can alter the symmetry and magnitude of the electronic polarizability and, hence, the optical properties of the crystal.

In the paraelectric phase, KDP is optically uniaxial with the optic axis along the tetragonal Z axis. Light propagating along Z travels with the same velocity irrespective of the plane of polarization. The application of an electric field E along Z reduces the crystal symmetry to orthorhombic and the optical symmetry to biaxial.[3] Hence, the index of refraction for light propagating along Z is different for light polarized in the two principal planes. After passing through a length L, the phase retardation Γ between the principal waves is

$$\Gamma = \pi EL/V_0, \qquad (1)$$

where V_0 is the (zero-strain) value of EL for half-wave retardation.

Measurements of the dielectric constant at a frequency of 25 kMc/sec (at 25°C) agree with the low-frequency dielectric constant of a clamped crystal.[1,4] Since the electro-optic effect is proportional to the polarization,[1] one would not expect any appreciable reduction in V_0 below 25 kMc/sec.[5] Previous measurements have shown V_0 to be frequency independent to 500 Mc/sec.[6] We have observed the electro-optic effect in KDP at room temperature and 9.25 kMc/sec and find V_0 to be of the same order as the low-frequency value.

The apparatus [Fig. 1(a)] consists of a 25-watt zirconium concentrated arc lamp with a Corning 7-69 infrared filter peaked at 8000 A, a Glan-Thompson polarizer and crossed analyzer, an RCA 7102 (S-1) photomultiplier, and a pulsed X-band magnetron which feeds a cylindrical cavity containing the KDP rod. The cavity is filled with polystyrene and the dimensions are

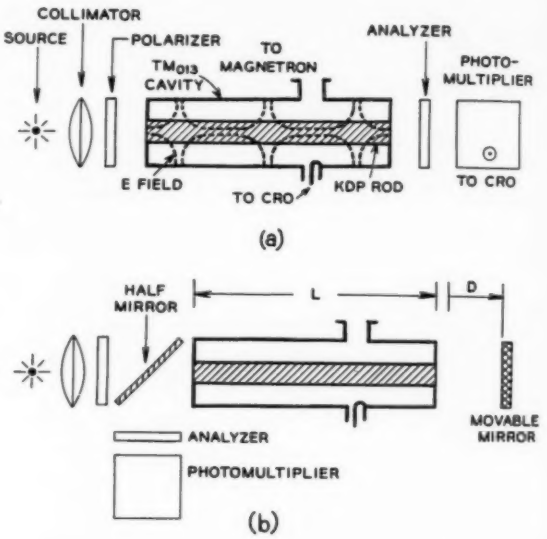

FIG. 1. (a) Transmission apparatus. (b) Reflection apparatus.

adjusted so that the microwave phase velocity approximates the light velocity when the cavity is excited in the "TM_{013}-like" mode. If the cavity standing wave is decomposed into a forward and a backward travelling wave, it can be shown that, to good approximation, the backward wave produces no net retardation when the velocities are matched, while the forward wave provides a constant E at a given point in the light wave train as it passes through the crystal.[7] The light velocity in the crystal is $c/1.47$; the microwave velocity at 9.25 kMc/sec is $c/1.38$.

With the polarizer and analyzer crossed, pulses from the photomultiplier are observed coincident with the microwave pulses (3 μsec at 60 pulses/sec). In order to obtain direct evidence of microwave modulation, a movable mirror and half mirror are placed as shown in Fig. 1(b). When the transit time for light leaving the end of the crystal, reflecting from the movable mirror, and re-entering the crystal is equal to an odd multiple of the microwave half-period, light pulses are observed in the photomultiplier. When the mirror is moved a distance D equal to one-quarter the free-space microwave wavelength, no pulses are observed

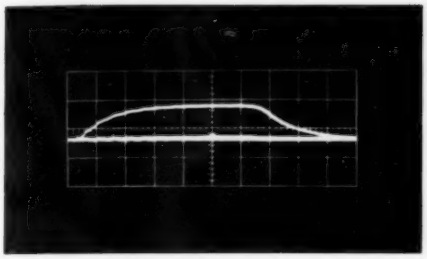

FIG. 2. Photomultiplier response with mirror set for maximum signal (top). With mirror displaced $\lambda/4$, the response is nearly coincident with that obtained by covering the source (bottom). ($\frac{1}{2}$ μsec/div. Circuit time constant ~ $\frac{1}{2}$ μsec.)

(Fig. 2). In the first case, the retardation is doubled, while in the latter the net retardation is zero.

The time-average relative intensity for modulated light with crossed polarizers, $\rho_\perp$, and with parallel polarizers, $\rho_\parallel$, is[6]

$$\rho_\perp = \tfrac{1}{2}[1 - J_0(\Gamma_p)], \quad \rho_\parallel = \tfrac{1}{2}[1 + J_0(\Gamma_p)], \qquad (2)$$

where J_0 is the zero-order Bessel function and Γ_p is the peak retardation. With a peak power P of 760 watts absorbed in the cavity, $\rho_\perp = \rho_\parallel$ (Fig. 3) and $\Gamma_p = 2.40$.

The peak field intensity in the forward wave E may be estimated by assuming a uniform longitudinal E across the rod with sinusoidal variation along the rod and assuming all the power P to be dissipated in the rod. Then

$$E \sim (QP/\omega\epsilon\epsilon_0 v)^{1/2} \sim 70 \text{ volts/mm}, \qquad (3)$$

in which ϵ and Q are the dielectric constant and dielectric Q for the rod at angular frequency ω and v is the rod volume ($L = 35.5$ mm, diameter 4 mm). In the absence of 9-kMc/sec data, we have used the 25-kMc/sec values[4] $\epsilon \sim 20$, $Q \sim 30$. For $\Gamma_p = 2.40$,

$$V_0 = \pi E 2L/\Gamma_p \sim 7 \text{ kv}. \qquad (4)$$

This estimate may be compared with the low-frequency clamped value of 11 kv obtained by extrapolating measurements of W. L. Bond to 8000 A.

KDP is transparent between 4000 A and 13 000 A. Since V_0 decreases with decreasing wavelength,[6] the effect may be enhanced by operating at shorter wavelengths. Further enhancement, with increased loss, may be obtained by increasing L and by operating nearer to the Curie temperature, either by reducing the temperature, or by choosing an isomorphous compound with a higher Curie temperature.[2]

The tunnelling frequency[2] for protons in the double minimum potential occurs at ~200 cm^{-1} (6000 kMc/sec). Therefore, it may be possible to extend the modulating frequency to much higher frequencies than the 9.25 kMc/sec used here.

It may also be possible to construct a broadband low-power microwave light modulator, using more sophisticated structures or other materials, for use in a practical optical communication system.[9] The bandwidth for the present structure is limited by the cavity Q: $\Delta f \sim f/150 \sim 60$ Mc/sec. In a pure travelling wave structure, a limitation would be the band over which the microwave and light velocities can be matched.

A microwave light modulator might also be used as an instrument for studying short relaxation times and other effects in optically pumped systems or for refined measurements of the velocity of light.

It is a pleasure to acknowledge instructive discussions with R. Kompfner, A. G. Fox, E. H. Turner, and R. F. Trambarulo, and the assistance of F. A. Dunn.

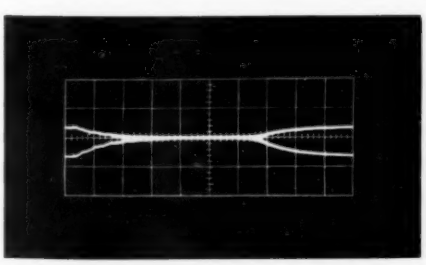

FIG. 3. Photomultiplier response with parallel polarizers (upper) and with crossed polarizers (lower) for $\rho_\perp = \rho_\parallel$.

[1]W. Känzig, in Solid State Physics, edited by F. Seitz and D. Turnbull (Academic Press, Inc., New York, 1957), Vol. 4.

[2]R. Blinc, J. Phys. Chem. Solids 13, 204 (1960).

[3]B. H. Billings, J. Opt. Soc. Am. 39, 797 (1949).

[4]W. A. Yager, quoted in Piezoelectric Crystals and Their Application to Ultrasonics, edited by W. P. Mason (D. Van Nostrand and Company, New York, 1950), p. 258.

[5]N. Bloembergen, P. S. Pershan, and L. R. Wilcox, Phys. Rev. 120, 2014 (1960).

[6]R. O'B. Carpenter, J. Opt. Soc. Am. 40, 225 (1950).

[7]The use of a travelling wave structure has been suggested by N. Bloembergen [talk, NEREM, Boston, No. 1960] and the possibility of using the standing wave structure by R. Kompfner.

[8]Clark, Holshouser, and von Foerster, Technical Note 1-2, Engineering Experimental Station, University of Illinois, 1957 (unpublished).

[9]E. H. Turner attempted to observe microwave light modulation (1952) using $NH_4H_2PO_4$ (ADP) in a rectangular TE_{101} cavity but was unsuccessful because of the short length of ADP permitted by the structure. Bloembergen, Pershan, and Wilcox[5] have suggested, independently, the use of dihydrogen phosphates for microwave modulation of light.

EVIDENCE FOR FOCUSING COLLISIONS IN IRRADIATED PLATINUM

E. Ruedl, P. Delavignette, and S. Amelinckx
Solid State Physics Department, Centre D' Etude de L' Energie Nucléaire, Mol, Belgium
(Received April 21, 1961)

Focusing collisions along close-packed directions in face-centered cubic metals were first predicted by Silsbee.[1] A more elaborate theory has recently been developed by Leibfried and co-workers,[2] for the case of ⟨110⟩ focusing.

Gibson, Goland, Milgram, and Vineyard[3] found evidence for this process by means of machine calculations on a dynamical model. They showed, moreover, that focusing also occurs along ⟨100⟩ and ⟨111⟩ directions; this was attributed to the influence of the neighboring rows.

Direct experimental evidence is practically limited to the sputtering experiments of Thompson.[4] He found that preferential ejection of atoms occurs along ⟨110⟩, ⟨100⟩, and ⟨111⟩ directions. The focusing effect along the non-close-packed rows was explained using an optical analogy.[5]

The rapid decrease in internal friction on irradiation has been attributed to the preferential formation of defects at dislocations as a consequence of focusing collisions.[6]

In this note we wish to present some rather direct evidence of a completely different type, which was obtained during the electron optical examination of irradiated platinum foils.

The specimens consisted of about 0.1-micron thick beaten foil, annealed for one hour at 800°C in order to eliminate part of the dislocations and to obtain a reasonable grain size. The anneal also resulted in the formation of annealing twins, generally limited by coherent twin boundaries.

Such specimens were mounted in contact with uranium foils and irradiated at reactor temperature (≈80°C) in the BR-1 reactor over periods of $\frac{1}{2}$, 2, and 5 hours. The number of fission fragments that penetrated into the platinum foil under these circumstances were, respectively, 2.5×10^{9}, 1×10^{10}, and 2.5×10^{10} cm^{-2}. After the irradiation the specimens were examined with the Philips electron microscope operated at 100 kv. Figure 1 shows the increasing concentration of black dots with increasing dose. Such "measles" have been observed previously in other irradiated materials.[7-9]

By pulse annealing it was verified that the "measles" disappear at about 400-500°C in accord with the annealing peak found by Piercy[10] and attributed by him to the motion of vacancies. From this evidence and from the approximate proportionality of their concentration with dose, it is reasonable to accept that the black dots correspond to defect clusters. The most significant feature of this investigation is, however, that measles appear preferentially along coherent twin boundaries as shown in Fig. 2; and much less pronounced along ordinary boundaries. This fact can, of course, not be attributed to preferential impinging of fission fragments along the coherent twin interface.

It is therefore difficult to avoid the conclusion that momentum transfer has taken place resulting in the preferential creation of defects along the twin boundary. Since coherent twin boundaries do not act as sources or sinks for point defects, as shown by Barnes,[7] the defects would not easily disappear there as would be the case if they were formed at ordinary boundaries.

The preferential formation of defects at coherent twin boundaries can easily be understood on the basis of the theory of focusing collisions. Suppose that momentum transfer occurs along a ⟨110⟩ direction, as would be the case in the Silsbee type of focusing. The ⟨110⟩ direction

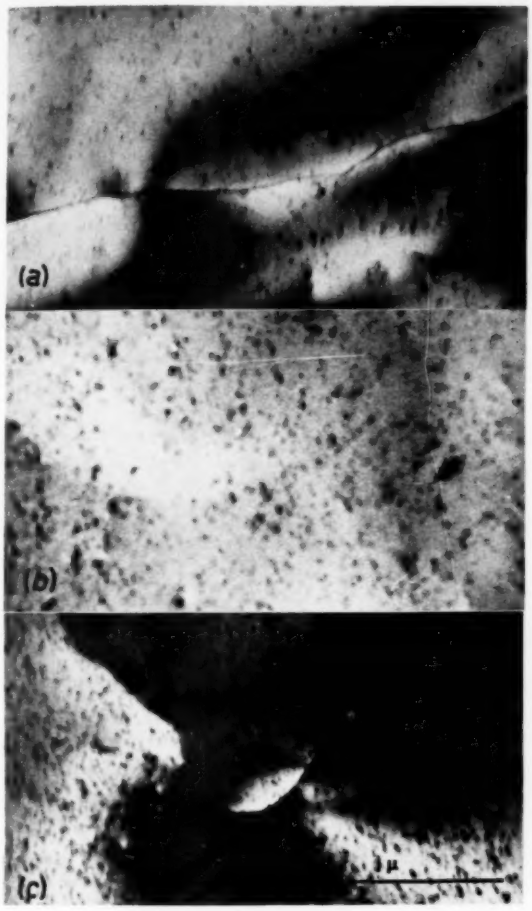

FIG. 1. Increasing concentration of defects in platinum irradiated in contact with uranium foil. The doses were, respectively, (a) 2.5×10^{15} n/cm^2, (b) 1×10^{16} n/cm^2, and (c) 2.5×10^{16} n/cm^2.

in one of the crystals of the twin becomes a nonfocusing ⟨114⟩ direction in the other. Coherent twin boundaries are in fact effective barriers for focused collision chains, without being sinks for the defects.

Primary collisions occurring in a strip of material on both sides of the twin boundary and causing focusing along ⟨110⟩ rows, intersecting the twin interface, will produce defects on passing the latter. The width of this strip is determined, either by a purely geometrical factor, namely, the possibility of reaching the twin interface along ⟨110⟩ directions, or by the range of the focusing chains. This width is clearly a function of the foil thickness, at least for thin

FIG. 2. Preferential formation of defects along coherent twin boundaries (Tw) in irradiated platinum.

foils. In very thin foils one would not expect to find a detectable effect since the strip becomes too narrow. This may explain why, e.g., Grenall[9] did not find any such effect in very thin gold particles, although they also contained twins and stacking faults.

It is clear that similar considerations apply to other focusing directions.

A more detailed account concerning the electron microscopic observation of dislocations and radiation effects in platinum is being published elsewhere.

This work is part of a research program undertaken at Centre d'Etude de l'Energie Nucléaire, Mol, Belgium, on behalf of the joint research and development program of the agreement for cooperation between Euratom and the United States.

We would like to thank Mr. J. Finet for skillful preparation of specimens and Mr. H. Beyens for careful photographic work.

[1]R. H. Silsbee, J. Appl. Phys. 28, 1246 (1957).
[2]C. Lehman and G. Leibfried (to be published).
[3]J. B. Gibson, A. N. Goland, M. Milgram, and

G. H. Vineyard, Phys. Rev. 120, 1229 (1960).
[4]M. W. Thompson, Phil. Mag. 4, 139 (1959).
[5]M. W. Thompson and R. S. Nelson, Atomic Energy Research Establishment Report AERE-R 3320, 1960 (unpublished).
[6]D. O. Thompson, T. H. Blewitt, and D. K. Holmes, J. Appl. Phys. 28, 275 (1957).
[7]R. S. Barnes, Phil. Mag. 5, 635 (1960).
[8]J. Silcox, Proceedings of the European Regional Conference on Electron Microscopy, Delft, 1960 (to be published).
[9]A. Grenall, North American Aviation Report NAA-SR-5062 (unpublished).
[10]G. R. Piercy, Phil. Mag. 5, 635 (1960).

SUPERCONDUCTIVITY OF Nb_3Sn IN A PULSED MAGNETIC FIELD*

J. O. Betterton, Jr., R. W. Boom, G. D. Kneip, and R. E. Worsham
Oak Ridge National Laboratory,† Oak Ridge, Tennessee
and
C. E. Roos
Vanderbilt University, Nashville, Tennessee
(Received April 24, 1961).

Kunzler, Buehler, Hsu, and Wernick[1] have shown that quenching of superconductivity in a niobium-clad wire with a Nb_3Sn core occurs at magnetic field strengths greater than 88 kilogauss and at core current densities in excess of 10^5 amp/cm^2. Samples of this wire were prepared by methods suggested in reference 1. Critical current as a function of field was measured by a pulsed-field, pulsed-current method at 4.2°K in the Vanderbilt University 200-kilogauss magnet. The transition time from superconducting to normal state and the resistance were also determined.

A longitudinal specimen (0.38-mm diam and 2.5 cm long) and a constantan standard resistor were mounted at the end of two pieces of 3-mm diam, thin-wall Monel tubing as shown in Fig. 1. The Monel tubes served as the outer shields of coaxial lines which carried the sample voltage and current signals. A pickup coil to measure the field strength was placed adjacent to the test samples. The coils of the Vanderbilt magnet are arranged in a Helmholtz configuration to provide a field uniform to 2% over an experimental volume of 30 cm^3. Current pulses of 30 to 150 microseconds were used at the peak of the magnetic field (half-period 1.2 milliseconds). The magnetic field was constant to within 2% during the longest current pulses. By mounting the sample as noninductively as practicable, a resistive sensitivity of 10 μohm was achieved, as checked with copper samples at a series of temperatures. A transverse specimen was mounted in a similar way.

Typical oscilloscope traces of the measured current and voltage are shown in Fig. 2. In the upper set, the voltage across the sample illustrates a purely inductive response for a nonresistive superconductor. In the lower set, the voltage across the sample increases abruptly when the sample becomes resistive. The critical current is determined by measuring the current at the point where a resistive component is first detected. After the inductive voltage is subtracted, the normal-state resistance is approximately

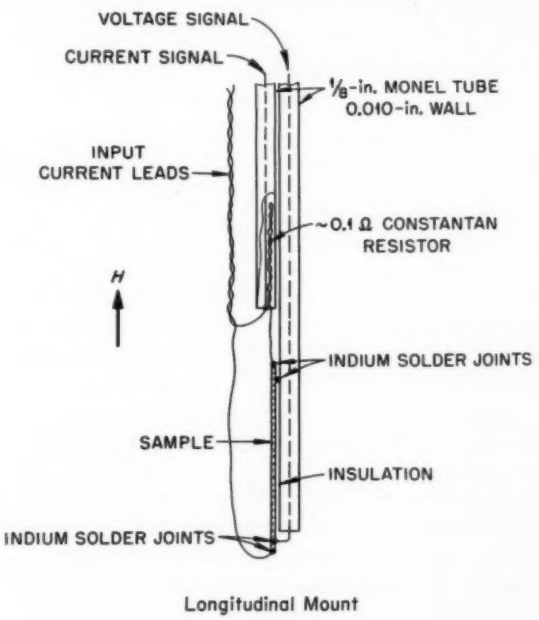

FIG. 1. Specimen holder.

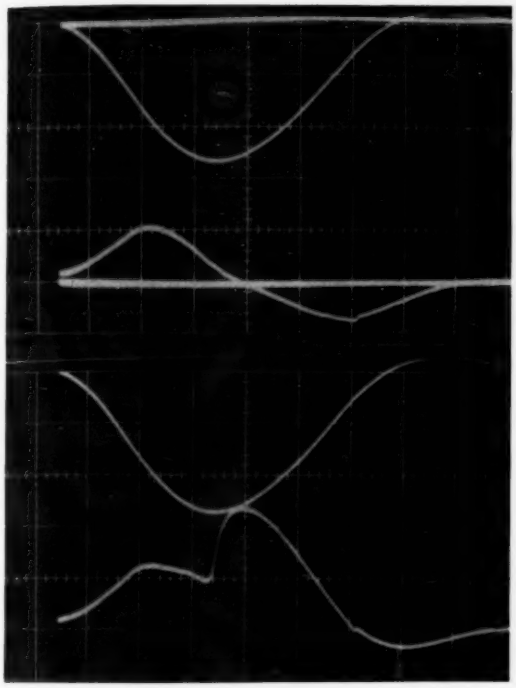

FIG. 2. Upper set: superconducting sample, $L\,di/dt$ response. Lower set: superconducting-to-normal transition, $L(di/dt)+iR$ response. Top traces: sample current, 89.5 amp/cm, positive direction downward. Bottom traces: sample voltage, 100 mv/cm, positive direction upward.

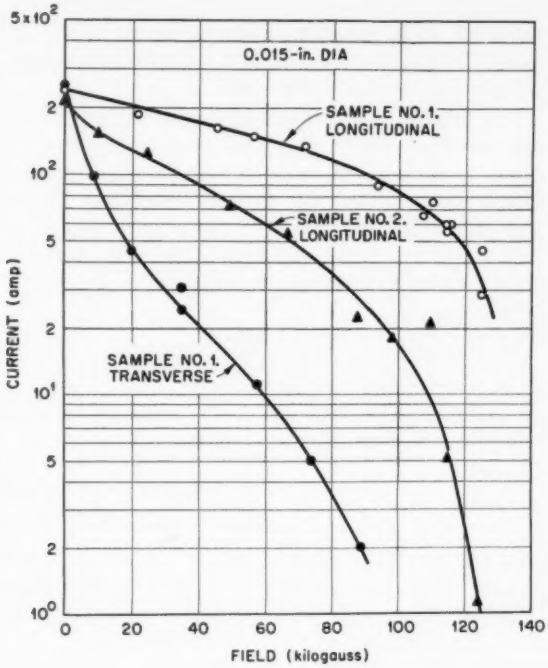

FIG. 3. Critical current vs applied magnetic field for Nb-Nb_3Sn wires at 4.2°K. (Wire diameter, 0.038 cm; core diameter, 0.015 cm.)

one milliohm. Both the transition time and the normal resistance depend on the previous history of the sample. Resistances as small as 10 μohm and transition times as short as 2 μsec were observed. These effects are being investigated and will be reported in a later communication.

The critical current was plotted as a function of field for two samples; see Fig. 3. Sample No. 1 was measured both parallel and transverse to the field, while sample No. 2 was oriented parallel to the field only. The curves show that all samples carry currents of 210 to 260 amp in a zero external field. Sample No. 1 carries 100 amp at 100 kilogauss with the field parallel to the wire axis. A much smaller critical current occurs with the field oriented in a transverse direction. Both the current-carrying capacity and the maximum field at which current is carried are lower in sample No. 2. The difference between specimens, shown in Fig. 3, is not entirely unexpected; the properties of hard superconductors are known to vary with slight differences of strain and defect structure.

Domain structure would appear to explain the differences obtained for parallel and transverse orientations. Only a small volume of the Nb_3Sn is superconducting at higher fields according to the magnetization curve of Bozorth, Williams, and Davis.[2] Studies of the intermediate state of various superconductors by Schawlow,[3] DeSorbo,[4] and Haenssler and Rinderer[5] suggest that the internal structure tends to become arranged in domains with interfaces parallel to the field and normal to the current. A domain structure of this type in Nb-Nb_3Sn could account for the much smaller critical currents for transverse orientation. This can explain the differences found between the transverse and parallel orientations in soft superconductors. In a hard superconductor such as Nb_3Sn, however, the superconducting regions should be determined primarily by the macroscopic physical structure of the specimen.

Since this structure is oriented along the axis of the wire, it is somewhat surprising that such large differences between the parallel and transverse orientations were found.

The critical current at zero external field was also measured with direct currents in the samples. The direct-current values were 1/3 lower than those obtained with pulsed techniques. This is attributed to heating at the current joints or in the cladding which surrounds the Nb_3Sn core. This heating is substantially reduced with pulse techniques.

*Work supported in part by the National Science Foundation and T.E.A.S.P.

†Operated for the U. S. Atomic Energy Commission by the Union Carbide Corporation.

[1]J. E. Kunzler, E. Buehler, F. S. Hsu, and J. H. Wernick, Phys. Rev. Letters 6, 89 (1961).

[2]R. M. Bozorth, A. J. Williams, and D. D. Davis, Phys. Rev. Letters 5, 148 (1960).

[3]A. L. Schawlow, Phys. Rev. 101, 573 (1956).

[4]W. DeSorbo, Proceedings of the Seventh International Conference on Low-Temperature Physics (University of Toronto Press, Toronto, Canada, 1960).

[5]F. Haenssler and L. Rinderer, Proceedings of the Seventh International Conference on Low-Temperature Physics (University of Toronto Press, Toronto, Canada, 1960).

FERMI SURFACE TOPOLOGY OF EVEN-VALENT METALS FROM THEIR MAGNETORESISTANCE ANISOTROPY

E. Fawcett

Physics Department, Royal Radar Establishment, Malvern, England

(Received March 27, 1961)

The anisotropy of the magnetoresistance of Au and Cu has recently been successfully interpreted by employing the concept of open orbits on a multiply-connected Fermi surface in a periodically extended zone scheme.[1] Open orbits occur for a limited range of field directions, and the transverse magnetoresistance $\rho_{\alpha\alpha}$ in a sufficiently high field H with the current making an angle α with the direction of the open orbits is then of the form,[2]

$$\rho_{\alpha\alpha} = A + BH^2\cos^2\alpha. \qquad (1)$$

A plot of the resistance in a fixed high field whose direction varies is characterized by sharp maxima for field directions permitting some open orbits (with $\alpha \neq \pi/2$), which rise above the low resistance obtained for most field directions for which only closed orbits occur and the resistance saturates.

This behavior is in marked contrast with the anisotropy of the magnetoresistance observed for Mg,[3] Zn,[4] Cd,[4] Pb,[5] and Sn[5] (the transition metals are not considered here and insufficient data are available for other even-valent metals). For these metals the resistance varies quadratically with field and is uniformly high for most field directions, falling to sharp minima for certain field directions where it varies less rapidly.

The proposed explanation of this behavior in the even-valent metals is as follows. Consider the range of field directions for which closed cyclotron orbits occur over the whole Fermi surface, and fields so large that for all such orbits $\omega_c\bar{\tau} \gg 1$, ω_c being the cyclotron frequency and $\bar{\tau}$ the relaxation time averaged over the orbit. If the component σ_{xy} of the conductivity tensor with field H along the z axis is expanded in ascending powers of $1/H$, the leading term is of the form,[2]

$$\sigma_{xy} = -\frac{e}{cH}\frac{2}{h^3}\sum_i \int S_i(p_z)\,dp_z. \qquad (2)$$

Here the area $S_i(p_z)$ enclosed by the intersections with the sheet i of the Fermi surface by the plane p_z = constant will, in general, be the sum of positive terms for closed orbits containing occupied electron states of lower energy within and immediately adjacent to each orbit, and of negative terms for orbits containing hole states. For the case where all sheets of the Fermi surface are simply connected, the range of integration need be only over a single Brillouin zone (with suitable remapping), and Eq. (2) results in the well-known expression,[2-6]

$$\sigma_{xy} = -\frac{e}{cH}(n_e - n_h)N_a. \qquad (3)$$

Here N_a is the number of atoms per unit volume, and n_e and n_h are the numbers of electron and hole states per atom, which are well defined since each sheet consists of closed surfaces containing either electrons or holes.

But Eq. (3) also applies to the case where one or more sheets of the Fermi surface are multiply connected, provided no open orbits occur in the range of field directions considered and $\omega_c\bar{\tau} \gg 1$ for all closed orbits. This may be seen by extending the range of integration to sufficient periodically extended zones to include the most extended orbits of any practical significance. The value of the integral for each sheet in Eq. (2) is still independent of the field direction: Its sign determines the electron or hole character of the sheet, and its numerical value is accordingly the electron volume $n_e N_a h^3/2$ or the hole volume $n_h N_a h^3/2$ enclosed by the sheet. This is true despite the fact that on the same multiply-connected sheet both electron and hole orbits may occur, since in the case of an electron sheet every hole orbit will be surrounded by an electron orbit and vice versa for a hole sheet.[7] This provides a useful criterion for determining the electron or hole character of a multiply-connected sheet.

Moreover, inspection of the proposed Fermi surface topologies for the metals considered here according to this criterion shows that n_e and n_h are equal (and it seems a reasonable hypothesis to suppose this to be true for any even-valent metal). It follows that the leading term in σ_{xy} vanishes for all field directions for which only closed orbits with $\omega_c\bar{\tau} \gg 1$ occur, and the components ρ_{xx} and ρ_{yy} of the resistivity tensor then rise quadratically with the field.[6]

The transverse magnetoresistance in a fixed high field will therefore be uniformly high except for minima in field directions where there are open orbits making an angle $\alpha \sim \pi/2$ with the current direction, or where there are closed orbits for which $\omega_c\bar{\tau} \leq 1$. In the first case the field dependence of the resistance is given by Eq. (1), saturating at the highest fields when $\alpha = \pi/2$, while in the second case the resistance will saturate at intermediate fields but again rise quadratically at fields sufficiently high to make $\omega_c\bar{\tau} \gg 1$ for all orbits.

The multiply-connected hole surface for Mg is shown in Fig. 1; another hole surface is split off by the spin-orbit coupling,[8] but this need not be drawn since it is simply connected, as are the electron surfaces.[9] Measurements of the de Haas-van Alphen effect in Mg and Zn are consistent with this picture of the Fermi surface, while similar measurements for Cd suggest that the arms of the "ring" parallel to the basal plane are pinched off.[10]

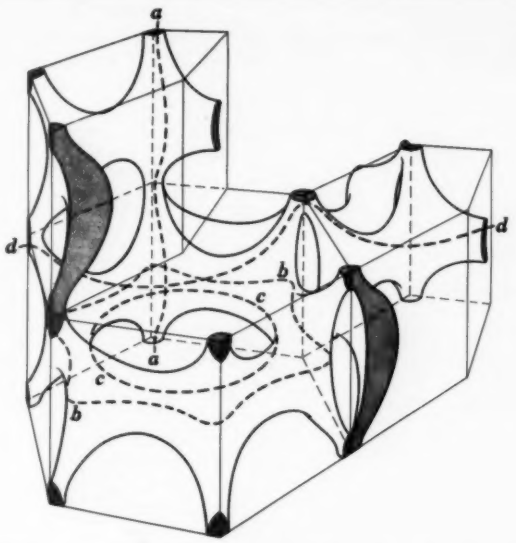

FIG. 1. The multiply-connected Fermi surface containing holes in the first Brillouin zone for Mg[9] (and probably Zn[10]), drawn in a periodically extended zone scheme. *aa*—open orbit along the hexagonal axis; *bb*, *cc*—closed orbits around the "ring"; *dd*—open orbit parallel to the basal plane.

The connectivities of these hole surfaces are consistent with most features of the observed anisotropy and field dependence of the transverse magnetoresistance. For example, the experimental results illustrated in Fig. 2, with the current J near the basal plane and the field H making an angle θ with the basal plane, show a sharp minimum in the resistance at $\theta = 0°$ in both Zn and Cd, which is due to open orbits along the hexagonal axis (for example orbit *aa* in Fig. 1). A minimum is observed in Zn also at $\theta = 90°$, which is attributed to the lower value of ω_c for orbits around the circumference of the ring (orbits *bb* and *cc* in Fig. 1) than for orbits embracing its arms; the absence of this minimum confirms that the ring is pinched off in Cd. Measurements in this orientation have not been published for Mg, but the minimum observed when H and J are coplanar with the hexagonal axis and J makes an angle of 25° with the basal plane (and in several other specimens of unspecified orientations[3]) may be due to open orbits parallel to the basal plane (orbit *dd* in Fig. 1). For Mg and Cd (and probably also for Zn) with J along the hexagonal axis and H in the basal plane, the resistance is roughly isotropic and varies quadratically with H due to open orbits along the hexagonal axis.[8]

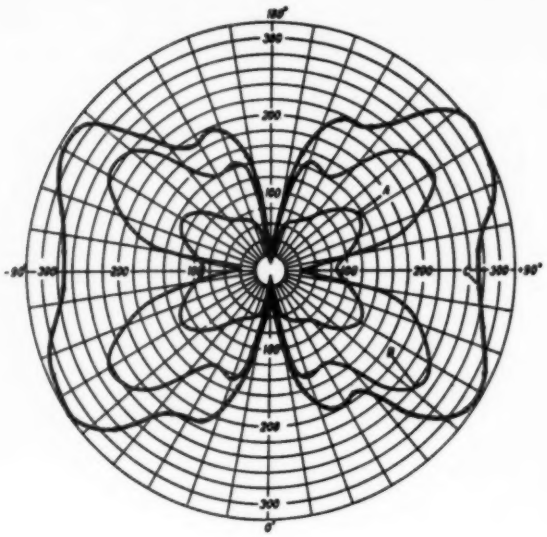

FIG. 2. Polar diagram of the transverse magnetoresistance, $\Delta\rho_H/\rho_0$, in Zn and Cd at 4.2°K. α is the angle between the current J and the hexagonal axis, and r the resistance ratio, $\rho_{273}/\rho_{4.2}$, in zero field (after Justi et al.[4]).

A – Cd2,	H = 12.9 kgauss,	α = 87°,	r = 800.
B – Zn10,	H = 12.9 kgauss,	α = 88°,	r = 2100.
C – Cd47,	H = 14.8 kgauss,	α = 84°,	r = 2000.

A multiply-connected electron surface in the third Brillouin zone for Pb, consisting in a periodically extended zone scheme of thick cylinders along the edges of the zone intersecting at its corners, was proposed by Gold.[11] With J along both [111] and [001] the transverse magnetoresistance of Pb is uniformly high and varies quadratically with the field, except for sharp minima where it saturates when H is along [110]. It is difficult to explain this result employing open orbits since, for any direction of the orbit, the angle α in Eq. (1) must differ from $\pi/2$ for one or the other of these current directions. But with H along [110] a large closed orbit exists around the inside of the multiply-connected surface in a single zone, of which there is some evidence from magnetoacoustic measurements.[12] One might expect a large cyclotron mass and hence small ω_c for this orbit, and if $\omega_c\bar{\tau} \lesssim 1$ for the fields and specimens used, one has a ready explanation of the observed anisotropy of the magnetoresistance. But this interpretation is necessarily tentative since, although the de Haas–van Alphen measurements indicate that the hole surface in the second zone is closed,[11] the behavior of the magnetoacoustic attenuation in high fields suggests that this surface also is multiply connected.[12] In any case open orbits on the surface in the third zone probably occur for some field directions.

The Fermi surface of Sn is so complex, consisting of several sheets one or more of which may be multiply connected, as to have evaded attempts at its determination using several different experimental methods.[13] The anisotropy of the magnetoresistance suggests that open orbits occur [for example, the resistance at the minimum for one field direction changes according to Eq. (1) as the current direction is varied in a plane normal to the field[11]], and the predominantly quadratic field dependence of the resistance is consistent with the hypothesis that $n_e = n_h$ for all even-valent metals.

The author has benefited from stimulating discussions with his colleagues at the Royal Radar Establishment, particularly Dr. J. M. Lock and Dr. M. D. Sturge; he is also indebted to Dr. D. H. Parkinson for his encouragement and to D. W. Charles for drawing Fig. 1.

[1]Yu. P. Gaidukov, J. Expti. Theoret. Phys. (U.S.S.R.) 37, 1281 (1959) [translation: Soviet Phys.–JETP 37(10), 913 (1960)]; M. G. Priestley, Phil. Mag. 5, 111 (1960); J. R. Klauder and J. E. Kunzler, Proceedings of the International Conference on the Fermi Surface (John Wiley & Sons, New York, 1960), p. 125.

[2]I. M. Lifshitz, M. Ia. Azbel', and M. I. Kaganov, J. Exptl. Theoret. Phys. (U.S.S.R.) 31, 63 (1956) [translation: Soviet Phys.–JETP 31(4), 41 (1957)]; I. M. Lifshitz and V. G. Peschanskii, J. Exptl. Theoret. Phys. (U.S.S.R.) 35, 1251 (1958) and 38, 188 (1960)[translations: Soviet Phys.–JETP 35(8), 875 (1959) and 38(11), 137 (1960)].

[3]N. E. Alekseevskii and Yu. P. Gaidukov, J. Exptl. Theoret. Phys. (U.S.S.R.) 38, 1720 (1960) [translation: Soviet Phys.–JETP 38(11), 1242 (1960)].

[4]B. G. Lazarev, N. M. Nakhimovich, and E. A. Parfenova, Zhur. Eksp. i Teoret. Fiz. 9, 1169 (1939); E. Justi, J. Kramer, and R. Schulze, Physik. Z. 41, 308 (1940); E. S. Borovik, J. Exptl. Theoret. Phys. (U.S.S.R.) 30, 262 (1956) [translation: Soviet Phys.–JETP 30(3), 243 (1956)]; C. A. Renton, Proceedings of the Seventh International Conference on Low-Temperature Physics, Toronto, 1960 (University of Toronto Press, Toronto, 1960), p. 153.

[5]N. E. Alekseevskii and Yu. P. Gaidukov, J. Exptl. Theoret. Phys. (U.S.S.R.) 36, 447 (1959) and 37, 672 (1959) [translations: Soviet Phys.–JETP 36(9), 311 (1959) and 37(10), 481 (1960)].

[6]R. G. Chambers, Proc. Roy. Soc. (London) A238, 344 (1956); Proceedings of the International Confer-

ence on the Fermi Surface (John Wiley & Sons, New York, 1960), p. 100.

[7]This statement is valid even for those field directions in a plane of high symmetry for which open orbits of type A [6] occur, if such an orbit is regarded as the limiting form of a highly extended orbit. It is not true when the field is in the isolated direction of high symmetry which lies at the center of a solid angle of field directions for which open orbits of type B [2,6] occur (for example, the [100], [110], and [111] axes in Au and Cu[1]). In fact the integral in Eq. (2) cannot be defined where orbits of type B occur, and one may envisage the transformation of an electron sheet into a hole sheet as the volume occupied by electrons is expanded to fill more than half the zone by supposing the sheet to pass through intermediate stages for which orbits of type B occur for all field directions.

[8]M. H. Cohen and L. M. Falicov, Phys. Rev. Letters 5, 544 (1960).

[9]L. M. Falicov (to be published); the author is indebted to Dr. L. M. Falicov for communicating the results of his band structure calculations for Mg before publication.

[10]W. L. Gordon, A. S. Joseph, and T. G. Eck, Proceedings of the International Conference on the Fermi Surface (John Wiley & Sons, New York, 1960), p. 84; W. A. Harrison, Phys. Rev. 118, 1190 (1960); see also E. Fawcett, J. Phys. Chem. Solids (to be published).

[11]A. V. Gold, Phil. Trans. Roy. Soc. (London) A251, 85 (1958).

[12]A. R. Mackintosh, Proceedings of the International Conference on the Fermi Surface (John Wiley & Sons, New York, 1960), p. 233.

[13]See, for example, A. V. Gold and M. G. Priestley, Phil. Mag. 5, 1089 (1960), who describe the free-electron model of the Fermi surface of Sn.

RESOLVED ISOTROPIC HYPERFINE STRUCTURE OF THE ELECTRON PARAMAGNETIC RESONANCE ABSORPTION OF F CENTERS IN NaH†

W. T. Doyle and W. L. Williams

Physics Department, Dartmouth College, Hanover, New Hampshire

(Received April 21, 1961)

The wide, inhomogeneously broadened electron paramagnetic resonance lines of F centers in alkali halides are due to the hyperfine interactions between the center electron and the surrounding nuclei.[1,2] These lines are commonly structureless and the hyperfine interactions must be studied using the electron nuclear double resonance (ENDOR) method.[3] When the first shell contact interaction predominates, however, and the nuclear spin of the alkali ion is 3/2, one expects a nineteen-line spectrum with relative intensities of the components of 1, 6, 21, 56, 120, 216, 336, 456, 546, and 580, corresponding to total shell nuclear magnetic quantum numbers of $\pm 9, \cdots, 0$, respectively.[1] In a few crystals, viz., LiF and NaF,[4,5] and RbCl,[6] a partially resolved spectrum has been observed. The structure of the LiF line, originally reported to be isotropic,[4,5] is now known to possess many more than the predicted nineteen lines[7] and to be anisotropic.[8] ENDOR studies[9] have shown that the first shell interaction does not predominate in this case, but subsequent calculations[10] have established that the resolved spectrum is consistent with the ENDOR results and with the de Boer model. It seems likely that in RbCl, too, the spectrum is due to more than the first shell nuclei alone, since the spectrum could not be reconciled with the known isotopic abundances of the alkali ions.[6] In NaF, on the other hand, we believe that the resolved spectrum is due to the first shell interaction as originally reported.[4,5] We have found that the resolution of the NaF spectrum is unimpaired when the sample is in the form of a powder, whereas in LiF the resolution is washed out when the sample is powdered. NaF is thus the only alkali halide in which the hyperfine interaction with the first shell nuclei has been seen directly. However, even in NaF not all of the nineteen lines have been observed, and the signals observed were neither well enough resolved nor strong enough to permit a direct comparison with the predicted relative strengths of the nineteen lines. Since the favorable circumstances in NaF may be traced in part to the relatively large hyperfine interaction constant of sodium, and in part to the low atomic number of fluorine, we were led to examine the spectrum of the very similar crystal NaH, in which it was to be expected that the situation should be even more favorable for the appearance of a resolved first shell structure.

It is known that the hydrides may be colored by radiation and that in LiH the principal product

is colloidal lithium when the irradiation is carried out at room temperature.[11] In contrast with this, x-ray induced F centers in sodium hydride are stable at room temperature, although they are thermally bleached within minutes at temperatures around 100°C. The rate of production of F centers, as well as the optical and thermal bleaching properties, monitored using the electron spin resonance signal, were all found to parallel closely the corresponding properties in the halides.

In view of the difficulty of producing single crystals of NaH, the observations reported here were made using commercial sodium hydride powder. This has the advantage of tending to smear out the small anisotropic contribution. This material usually contains an appreciable amount of excess sodium, so the samples used were additively colored at the start. All of the samples exhibited a strong, narrow electron paramagnetic resonance (EPR) line which was identified by its shape, g value, and temperature independence, as conduction electron spin resonance in sodium metal. The narrow resonance was not changed by irradiation and, since it could not be saturated with the microwave power available, it was a simple matter to subtract it from the easily saturated F-center resonance developed by the irradiation.

In Fig. 1 the F-center resonance alone is shown. This curve was obtained by taking the difference between a high- and low-power spectrum. The shape of the spectrum agrees in detail with the predictions of the de Boer model. There are 19 well-resolved lines. The spacing is determined by the first shell hyperfine interaction constant $A(1)$. All of the relative intensities agree with the theoretical distribution to within the experimental error of a few percent, as judged by comparison with computed curves of sums of Gaussian derivatives. It appears from such curves that the ratio of peak separation A to the full width, 2σ, between points of maximum and minimum slope (rms width for a Gaussian shape) is about 1.25 ± 0.1. Since the ENDOR studies on LiF have shown that only the first two shells interact strongly with the F-center electron, it is probably safe to assume that the width of the individual peaks is due primarily to the twelve second shell nuclei. When, as in NaH, these have spin 1/2, the relationship of the hyperfine constant to the linewidth is $A = \sigma/\sqrt{3}$.[5] The observed values of A as well as the modulus of the F-center wave function at the nuclei, $|\psi|^2 = 3IA/8\pi\mu$, for the first and second shell are given in Table I. Because they are based upon peak widths rather than resolved spacings, the second shell values are somewhat less reliable. The g value tabulated was corrected to second order in A/H using the Breit-Rabi equation. For this purpose the first shell is treated as a single entity with shell spin $I = 9$.[5] As expected, the g shift is negative and agrees in order of magnitude with the shifts found in the halides.

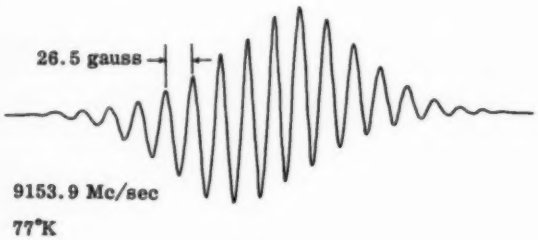

FIG. 1. Derivative of EPR absorption curve for F centers in NaH, showing a well-resolved 19-line spectrum of de Boer shape.

Table I. Experimental results. The g value has been corrected to second order in A/H_0 using the Breit-Rabi equation. The uncertainty quoted for g is the rms deviation from the mean of 15 determinations. The hyperfine interaction energy, A, and the modulus of the wave function at the nucleus, $|\psi|^2$, for the first and second shells were obtained from the peak separation and width, respectively.

$g = 1.9979 \pm 0.0004$	$\lvert\psi(1)\rvert^2 = 4.3 \times 10^{23}$ cm^{-3}
$A(1) = 26.5 \pm 0.2$ gauss	$\lvert\psi(2)\rvert^2 = 0.26 \times 10^{23}$ cm^{-3}
$A(2) = 6.1 \pm 0.3$ gauss	

It appears that sodium hydride is a particularly favorable crystal for viewing the hyperfine interaction of the F-center electron with the first shell nuclei. The validity of the de Boer model is immediately apparent in the resolved spectrum.

†Research supported by a grant from the National Science Foundation.

[1]A. F. Kip, C. Kittel, R. A. Levy, and A. M. Portis, Phys. Rev. 91, 1066 (1953).
[2]A. M. Portis, Phys. Rev. 91, 1071 (1953).
[3]G. Feher, Phys. Rev. 105, 1122 (1957).
[4]N. Lord, Phys. Rev. 105, 756 (1957).
[5]G. J. Wolga and M. W. P. Strandberg, J. Phys. Chem. Solids 9, 309 (1959).
[6]H. C. Wolf and K. H. Hausser, Naturwissenschaften 46, 646 (1959).

[7]Y. W. Kim, R. Kaplan, and P. J. Bray, Bull. Am. Phys. Soc. 3, 178 (1958).
[8]Y. W. Kim, R. Kaplan, and P. J. Bray, Phys. Rev. Letters 6, 4 (1961).
[9]W. C. Holton, H. Blum, and C. P. Slichter, Phys. Rev. Letters 5, 197 (1960).
[10]H. Blum and W. C. Holton, Bull. Am. Phys. Soc. 6, 112 (1961).
[11]W. T. Doyle, D. J. E. Ingram, and M. J. A. Smith, Phys. Rev. Letters 2, 497 (1959).

MAGNETIC COOLING WITH PARAMAGNETIC METALS*

R. D. Parks and W. A. Little
Department of Physics, Stanford University, Stanford, California
(Received April 19, 1961)

In this Letter we report on an investigation of the magnetic properties at low temperatures of a series of thorium-erbium alloys. These alloys are unique in that even for high spin densities magnetic ordering occurs only at temperatures well below 1°K. For this reason it is possible to use such alloys as the cooling agents in adiabatic demagnetization experiments.

Conventional paramagnetic salts used for this purpose such as potassium chrome alum and ferric ammonium alum, being dielectric crystals, have a thermal conductivity due to the lattice which varies as T^3. Consequently, at temperatures below 0.1°K this becomes exceedingly small, resulting in very low rates of heat transfer between the paramagnetic salt and the sample being cooled. In a metal, however, the thermal conductivity which is due to the conduction electrons varies linearly with T. For temperatures below 0.1°K this greatly exceeds that of a dielectric crystal. In addition a metal is more durable than conventional cooling salts which decompose on exposure to air or heat. For these reasons we have looked for a paramagnetic alloy which could be used instead of a paramagnetic salt for magnetic cooling. This search led us to the study of thorium–rare earth alloys. As reported earlier,[1] we found some magnetic cooling below 1°K with thorium-dysprosium alloys. We have now investigated the thorium-erbium system and have found excellent cooling properties to temperatures below 0.1°K.

The alloys were prepared by melting thorium and erbium metals together under argon in an arc furnace. This method is described in more detail elsewhere.[1] A series of Th-Er samples were adiabatically demagnetized from initial temperatures of 0.73°K and varying magnetic fields up to 8400 gauss. The cooling curves appear in Fig. 1. When demagnetized from fields of about 8000 gauss, all the samples cooled

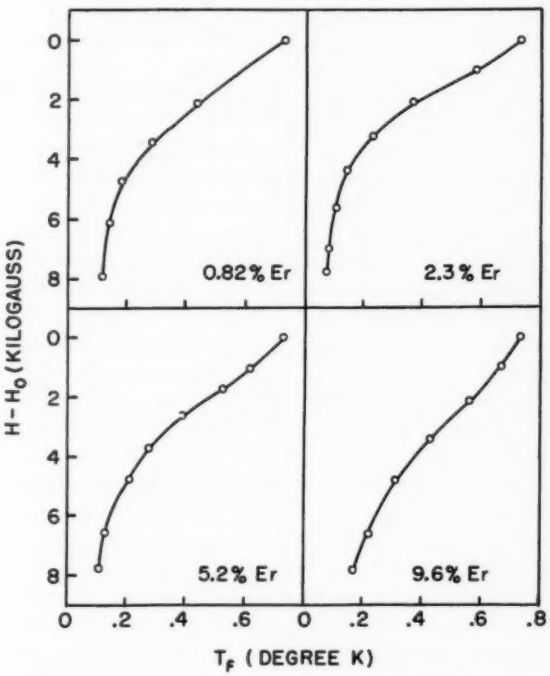

FIG. 1. Magnetic cooling curves of different Th-Er alloys. T_f is the final temperature reached by the samples when demagnetized from an initial temperature of 0.73°K and from a magnetic field of H. A residual field of 500 gauss (H_0) was left on the sample to suppress either superconductivity or antiferromagnetic ordering. The complete removal of H resulted in a small increase in temperature which is characteristic of the onset of either phenomenon.

to temperatures below 0.2°K. The 2.3% Er sample reached a final temperature of 0.07°K. From these curves one should expect that for larger values of H/T_i (T_i = initial temperature) the samples should reach even lower final temperatures. In the most dilute sample (0.82% Er) the electronic entropy is an appreciable fraction

of the spin entropy removed and therefore limits T_f. In the most concentrated samples T_f is limited by the larger internal interactions which lower the entropy. The cooling curves suggest that Th-Er alloys with concentrations of Er in the range 1-4 atomic percent would be most useful for cooling below 0.1°K.

We believe that Th-Er should exhibit better magnetic cooling properties than other thorium–rare earth alloys. The requirements of a metal for magnetic cooling are that it have a large total spin entropy per unit volume, $N_m k \ln(2J+1)$ (where N_m is the number of magnetic ions per unit volume), and that it have a low magnetic transition temperature, T_c (the temperature at which magnetic ordering occurs). In the rare earth metals the indirect exchange interaction between the $4f$ electrons and the conduction electrons determines T_c.[2] Liu[3] and de Gennes[4] have shown that T_c should vary as $N_m(\vec{J}\cdot\vec{S})^2/J(J+1)$. Of the 14 rare earth elements, these requirements are best satisfied by cerium, ytterbium, and erbium. However, Ce[5] and Yb[6] exhibit anomalous behavior which indicates that they would not be suitable.

We have made specific heat measurements on the Th-Er alloys which give further evidence that the indirect exchange interaction is small. Figure 2 shows the specific heat of Th-19% Er in the temperature range 0.3-4.2°K. From this curve we find that 80% of the total spin entropy remains below 0.4°K.[7] This is quite remarkable since in pure erbium magnetic ordering occurs at 84°K.[8]

To determine the usefulness of the Th-Er alloys for magnetic cooling, a comparison can be made between Th-3% Er and ferric ammonium alum with respect to cooling power, which is proportional to the total spin entropy, and thermal conductivity. Th-3% Er has a total spin entropy per unit volume of 33×10^{-3} joule/cm^3 deg,[9] compared to that of 53×10^{-3} joule/cm^3 deg for ferric ammonium alum. From measurements of the residual resistivity the value of the thermal conductivity, k, due to the electrons, was calculated. This gives a value of $k = 2.8\times10^{-3}T$ joule/cm sec for the Th-3% Er alloy. At 0.05°K this is about 100 times larger than the thermal conductivity reported for compressed powdered ferric ammonium alum.[10]

In a cyclic magnetic refrigerator, described elsewhere,[11] we have used a Th-3.5% Er alloy to reach a final reservoir temperature of 0.2°K with a starting temperature of 0.73°K. This is as low a final temperature as has been obtained by using a salt.[11] The refrigerator is now being modified for He^3 pumping which will give a starting temperature of 0.35°K. By using a Th-Er alloy instead of a salt in this new refrigerator, we expect to reach a reservoir temperature below 0.1°K and obtain high heat extraction rates at this temperature.

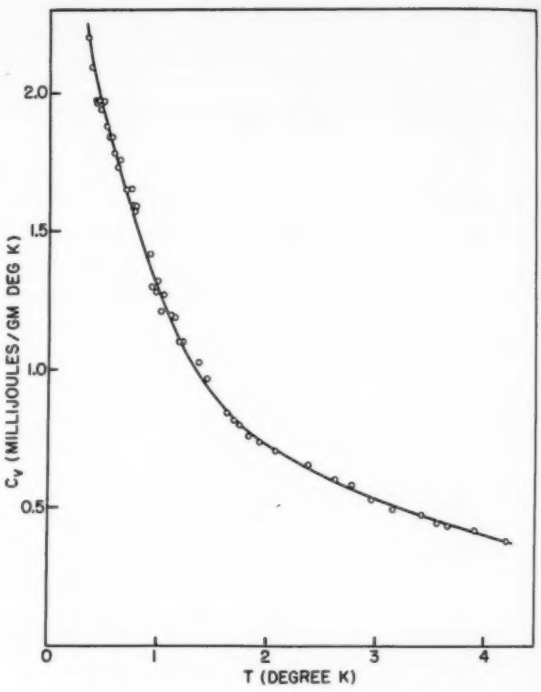

FIG. 2. Specific heat of a thorium-19% erbium alloy.

*Work supported by the Office of Naval Research and the U. S. Atomic Energy Commission.

[1]R. D. Parks and W. A. Little, Proceedings of the Seventh International Conference on Low-Temperature Physics, 1960 (University of Toronto Press, Toronto, Canada, 1960), p. 114.

[2]T. Kasuya, Progr. Theoret. Phys. (Kyoto) 16, 45 (1956).

[3]S. H. Liu, Phys. Rev. 121, 451 (1961).

[4]P.-G. de Gennes, Compt. rend. 247, 1836 (1958).

[5]There is strong evidence that in Ce part of the $4f$ electron is promoted to the $5d$ shell at lower temperatures. This greatly increases the indirect exchange interaction. See B. T. Matthias, H. Suhl, and E. Corenzwit, Phys. Rev. Letters 1, 92 (1958).

[6]In Yb the $6s$ electron apparently falls to the $4f$ shell, completing the shell, and thus destroying the paramag-

netism. See F. H. Spedding, S. Legvold, A. H. Daane, and L. D. Jennings, Progress in Low-Temperature Physics, edited by J. C. Gorter (North-Holland Publishing Company, Amsterdam, 1957), Vol. II, p. 391.

[7]This calculation is based upon $J=15/2$ for Er which is the theoretical value. There may be a decrease in J because of crystalline field effects. For pure Er the saturation moment gJ at 4.2°K was found to be about 10-15% less than the theoretical value. [See R. W. Green, S. Legvold, and F. H. Spedding, Phys. Rev. 122, 867 (1961).] A change in J of this size would have little effect upon the spin entropy which varies as $\ln(2J+1)$.

[8]R. E. Skochpole, M. Griffel, and F. H. Spedding, J. Chem. Phys. 23, 2258 (1955).

[9]Based upon $J=15/2$. See reference 8.

[10]H. van Dijk and W. H. Keesom, Physica 7, 970 (1940).

[11]W. A. Little, R. D. Parks, and N. P. Shah, Progr. Theoret. Phys. (Kyoto) 16, 112 (1956).

ANOMALOUS LATTICE SPECIFIC HEAT OF SUPERCONDUCTORS*

Richard A. Ferrell
University of Maryland, College Park, Maryland
(Received April 25, 1961)

Bryant and Keesom[1] have discovered that the lattice specific heat of indium is significantly less in the superconducting than in the normal state. A similar effect has been detected in niobium by Boorse, Hirshfeld, and Leupold.[2] Daunt and Olsen[3] have proposed to account for the difference in terms of a temperature dependence of the zero-point energy in the superconducting state. But according to the second law of thermodynamics, a physical system can only take on heat by means of an increase in its entropy, or disorder. If the high-frequency lattice oscillators remain in their ground states, their quantum numbers do not change and they cannot directly contribute any disorder to the system. Their energy is indeed temperature dependent because of their interaction with the low-lying electron excitations,[4] but this interaction energy is customarily included as part of the electron excitation energy and must not be counted twice. Thus the zero-point energy does not constitute a new and independent source of heat, but instead simply contributes to the "renormalization" of the single-electron excitation energies. In any case, it cannot produce a specific heat anomaly at very low temperatures ($T \ll T_c$) because of the "freezing-out" of the electrons in the superconducting state.[5]

The purpose of the present note is to emphasize that the specific heat anomaly is clear and unmistakable evidence for an anomalous dispersion in the phonon spectrum of the superconducting state. Although a more complete report is in preparation, we shall also indicate here the a priori basis of such a dispersion, and show that it gives a good quantitative account of the data. In addition we propose several straightforward experimental tests of the theory.

Consider a constant shift upwards of $\Delta\omega$, in the range of the angular frequencies involved. The specific heat of any given lattice mode is $kf(\hbar\omega/2kT)$, where k and $2\pi\hbar$ are Boltzmann's and Planck's constants, T is the temperature, ω is the angular frequency of the oscillator, and

$$f(x)=(x/\sinh x)^2. \tag{1}$$

The fractional decrease in the total lattice specific heat is

$$\Delta C_S/C_S = T_S/T, \tag{2}$$

where

$$T_S = 0.556\hbar\Delta\omega/k, \tag{3}$$

and it is assumed that $T \gg T_S$. The numerical factor is one half of the ratio of the sum of the inverse cubes of the integers to the sum of the inverse fourth powers. To first order in the anomaly, the lattice specific heat in the superconducting state is

$$C_S = \alpha T^3 - BT^2, \tag{4}$$

where the coefficient of the T^2 anomalous term is $B=\alpha T_S$.

Figure 1 shows the data of Bryant and Keesom[1] divided by T^2 and replotted vs T. The slope of the lines is not adjusted but is instead fixed by the value computed by Chandrasekhar and Rayne[6] from their measurements of the elastic constants of indium. The dashed line passing through the origin represents the Debye specific heat in the

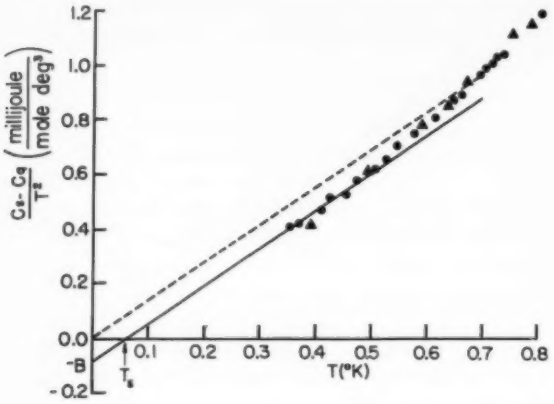

FIG. 1. Specific heat divided by the square of temperature vs absolute temperature, for the superconducting state of indium. (The nuclear quadrupole specific heat C_q is subtracted from the measured total.) The solid line is shifted downwards by the dispersion resulting from the self-energy process of Fig. 2.

absence of the dispersion. It is seen that the displaced line, which contains only one adjustable parameter, its displacement, gives a fit at the very low temperatures which could hardly be excelled by any temperature dependence other than that of Eq. (4). The vertical and horizontal intercepts are $B = 0.09$ millijoule mole^{-1} deg^{-3} and $T_S = 0.065$°K, which inserted into Eq. (3) give $\Delta\omega = 1.6\times10^{10}$ sec^{-1}, or a frequency shift of 2.5×10^9 cycles per sec. At the higher temperatures ($0.55°K < T < 0.85°K$) the difference between the heavy line and the experimental points is fitted well by the exponential $ae^{-bT_C/T}$, where T_C is the transition temperature of 3.37°K and the coefficients are $a = 7.3$ and $b = 1.43$. These values can be compared with the predictions[7] of the BCS theory of $a = 8.5$ and $b = 1.44$. The good agreement with the BCS exponent is consistent with the similar agreement with BCS theory in the temperature dependence of ultrasonic attenuation found by Morse and Bohm[8] for indium. Turning to the niobium anomaly, we find that the data are not fitted quite as well by our T^2 dependence. If we assume, however, that the corrections referred to in reference 2 will lower the lowest temperature points the most, the fit becomes satisfactory.

The microscopic basis for the shift in the frequency of the phonons in the superconducting state is the well-known result of Bardeen and

FIG. 2. Phonon self-energy Feynman diagram. The absorption of the phonon produces an electron-hole pair which can then re-create the phonon, resulting in a frequency shift. The same electron excitations are involved in both the real and imaginary parts of the frequecny shift. Thus the dispersion in the superconducting state is related to the ultrasonic attenuation in the normal state [Eq. (8) of the text].

Pines[9] and others that the frequency of a sound wave is very much dependent on the response of the conduction electrons. This is illustrated by the phonon self-energy Feynman diagram in Fig. 2. The phonon (represented by a wavy line) continually causes electrons to be excited out of their normal state. The electrons then act back on the phonon, changing its energy. (Time is imagined to flow from right to left.) The dispersion of the sound waves depends upon the real part of the matrix element corresponding to Fig. 2. We want to calculate the change in the real part when the metal passes from the normal to the superconducting state. It is useful, however, first to consider the imaginary part, which represents the damping calculated by Kittel,[10] and which can be written as $\omega/4\pi Q$, where ω is the angular frequency of the sound wave, and Q is a dimensionless number measuring the phonon mean free path in units of the wavelength. Kittel's result is

$$Q = \hbar^3 \rho c_s / (m^* C)^2, \qquad (5)$$

where $2\pi\hbar$ is Planck's constant, ρ is the mass density of the metal, c_s is the velocity of sound, m^* is the electron effective mass, and C is the usual electron-phonon coupling constant.[11] It is clear that there is not only a contribution to the imaginary part of the phonon frequency, but that a real contribution must also result, from virtual excitation of the same type of electron states as contribute to the damping.

The general features of Kittel's formula have been verified by Morse and Bohm,[8] including the frequency independence of Q. They have also shown that at temperatures very much below the transition temperature the Kittel damping disappears completely. This result follows readily from an energy gap picture of superconductivity:

If the phonon energy is less than the gap, there is no continuum of excited states into which a transition can take place. But this same deficiency of states in the gap will also lead to a loss in the virtual excitations, and thereby produce a change in the real part of the phonon frequency. Introducing $\hbar\bar{\omega}_g$ as the effective energy gap within which the normal density of electron excitations per unit excitation energy ϵ, $\rho(\epsilon)$, is replaced by zero in the superconducting state, we can write the difference in the complex phonon self-energy between the normal and superconducting state as the following integral:

$$\hbar\left(-\Delta\omega - \frac{i\omega}{4\pi Q}\right) = 2\int_0^{\hbar\bar{\omega}_g} \frac{|H_q|^2 \rho(\epsilon)\epsilon}{(\hbar\omega)^2 - (\epsilon - i\delta)^2} d\epsilon. \quad (6)$$

H_q is the matrix element for the production of an electron-hole pair by the absorption of a sound wave of wave number q and is independent of ϵ, while δ is an infinitesimally small positive quantity. Since $\rho(\epsilon)$ vanishes for $\epsilon = 0$, we can use the Taylor series expansion $\rho(\epsilon) = \epsilon\rho'$, where ρ' is the derivative. [We now restrict our attention to values of q sufficiently large that the maximum value of ϵ for which $\rho(\epsilon) \neq 0$ is much larger than $\hbar\bar{\omega}_g$; i.e., we consider wavelengths considerably smaller than the coherence length.] Both $|H_q|^2$ and ρ' can now be taken outside the integral sign, and elementary integration yields

$$\Delta\omega + (i\omega/4\pi Q) = |H_q|^2 \rho'(2\bar{\omega}_g + i\pi\omega). \quad (7)$$

We verify that insertion of the usual expressions for H_q and ρ' reduces the imaginary part of this equation to Eq. (5). The real increase in the sound-wave frequency in the superconducting state can now conveniently be compared with the imaginary part, giving us our basic equation,

$$\Delta\omega = \bar{\omega}_g/(2\pi^2 Q). \quad (8)$$

This is a type of dispersion relation, relating the dispersive behavior of the metal to its absorptive properties.

It is now desirable to see if Eq. (8) yields a reasonable value for Q. For our present purposes, we can approximate the effective gap by the actual energy gap, $\hbar\bar{\omega}_g \approx \hbar\omega_g \approx 4kT_c$. Sum rule arguments indicate that this is probably an overestimate, but not by more than 50%.[12] With this sort of accuracy understood, we can write

$$Q \approx 0.11\, T_c/T_s, \quad (9)$$

from which we obtain for indium, $Q \approx 5.8$. Equation (5) enables us to go further, and deduce the mean electron-phonon coupling strength. From the Debye temperature[6] of 111.3°K we infer $c_s \approx 0.83 \times 10^5$ cm/sec, while the normal state specific heat of indium[1] gives m^* equal to 1.21 times the free electron mass. We find $C \approx 7.9$ ev, which happens to be just equal to the Sommerfeld-theory Fermi energy. This result is not unreasonable for a metal with a complicated energy band structure sensitive to lattice changes, and indicates that a given percentage elastic strain must change the individual single-electron energies in about the same proportion. Since all superconductors do not necessarily have such large deformation potentials, it is clear that the specific heat anomaly cannot always be expected to appear. Furthermore, the lowest shear mode, with which the anomaly is primarily associated, has a longitudinal admixture for nonsymmetry directions. The resulting longitudinal deformation potential and electric field could in some cases interfere destructively with the shear coupling constant for the low-energy electron excitations. Therefore, it is clearly not feasible to predict a priori which superconductors will exhibit the anomaly. Nevertheless, it is possible to measure the quantity Q directly from ultrasonic absorption (for the lowest velocity mode averaged over propagation directions) and thereby employ Eq. (9) to predict the value of T_s. This would yield a quantitative prediction of the heat anomaly in advance of actual thermal measurements. Conversely, it would be highly desirable to have a check on the present considerations by means of an actual ultrasonic measurement of Q for indium (and, of course, also niobium for which $T_s \approx 0.2$°K and $Q \approx 5$). Such a measurement has already been made on the (001) shear wave in tin,[13] yielding $Q \approx 60$. Assuming that this is representative of the other propagation directions, we can predict that the specific heat anomaly is an order of magnitude smaller in tin than in indium. A further indication of an especially strong coupling of the shear waves to the electrons in indium is the strong temperature dependence found by Simmons and Slichter[14] in the nuclear quadrupole resonant frequency.

An alternative ultrasonic experimental check on the present considerations would be a direct measurement of the dispersion in the superconducting state, rather than of the attenuation in the normal state. Wavelengths λ smaller than the

coherence length ξ_0 are required, because of the general principle that the bulk elastic constants must give a correct description of sound waves for $\lambda > \xi_0$. (The very small normal-superconducting difference in the elastic constants results in turn from the fact that the transition energy depends parametrically on the lattice strains and forms only an extremely small fraction of the total ground-state energy.) Since the coherence length can be estimated for indium at $\xi_0 = 6300$ A, the minimum frequency for detecting appreciable dispersion is about 1.3×10^9 cycles per second. As a consequence of this minimum frequency, the lattice specific heat must return to its undisplaced Debye value in the limit $T \to 0$. That is, if it were possible to extend the measurements to such low temperatures, the points in Fig. 1 would leave the solid line and rejoin the dashed line.

It should also be noted that the constant frequency shift follows from Eq. (6) only for $\omega \ll \bar{\omega}_g$. At higher frequencies a more complicated dispersion results, leading for $\omega \gg \bar{\omega}_g$ to a very small shift [reduced by the order of $(\bar{\omega}_g/\omega)^4$]. Consequently, inelastic neutron scattering or the Mössbauer effect, for example, does not offer a feasible alternative method of detecting the dispersion.

An additional experimental test of Eq. (8) is suggested by Pippard's[15] study of the effect of the electron mean free path l on the ultrasonic attenuation. He finds that the Kittel damping is reduced by a factor proportional to l/λ for $l < \lambda$, in agreement with similar studies by Kittel,[10] Mason,[16] and Morse.[17] This suggests that if a metal showing the heat anomaly were heavily enough doped with an alloying impurity to reduce significantly the coherence length (as would be indicated by a decrease in the superconducting skin depth), then the anomaly would disappear.

*Research supported in part by the Air Force Office of Scientific Research and by the Office of Naval Research.

[1]C. A. Bryant and P. H. Keesom, Phys. Rev. Letters 4, 460 (1960).

[2]H. A. Boorse, A. T. Hirshfeld, and H. Leupold, Phys. Rev. Letters 5, 246 (1960).

[3]J. G. Daunt and J. L. Olsen, Phys. Rev. Letters 6, 267 (1961).

[4]Anharmonicity would couple the low-lying phonon excitations to the high-frequency oscillators, but for the sake of simplicity and without essential loss in generality, we neglect this effect here.

[5]The T^3 term of Eq. (8) of reference 3 results from the assumed parabolic shape of the threshold field curve, and would be replaced by an exponential for a more realistic shape. The linear term of this equation expresses the well-known Fröhlich enhancement of the Sommerfeld specific heat resulting from the electron-phonon interaction [see, for example, R. A. Ferrell, Bull. Am. Phys. Soc. 3, 203 (1958), and references cited there]. The difficulty encountered by Daunt and Olsen of a predicted negative specific heat in the superconducting state is instead simply this enhancement of the electron specific heat in the normal state, and is absorbed in the usual fit of the Sommerfeld parameter γ to the experimental data. This can also be seen from the fact that the entire temperature dependence for $T \ll T_c$ of their Eq. (3) (giving the normal-superconducting difference in the compressibility) is associated with the normal state (because of the T^2 term in the normal-state Gibbs function), and is equivalent to the use of the threshold field curve in the limit $T \to 0$ to deduce the Sommerfeld parameter [see, for example, J. G. Daunt, in Progress in Low Temperature Physics (Interscience Publishers, Inc., New York, 1955), Vol. 1, p. 202].

[6]B. S. Chandrasekhar and J. A. Rayne, Phys. Rev. Letters 6, 3 (1961).

[7]H. A. Boorse, Phys. Rev. Letters 2, 391 (1959).

[8]R. W. Morse and H. V. Bohm, Phys. Rev. 108, 1094 (1957).

[9]J. Bardeen and D. Pines, Phys. Rev. 99, 1140 (1955).

[10]C. Kittel, Acta Metallurgica 3, 295 (1955).

[11]A. H. Wilson, Theory of Metals (Cambridge University Press, New York, 1953), 2nd ed., Eq. (9.3.8).

[12]Detailed matrix element computations bearing on this point are being carried out by J. R. Schrieffer and D. Markowitz.

[13]H. Bommel (private communication).

[14]W. W. Simmons and C. P. Slichter, Phys. Rev. 121, 1580 (1961).

[15]A. B. Pippard, Phil. Mag. 46, 1104 (1955).

[16]W. P. Mason, Phys. Rev. 97, 557 (1955).

[17]R. W. Morse, Phys. Rev. 97, 1716 (1955).

ANOMALOUS CAPACITANCE OF THIN DIELECTRIC STRUCTURES

C. A. Mead

California Institute of Technology, Pasadena, California

(Received March 9, 1961; revised manuscript received April 10, 1961)

The classical analysis of a plane parallel capacitor gives a capacitance which becomes infinite as the spacing between the metal electrodes approaches zero. The fact that real capacitors show a marked deviation from this behavior has not generally been recognized.[1,2] This communication describes experiments in which the deviations have been measured with some care.

In order to determine the dependence of capacitance upon thickness it is necessary to have a reliable measure of the relative thickness of the device and also a method for producing very thin, uniform dielectric layers. Normal methods for measuring thickness are quite inconvenient for the thin layers used here. Consequently the voltage required to obtain a given tunneling current density[3,4] was used as a measure of the thickness. This procedure is considered to be a good approximation if the difference in metal-insulator work functions of the two metals under the conditions used is small, since the tunneling current density is only a function of the electric field at the interface, and not of the thickness of the dielectric. Investigation of the slight asymmetry of the volt-ampere characteristic of the structures used indicated that differences in the metal-insulator work functions were indeed small.

The present experiments were all carried out on a tantalum sheet which had been recrystalized in a dry argon atmosphere at 2700°C for 1/2 hour. The sheet was then composed of many crystals approximately 1 mm across, and was subsequently electropolished to a mirror finish. Tantalum oxide was formed on the surface anodically in dilute ammonium citrate solution. The samples were then placed in a vacuum system where they were baked at 300°C at residual pressure of 3×10^{-9} mm Hg while counter electrodes of gold were evaporated through a mask. The resulting structure was a large number of gold squares approximately 5 mils (0.005 in.) across on the tantalum oxide surface. Measurements of capacitance and tunnel voltage were made by standard techniques on a large number of squares on each sample. Only squares lying wholly on one crystal were used. The tunnel current density used was approximately 0.05 ma per square mil. Previous experience had indicated that a very small amount of contamination of the surface resulted in large variations of capacitance between squares on one sample. On the samples tested it is believed that surface contamination has essentially been eliminated since variations were in many cases less than 1% and in all cases were well within the limits placed upon the measurement of the variation of area between squares. The results of this experiment are shown in Fig. 1. It is seen that instead of having zero intercept, the plot of inverse capacitance versus tunneling

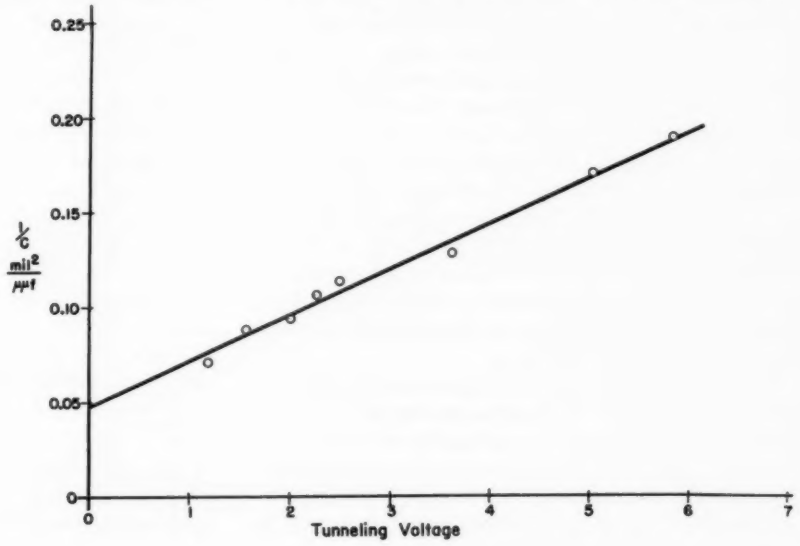

FIG. 1. Inverse capacitance as a function of tunnel voltage for Ta-Ta_2O_5-Au structures.

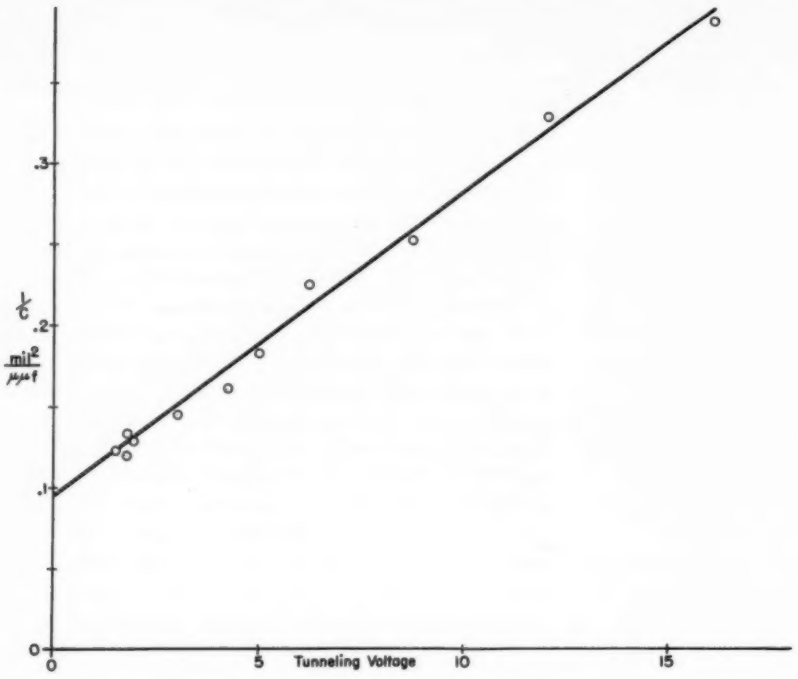

FIG. 2. Inverse capacitance as a function of tunnel voltage for Ta-Ta_2O_5-Bi structures.

voltage intercepts at approximately 0.05 square mil per $\mu\mu f$. This intercept corresponds to an ϵ_0 layer approximately 2.75 A thick. It was felt that perhaps variations in the capacitance with applied dc electric field could be observed. The experiment was performed but no detectable variation was observed up to electric fields where tunneling current made the measurements unreliable.

Theoretical work[5] indicates that the dielectric constant of an insulator should be preserved down to a few atomic layers. If this is true, we should expect the basic limitation of the capacitance to be electric field penetration into the metal. A crude classical calculation using a method similar to that of Mott and Jones[6] gives a penetration depth of the order of one A for typical metals, varying inversely with the square root of the density of states in the metal. Although no real confidence can be placed in such a calculation, if this is indeed the mechanism of the capacitance limitation, the $1/C$ intercept should vary with the density of states in the metal.

This dependence was investigated by another set of experiments using bismuth counter electrodes. Because of its low density of states, bismuth should have a larger value of penetration depth and hence a higher intercept on the plot of $1/C$ versus tunneling voltage. That this is indeed the case is shown in Fig. 2. Here the intercept corresponds to an ϵ_0 layer approximately 5.5 A thick.

At present it has not been possible to achieve truly symmetric structures and hence the series capacitance contribution for each interface is not known, but only the sum of those for two interfaces. A symmetric structure plus a knowledge of the true dielectric constant within the metal would be necessary for a full determination of the parameters involved.

The author is indebted to H. M. Simpson for preparing the samples, and to C. H. Wilts and R. W. Gould for helpful suggestions and comments. The work was supported in part by grants from the International Telephone and Telegraph Company, the General Electric Company, and a contract with the Office of Naval Research.

---

[1]J. C. Fisher and I. Giaever, J. Appl. Phys. 32, 172 (1961).

[2]R. W. Berry and D. J. Sloan, Proc. Inst. Radio Engrs. 47, 1070 (1959).

[3]C. A. Mead, Proc. Inst. Radio Engrs. 48, 359, 1478 (1960).

[4]C. A. Mead, J. Appl. Phys. 32, 646 (1961).

[5]W. Kohn, Phys. Rev. 110, 857 (1958).

[6]N. F. Mott and H. Jones, Metals and Alloys (Dover Publications, New York, 1958), p. 87.

AMPLIFICATION OF 9.3-kMc/sec ULTRASONIC PULSES BY MASER ACTION IN RUBY

E. B. Tucker
General Electric Research Laboratory, Schenectady, New York
(Received April 27, 1961)

The observation of the attenuation of 9.3-kMc/sec ultrasonic pulses by the spin-phonon interaction[1] in ruby implies that amplification should be observable in the same system if the spin population is inverted. We have now observed the amplification of 9.3-kMc/sec pulses of ultrasonic energy in passing through a ruby rod in which the spin system was inverted. This is the first observation of amplification of energy other than electromagnetic in such a system.

The conditions for the observation of maximum gain from the inverted spin system are identical with the conditions for the observation of the maximum attenuation except for the inversion, rather than the normal thermal equilibrium, of the spin system. The published results for attenuation in ruby[1] show that one of the highest ultrasonic interactions occurs, for longitudinal waves, at an angle of 60° between the magnetic field and the ruby c axis ($\theta = 60°$) for the 2-3 transition at high field (3700 gauss for 9.3 kMc/sec). Fortunately, the conditions for use of push-pull pumping[2] (saturation of both the 1-3 and the 2-4 transitions) at a single frequency occur at $\theta = 55°30'$. The actual orientation used for the experiment is a compromise between the above requirements. Since the ultrasonic transition probability is a slow function of angle near $\theta = 60°$, it was found that the best inversion was obtained at an angle of 56° using pump power of 23.3 kMc/sec.

The experimental observations were made using the same methods previously described[1] except that the ruby was contained in a K-band pump cavity. The crystal configuration consists of a $1\frac{1}{2}$-cm X-cut quartz crystal bonded, with indium, to a $1\frac{1}{4}$-cm length of Linde pink ruby (Cr^{+++} in Al_2O_3). Both crystals are in the form of cylindrical rods 3 mm in diameter and the c axis of the ruby is parallel to the rod axis to within $\frac{1}{2}$ degree. The experiments were carried out at 1.5°K.

The traces of Fig. 1 illustrate the effects of the spin system on the first few echoes observed. The echo to the right of the center graticule has made a single return trip through the ruby while the echo to the left of center has made two passes through the ruby. The larger amplitudes of these two echoes in the top picture as compared to the bottom trace is due to the amplification through interaction with the spin system. Similarly, the smaller amplitudes of the center trace as compared to the bottom are the result of attenuation due to transfer of energy to the spin system in thermal equilibrium at 1.5°K. The gain observed is 0.12 per centimeter of travel in the ruby.[3] This is somewhat higher than the attenuation of 0.09 per centimeter and is an indication of the efficiency of inversion.

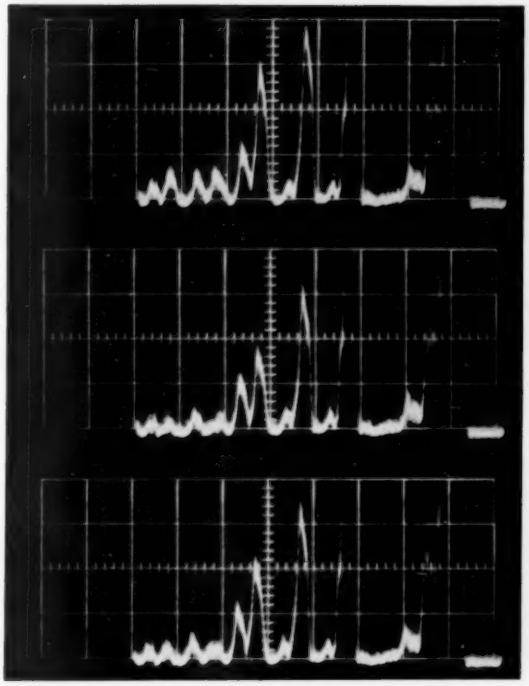

FIG. 1. Echo patterns observed for 9.3-kMc/sec ultrasonic pulse of 0.5-microsecond duration. Large echoes to the right and the left of the center graticule have passed through the ruby once and twice, respectively. Time increases from right to left. Top picture: magnetic field on resonance line and pump on. Center picture: magnetic field on resonance line, no pump. Bottom picture: magnetic field off resonance line.

The slower traces of Fig. 2 illustrate much more graphically the magnitude of the effect. The upper picture shows clearly a number of

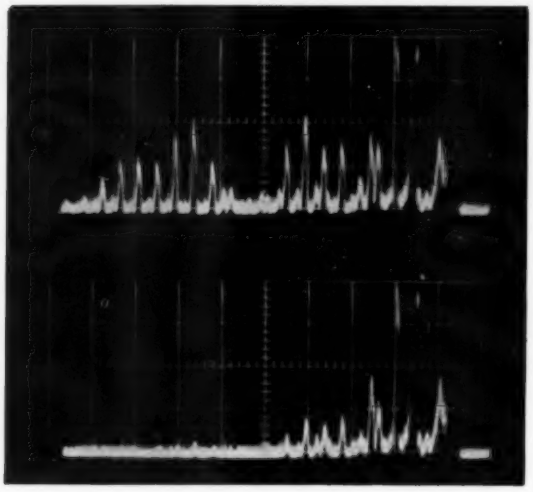

FIG. 2. Echo patterns observed for 9.31-kMc/sec ultrasonic pulse of 0.5-microsecond duration. The change in frequency accounts for the amplitudes of the first few echoes being different from those of Fig. 1. Sweep speed of oscilloscope is about 5 microseconds per centimeter. A round trip through the ruby requires 2.1 microseconds. Time increases from right to left. Top picture: magnetic field on resonance line and pump on. Bottom picture: magnetic field off resonance line.

echoes not visible without the aid of the amplification. From the spacing of these echoes it can be surmised that they are due to pulses which have traveled back and forth in the ruby for as many as eighteen round trips; and that their only traversal of the quartz has been the 3 cm travel to get to the ruby initially and, after the reflections in the ruby, to get back to the transducer end again. Echoes from the bond are almost nonexistent after 10 microseconds. The beating due to phase interference caused by the nonparallel ends and bond as well as crystal inhomogeneities and misalignment is very evident in the top trace of Fig. 2.

The physical perfection required to determine the true propagation characteristics of the quartz-indium-ruby combination is lacking, and hence conclusion of whether or not the gain obtainable from the spin system is sufficient to overcome the system losses is impossible. It is fairly obvious what conditions must be satisfied in order to realize over-all gain, i.e., a phonon maser. Just as in the case of the optical maser[4] the gain from the inverted population must be sufficient to overcome the losses due to attenuation in the materials and reflections at the ends of the cavity, in this case the optically polished ends of the crystals. If one assumes that an attenuation of 0.01 per centimeter (such as is observed in quartz[5]) is attainable in a good ruby crystal, the gain of 0.12 per centimeter is certainly sufficient. For appreciably higher losses either higher spin populations or spin systems with larger magnetoelastic coupling constants, or perhaps both, will be required.

This experimental demonstration of phonon amplification was undertaken after discussions, on the possibility of a phonon maser, with Dr. E. H. Jacobsen and Dr. N. S. Shiren. It is a pleasure to acknowledge their contributions.

---

[1]E. B. Tucker, Phys. Rev. Letters 6, 183 (1961).

[2]C. Kikuchi, J. Lambe, G. Makhov, and R. W. Terhune, J. Appl. Phys. 30, 1061 (1959).

[3]The pictures illustrate amplitudes proportional to voltage whereas the attenuations and gains are referred to power.

[4]A. L. Schawlow and C. H. Townes, Phys. Rev. 112, 1940 (1958).

[5]E. H. Jacobsen (private communication); 0.01 per cm includes end losses for a 3-cm X-cut quartz bar.

QUADRUPOLE MOMENT OF Li^7 AND QUADRUPOLE COUPLING CONSTANT OF Li_2†

S. L. Kahalas and R. K. Nesbet*
Department of Physics, Boston University, Boston, Massachusetts
(Received April 17, 1961)

Recently, the quadrupole coupling constant of Li^7 in LiH has been measured to high accuracy by Klemperer, Gold, and Wharton.[1] When combined with our calculated value of the electric field gradient at the Li^7 nucleus, this measurement leads to a definitive value for the quadrupole moment of Li^7, $Q(Li^7) = -3.56\times10^{-26}$ cm^2. We have also calculated the electric field gradient in Li_2. Using $Q(Li^7)$ calculated from LiH, we find the quadrupole coupling constant for the Li_2 molecule to be +0.049 Mc/sec compared with the value of +0.060 Mc/sec estimated by Logan, Coté, and Kusch.[2] This would indicate that the Logan, Coté, and Kusch value may be too large and that it would be desirable for the quadrupole coupling constant of Li_2 to be remeasured with higher accuracy in order to check the prediction. The remainder of this Letter presents some details of the molecular calculations.

Our electronic computer calculations of the molecular properties of the LiH and Li_2 molecules have been carried out by the Roothaan[3] (Hartree-Fock, self-consistent field, molecular orbital, linear combination of atomic orbitals) procedure as modified by Nesbet.[4,5] Extended sets of basis functions of the Slater type were employed and configuration interaction corrections to the energy and electric field gradient were calculated. For LiH, a basis set of 13 Slater-type orbitals were used, including $p\pi$ functions on both the lithium and hydrogen centers. For Li_2, 18 Slater-type orbitals were used (9 on each center), including $p\pi$ functions. In both cases the $p\pi$ functions were found to give large contributions in configuration interaction. For configuration interaction calculations in LiH, the 27 most important configurations are included in the energy and 19 configurations in the electric field gradient. For configuration interaction calculations in Li_2, the 28 most important configurations are included in the energy and 24 configurations in the electric field gradient. These calculations were carried out at three internuclear distances, including the internuclear distance corresponding to the minimum energy.

The accuracy to which the molecular wave function has been calculated may be indicated from the following results. For LiH, a total molecular energy of 99.3% of the experimental value, and a dissociation energy of 89.3% of the experimental value were calculated. Similar calculations in Li_2 resulted in 99.4% and 89.9%, respectively, for these two quantities. The energy of atomic Li, which enters the dissociation energy calculation, was calculated to comparable accuracy (99.4%).

Recently Klemperer, Gold, and Wharton have measured the quadrupole coupling constant of Li^7 in the LiH molecule[1]; the value $eqQ/h = +346\pm2$ kc/sec is found. Our calculated value for the electric field gradient at the Li nucleus is $q/2e = -0.02070\ a_H^{-3}$, evaluated at the internuclear distance corresponding to the minimum of the energy. e is the magnitude of the electron charge and a_H is the first Bohr radius. This leads to a value of -3.56×10^{-26} cm^2 for $Q(Li^7)$, in agreement with predictions from theoretical models of the nucleus.[6] This value is estimated to have an error associated with it of less than 10%. As distinct from the Li_2 case,[7] the electronic and nuclear contributions to the electric field gradient are not nearly equal, the latter being about 0.65 of the former.

For Li_2, $q/2e$ is calculated to be $-0.0029\ a_H^{-3}$. Together with $Q(Li^7)$ found above, this leads to a quadrupole coupling constant of +0.049 Mc/sec. The experimental value of Logan, Coté, and Kusch,[2] which is +0.060 Mc/sec, would thus appear to be too large.

A complete account of the molecular calculations will be presented later.

We wish to thank Professor W. Klemperer for permission to quote the LiH quadrupole coupling constant result prior to its publication. One of us (S.L.K.) gratefully acknowledges several helpful discussions with Dr. R. E. Watson. We wish to thank Professor N. F. Ramsey for a discussion concerning some measurements made in his laboratory. Professor P. Kusch is to be thanked for his correspondence concerning the Li_2 quadrupole coupling constant.

†Work partially supported by the National Science Foundation, the Computation Center of the Massachusetts Institute of Technology, and RIAS and the Martin Company at Baltimore, Maryland.

*On leave of absence from Boston University. Currently at Centre de Méchanique Ondulatoire Appliquée, Paris, France.

[1]W. Klemperer, L. P. Gold, and L. Wharton (private communication, 1961).

[2]R. A. Logan, R. E. Coté, and P. Kusch, Phys. Rev. 86, 280 (1952).

[3]C. J. J. Roothaan, Revs. Modern Phys. 23, 69 (1951).

[4]R. K. Nesbet, Quarterly Progress Report, Solid State and Molecular Theory Group, Massachusetts Institute of Technology, October 15, 1955 (unpublished), pp. 4-8.

[5]R. K. Nesbet, Revs. Modern Phys. 32, 272 (1960).

[6]See, for example, S. B. Welles, Phys. Rev. 62, 197 (1942).

[7]R. M. Sternheimer and H. M. Foley, Phys. Rev. 92, 1460 (1953).

INELASTIC SCATTERING OF 18.9-Mev NUCLEONS FROM THE 9.6-Mev STATE OF C^{12}

E. Bradford and B. A. Robson

Research School of Physical Sciences, The Australian National University, Canberra, Australia

(Received April 17, 1961)

Recently it has been suggested[1] that the 9.6-Mev state of C^{12} has spin and parity $J^{\pi}=3^-$ and not 1^- as previously supposed.[2] This Letter reports a new analysis of Peelle's[3] 18.9-Mev inelastic proton scattering data, which definitely favors 3^- for the 9.6-Mev state. The calculation uses a direct volume interaction with spin-dependent distorted waves.[4]

Peelle's[3] analysis of his data is based upon the direct surface interaction theory, which predicts a $j_K^2(kR)$ angular distribution. Using an interaction radius $R=3.3$ fermis, he found a best fit for $K=1$ giving $J^{\pi}=0^-$, 1^-, or 2^-. The same theory applied to inelastic scattering from the 4.4-Mev 2^+ state of C^{12} gave very poor agreement with experiment.

Levinson and Banerjee[5] showed that the direct-surface-interaction theory is probably inadequate for a nucleus as small as C, and Robson and Robson[4] found spin-orbit effects to be important for 12-Mev nucleons inelastically scattered from the 4.4-Mev level of C^{12}. Thus it was considered essential to take both these effects into account before using Peelle's data to determine the spin and parity of the 9.6-Mev state. In the following, only $J^{\pi}=1^-$ or 3^- are considered because there exists a reasonable amount of evidence[1] for eliminating other values.

The distorting potential is taken to be the usual Woods-Saxon optical potential plus a Thomas-Fermi spin-orbit potential,[6]

$$V_D(r) = -(V+iW)f(r) + (V_S+iW_S)\left(\frac{\hbar}{m_\pi c}\right)^2 \frac{1}{r}\frac{df}{dr}\vec{\sigma}\cdot\vec{L},$$

$$f(r) = \{1+\exp[(r-R)/a]\}^{-1}. \qquad (1)$$

The values of V, W, V_S, and W_S used are 45, 12,

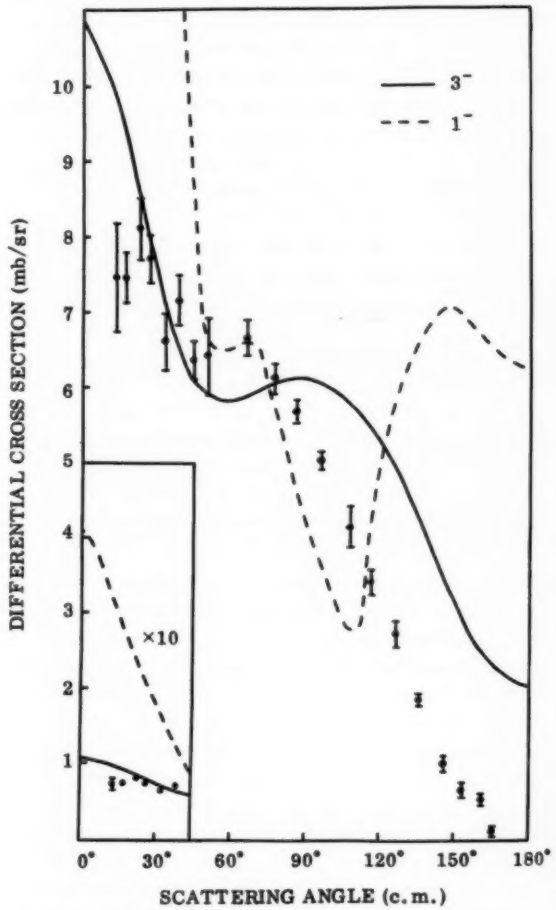

FIG. 1. Inelastic nucleon scattering from the 9.6-Mev state of C^{12}. The points are the experimental results of Peelle for 18.9-Mev protons. The theoretical curves are for 18.9-Mev neutrons. The normalization is arbitrary and both curves are fitted at 75°.

15, and -4 Mev for the incident energy of 18.9 Mev and 45, 8, 17, and -4 Mev for the emergent energy of 9.3 Mev, with $a = 0.4$ fermi and $R = 2.75$ fermis in both cases.

The direct-interaction two-body potential is assumed to be zero ranged and spin independent, and all forms of exchange are neglected.

Following Barker et al.,[1] the C^{12} ground state is taken as

$$\psi_0 = \psi(1s^4\,1p^8[4,4]000,0), \tag{2}$$

where the numbers following the configuration are values of $[\lambda]TSL, J$. The 9.6-Mev state is taken as

$$\psi_3 = \psi((1s^4\,1p^7[4,3]\tfrac{1}{2}\tfrac{1}{2}1, 1d)003, 3) \tag{3}$$

for $J^\pi = 3^-$, and

$$\psi_1 = \sum_{i=1}^{3} \alpha_i \psi_{1i} \tag{4}$$

for $J^\pi = 1^-$, where

$$\psi_{11} = \psi((1s^4\,1p^7[4,3]\tfrac{1}{2}\tfrac{1}{2}1, 2s)001, 1), \tag{4a}$$

$$\psi_{12} = \psi((1s^4\,1p^7[4,3]\tfrac{1}{2}\tfrac{1}{2}1, 1d)001, 1), \tag{4b}$$

$$\psi_{13} = \psi((1s^3[3]\tfrac{1}{2}\tfrac{1}{2}0, 1p^9[441]\tfrac{1}{2}\tfrac{1}{2}1)001, 1). \tag{4c}$$

For the Elliott and Flowers interaction, Barker et al.[1] found $\alpha_1 = 0.916$, $\alpha_2 = -0.399$, and $\alpha_3 = -0.028$. For simplicity, the values used in the present calculation are $\alpha_1 = 0.869$, $\alpha_2 = -0.494$, and $\alpha_3 = 0$. The $1p$, $1d$, and $2s$ wave functions are taken for an ideal harmonic oscillator with length parameter $b = 2.0$ fermis, obtained by fitting the $1p$ harmonic-oscillator wave function to the $1p$ square-well solution of the Schrödinger equation for a radius $R = 3.66$ fermis, which gives a reasonable fit to the 4.4-Mev data.[4]

Figure 1 shows the result of the calculation. It is seen that the theoretical curve for the 3^- assumption is a much better fit than for the 1^- assumption (both curves are normalized at 75°). Greater emphasis should perhaps be placed on fitting the scattering for angles $\theta < 90°$, since other processes like heavy-particle stripping[7] may become important for $\theta > 90°$. On account of the very lengthy calculations involved, no attempt was made to vary the parameters, which were selected by a consideration of the elastic scattering and inelastic scattering from the 4.4-Mev state data.[4,8]

---

[1]F. C. Barker, E. Bradford, and L. J. Tassie, Nuclear Phys. 19, 101 (1960).

[2]F. Ajzenberg-Selove and T. Lauritsen, Nuclear Phys. 11, 1 (1959).

[3]R. W. Peelle, Phys. Rev. 105, 1311 (1957).

[4]B. A. Robson and D. Robson, Proc. Phys. Soc. (London) 76, 611 (1960).

[5]C. A. Levinson and M. K. Banerjee, Ann. Phys. 3, 67 (1958).

[6]The Riesenfeld-Watson notation is used here. W. B. Riesenfeld and K. M. Watson, Phys. Rev. 102, 1157 (1956).

[7]G. E. Owen and L. Madansky, Phys. Rev. 99, 1608 (1955).

[8]J. S. Nodvik and D. S. Saxon, Phys. Rev. 117, 1539 (1960).

DECAY PROPERTIES OF K_2^0 MESONS*

D. Neagu, E. O. Okonov, N. I. Petrov, A. M. Rosanova, and V. A. Rusakov
Joint Institute of Nuclear Research, Moscow, U.S.S.R.
(Received April 20, 1961)

In this note we present preliminary data obtained by exposing the magnet cloud chamber to the beam of K_2^0 particles from the internal target of the Joint Institute for Nuclear Research synchrophasotron. Neutral particles emitted from the target at an angle of 97° to the direction of the circulating proton beam are used in the experiment. The cloud chamber is placed at a distance of 8 m from the target.

We have recorded so far more than 500 V^0 events interpreted as decays of K_2^0 mesons. Based on the selective analysis of experimental data, an estimation was made of the relative probability of a K_{e3} decay and quantitative data on the charge ratio in three-body decays were obtained. Only 225 V^0 events are measured completely. There is not a single 2π decay among them. We have found one four-prong event and four electron-positron pairs (with comparatively large opening angles) emitted at a large angle to the direction of K_2^0 flight.

(1) The passage of the charged decay products through a lead plate 5.8 g/cm^2 thick located in the operating volume of the chamber was studied in order to estimate the relative probability of K_{e3} decay. Out of 112 events we have found 24 events in which a particle either stops in the plate or undergoes a momentum loss of more than 30%. Making use of the Bethe-Heitler equation[1] (improved by Eyges[2]) which provides the probability of the given energy loss by an electron for radiation in traversing the definite lead thickness, we have found that the fraction of K_{e3}^0 decay with respect to all the decays with charged products constitutes 38%.[3] Taking into consideration the corrections for K_2^0-particle motion which leads to a relative increase in the number of pions and μ mesons traversing the plate, we determined the fraction of K_{e3}^0 to be equal to 42 $\pm$ 12%.

If one considers that the relative probability of $3\pi^0$ decay of K^0 mesons is not more than 20% for K_2^0 mesons,[4] then the probability of K_{e3} decay for these particles turns out to be equal to the twofold probability of K_{e3} decay for positive K mesons[5] within experimental error. Such a ratio between the two probabilities should occur if the isotopic spin selection rule[6] $\Delta T = \frac{1}{2}$ is valid. Therefore, the experimental data obtained point out, within statistical deviations, the extension of the above-stated selection rule to the decay processes involving leptons.

(2) Quantitative data on the charge ratio (i.e., the ratio of the number of decay events with the emission of π^- mesons to the number of events accompanied by the emission of π^+ mesons) are obtained both by identifying the charged decay products having momentum not larger than 120 Mev/c and by studying the passage of decay particles through the lead plate. In measuring the ionization, the electrons can be reliably selected when the momentum of decay particles does not exceed 100 Mev/c. When the momentum is between 100 and 120 Mev/c, it is only possible to determine whether a particle under study is a π meson or not.

The number of decays obtained which were accompanied by the emission of π^- mesons and π^+ mesons is equal to 46 and 51, respectively. They provide the value 0.90 ± 0.18 for the charge ratio. Within experimental errors this ratio does not differ from unity and is in disagreement with the analogous ratio 0.42 ± 0.27, estimated from the data of Bardon et al.[7]

Neither the authors of the quoted paper nor we have found any event of K_2^0-meson decay into two charged π mesons.

Combining our data with those obtained in reference 7, we set an upper limit of 0.3% for the relative probability of the decay $K_2^0 \to \pi^- + \pi^+$. Our results on the charge ratio and the degree of the 2π-decay forbiddenness are in agreement with each other and provide no indications that time-reversal invariance fails in K^0 decay.

(3) Up to now only three V^0 events[7-9] which might be interpreted as the decay of K_2^0 mesons according to the mode $K_2^0 \to \pi^- + \pi^+ + \pi^0$ have been recorded. We have found one four-prong event[10] which can be considered as the decay of a long-lived K^0 meson into two charged and one neutral π meson. In view of the presence of the Dalitz pair, in our experiment the nature of the neutral product of the decay is determined more directly than in the case of two-prong events; the observed four-prong decay is a direct proof for the existence of K_2^0-meson decay according to

Table I. Characteristics of observed electron-positron pairs.

	Momentum (Mev/c) (+)	(-)	Opening angle
1	55	42	7°– 9°
2	10	43	99°
3	111	103	18°–20°
4	26	79	25°

the above-mentioned mode.

(4) Among all the recorded V^0 events there were found 4 electron-positron pairs with comparatively large opening angles; the directions of three of these pairs make angles greater than 40° with that of the K_2^0-meson beam. The characteristics of these pairs are summarized in Table I.

There is not a single star with an electron-positron pair from the stars found in cloud-chamber gas. On the other hand, the probability of large opening angles for electron-positron pairs arising in the external conversion of γ rays is very small. These are the reasons to consider the pairs obtained to be Dalitz pairs resulting from K_2^0-meson decay into neutral π^0 mesons. Therefore, the fact of their observation can be treated as experimental evidence for the existence of the long-lived K^0-meson decay into three π^0 mesons. The observed quantitative ratio (1:4) of four-prong decay and single Dalitz pairs can also be considered as a support of this treatment.

The authors are grateful to Professor B. M. Pontecorvo for his constant interest in the work and for the discussion of the results. They would also like to thank Professor V. I. Veksler and Professor V. P. Dzhelepov for their interest in the experiment and their support.

---

*We feel it necessary to publish our communication exactly as it was submitted to the Rochester Conference, since in the Proceedings it appeared to be considerably distorted. See D. Neagu et al., Proceedings of the 1960 Annual International Conference on High-Energy Physics at Rochester (Interscience Publishers, Inc., New York, 1960), p. 603.

[1]H. A. Bethe and W. Heitler, Proc. Roy. Soc. (London) A146, 83 (1934).

[2]L. Eyges, Phys. Rev. 76, 264 (1949).

[3]Here the correction for π-meson nuclear absorption is already taken into account.

[4]L. M. Lederman, 1958 Annual International Conference on High-Energy Physics at CERN (CERN Scientific Information Service, Geneva, 1958), Vol. 5, p. 275.

[5]This can be easily shown if one compares the known mean lifetimes for K^+ and K_2^0 mesons [$\tau(K_2^0) = (6.1^{+1.6}_{-1.1}) \times 10^{-8}$ sec; F. S. Crawford, Jr., M. Cresti, R. L. Douglass, M. L. Good, G. R. Kalbfleisch, and M. L. Stevenson, Phys. Rev. Letters 2, 361 (1959)] with the relative probabilities of K_{e3} decays for the same particles.

[6]L. Okun', J. Exptl. Theoret. Phys. (U.S.S.R.) 34, 469 (1958) [translation: Soviet Phys.–JETP 34(7), 322 (1958)]; S. Okubo, R. E. Marshak, E. C. G. Sudarshan, W. B. Teutsch, and S. Weinberg, Phys. Rev. 112, 665 (1958).

[7]M. Bardon, K. Lande, L. M. Lederman, and W. Chinowsky, Ann. Phys. 5, 156 (1958).

[8]W. A. Cooper, H. Filthuth, J. A. Newth, O. Petrucci, R. A. Salmeron, and A. Zichichi, Nuovo cimento 6, 1433 (1956); 8, 471 (1958).

[9]M. L. Good, G. R. Kalbfleish, M. C. Stevenson, and K. Tiche, Phys. Rev. Letters 2, 266 (1959).

[10]E. Okonov, N. Petrov, A. Rosanova, and V. Rusakov, J. Exptl. Theoret. Phys. (U.S.S.R.) 39, 67 (1960) [translation: Soviet Phys.–JETP 12, 48 (1961)].

ELASTIC SCATTERING OF MUONS IN NUCLEAR EMULSION*

P. L. Connolly,† J. G. McEwen, and J. Orear
Laboratory of Nuclear Studies, Cornell University, Ithaca, New York
(Received April 24, 1961)

In the past 10 years several experiments have been performed to measure the nuclear scattering of cosmic-ray muons.[1] Many of these experiments are claimed to show, in addition to the Coulomb interaction, an anomalous muon-nuclear interaction. These cosmic-ray experiments suffer from several difficulties: (1) They measure inelastic as well as elastic scatterings; (2) the pion background is uncertain and difficult to correct for; (3) the incoming muon energy is not known; and (4) the use of thick scattering plates requires serious corrections for multiple scattering (also for successive single scatterings combined with multiple scattering). At high momentum transfer these scattering corrections require knowledge of the elastic and especially the inelastic cross sections. Such theoretical knowledge is yet only approximate.[2] Masek, Heggie, Kim, and Williams[3] have recently performed an experiment which overcomes most of the above difficulties. They measured a mixture of elastic and inelastic scattering of 2-Bev μ^- on carbon using a Bevatron separated muon beam; most of their scatterings with high momentum transfer should be inelastic, and their results are in agreement with the inelastic cross section estimates of Drell and Schwartz.[4]

Our experiment, on the other hand, measures only elastic scatterings as do the electron scattering experiments of Hofstadter.[5] The corresponding calculations can be done precisely so that detailed information on the charge distribution of the nucleus can be obtained from the elastic scattering measurements. A departure of the muon elastic scattering from these precise calculations would reveal a nonelectromagnetic muon-nuclear interaction, or a difference between the mean radii of the muon and electron charge distributions.

In this Letter we report the final results of our μ^+ scattering experiment and preliminary results of our μ^- scattering experiments. The μ^+ stack was exposed to 3.5×10^6 muons in the 43-Mev separated muon beam of the Carnegie Tech synchrocyclotron and the μ^- stack was exposed to 2.5×10^7 muons in the 60-Mev separated muon beam of the CERN synchrocyclotron. In the μ^+ experiment the small pion background is eliminated by observation of the π-μ decay. In the μ^- experiment the ratio of muon endings to pion endings is greater than 1000 to 1. Negative pions are also eliminated by observation of prongs at either the scattering or the ending. We have observed no inelastic scatterings. Most inelastic scatterings in our energy region would be expected to excite the giant resonance and thus show up as a large increase in grain density at the scattering.[6] Other inelastic scatterings could be distinguished by proton or conversion-electron prongs at the scattering.

Large effective path lengths are achieved by area scanning for muon endings in the region where muons are not supposed to end and tracing these endings back to a possible large-angle scattering. Since the geometry of the stack is known precisely, it is possible to make numerical calculations of the effective muon path scanned.

In our μ^+ experiment we have restricted our data to 14- to 40-Mev muons scattering at angles between 80° and 180°. Our energy and angle limits correspond to momentum transfers of 80 to 160 Mev/c. Figure 1 shows the number of events observed having a momentum transfer greater than the value q. The curve is the number of events predicted from the elastic scattering calculations of Rawitscher,[7] who used the nuclear charge distributions obtained by Hofstadter.[5] Figure 2 shows our experimental cross sections plotted against momentum transfer q, together with Rawitscher's calculated cross sections for 27-Mev μ^+ scattering elastically on Ag ($Z=47$) and Br ($Z=35$) averaged together. Rawitscher's cross sections when plotted against q are virtually independent of muon energy in the energy region studied. The statistical standard deviations are shown in Figs. 1 and 2, and it appears that the data are consistent with Rawitscher's calculations. The predicted number of events depends both on our geometry calculation and interpolations of Rawitscher's cross sections. We estimate an over-all accuracy of ±10% for our calculation of the predicted number of events. This possible systematic error is not shown in Figs. 1 or 2.

Early scanning on our μ^- experiment has yielded 10 events so far with $q>100$ Mev/c and this also appears to be consistent with Rawitscher's calculations.

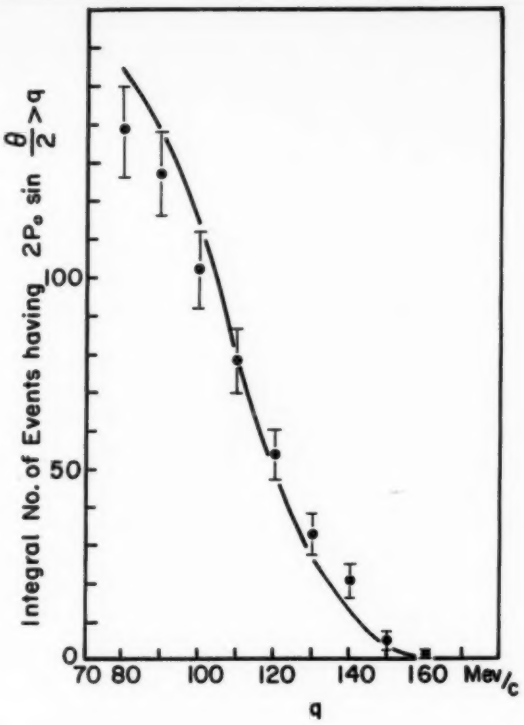

FIG. 1. The number of events having a momentum transfer greater than q is plotted vs q. The curve is the predicted number of events based on the elastic scattering cross sections calculated by Rawitscher.

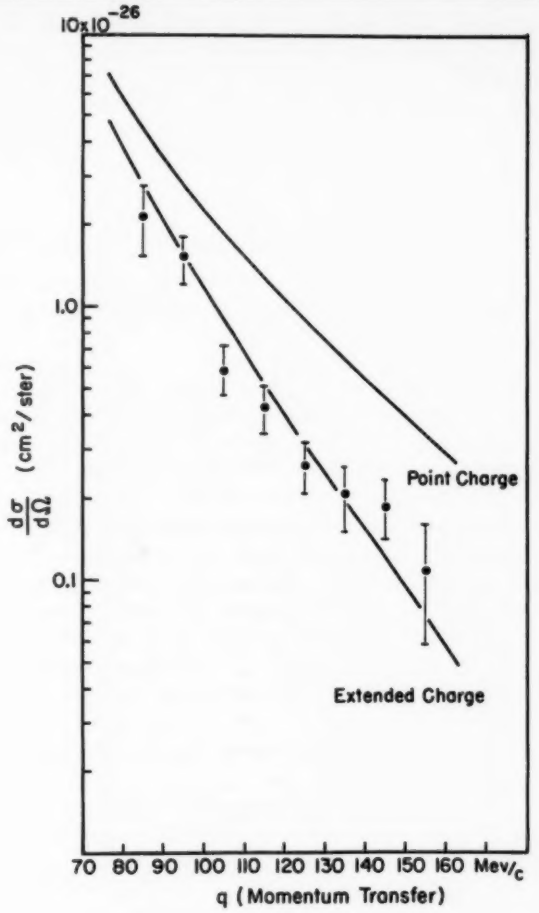

FIG. 2. One-half the sum of the differential cross sections for the elastic scattering of 27-Mev μ^+ on Ag and Br plotted against the momentum transfer q. The experimental points are based on a total of 138 observed scatters in nuclear emulsion. The curves for extended and point charge distribution are those calculated by Rawitscher.

We conclude that our positive muons behave as heavy positrons in the same momentum transfer region as was studied by the cosmic-ray experiments. We have no indication of an anomalous muon-nuclear interaction. If we make allowance for a possible finite size of the muon by multiplying Rawitscher's cross sections by $f^2(q)$, where $f(q) = (1 + \frac{1}{6}\langle R_\mu{}^2\rangle_{av} q^2)^{-1}$ is the form factor due to the muon charge distribution,[8] we find that our data determine an upper limit of 1.7×10^{-13} cm for the rms muon radius $(\langle R_\mu{}^2\rangle_{av})^{1/2}$.

We wish to thank Professor R. Siegel and Professor R. Sutton of Carnegie Tech and Dr. A. Citron and Dr. D. Michaelis of CERN for their generous help with the exposures. Professor G. Rawitscher of Yale University has kindly performed and forwarded to us additional calculations more appropriate to our experiment than those which appeared in his original paper.[7]

*Research supported by a National Science Foundation research grant.

†Now at Brookhaven National Laboratory, Upton, New York.

[1]For the most recent cosmic-ray experiments see R. L. Sen Gupta, S. Ghosh, A. Acharya, M. M. Biswas, and K. K. Roy, Nuovo cimento 19, 245 (1961). For a summary of the experiments up to 1958, see G. N. Fowler and A. W. Wolfendale, Progress in Elementary Particle and Cosmic-Ray Physics (North-Holland Publishing Company, Amsterdam, 1958), Vol. 4, p. 123.

[2]L. N. Cooper and J. Rainwater, Phys. Rev. 97, 492 (1935).

[3]G. E. Masek, L. D. Heggie, Y. B. Kim, and R. W.

Williams, Phys. Rev. 122, 937 (1961).
[4]S. D. Drell and C. L. Schwartz, Phys. Rev. 112, 568 (1958).
[5]R. Hofstadter, Ann. Rev. Nuclear Sci. 7, 231 (1957).
[6]Hans Bethe (private communication).
[7]G. H. Rawitscher, Phys. Rev. 112, 1274 (1958); also Bull. Am. Phys. Soc. 6, 301 (1961).
[8]S. D. Drell, Ann. Phys. 4, 75 (1958).

PROPOSED METHOD OF MEASURING THE SPIN OF THE K' MESON

M. Schwartz*
Columbia University, New York, New York and Brookhaven National Laboratory, Upton, New York
(Received April 27, 1961)

The recent discovery[1] of the K' meson with a mass of about 880 Mev has led to considerable speculation about its role in strange particle reactions. A knowledge of its spin is hence of obvious importance. It has already been verified that the K' has isotopic spin 1/2 and decays via the modes $K' \to K+\pi$. At the moment, one possibility for determining whether its spin is 0 or 1 is by observing the occurrence (or nonoccurrence) of the decay mode $K' \to K+\gamma$. It is the purpose of this note to point out another method of measuring the spin of the K', which, although no better than the above, is rather unique and perhaps somewhat elegant.

The reaction we shall consider is $\bar{p}+p \to K^0+\bar{K}^{0\prime}$ or $K^{0\prime}+\bar{K}^0$, where the antiproton capture takes place at rest. Only one assumption will be made here—namely that the capture proceeds from an S state. The justification for this assumption rests on the recent arguments of Day, Snow, and Sucher.[2] At any rate, there is an inherent check of this assumption in the experiment as will be seen below.

Subject to the above assumption, the initial state can be either the triplet or the singlet state. The triplet state is odd under charge conjugation and the singlet state is even. The parity of the initial system is odd.

The reaction $\bar{p}+p \to K^0+\bar{K}^0$. It is well known that if the above conditions are satisfied, then the outgoing $K^0\bar{K}^0$ system must be odd under charge conjugation. If this is so, the outgoing wave function will have the factor $K_{1a}{}^0K_{2b}{}^0 - K_{2a}{}^0K_{1b}{}^0$. Hence one K^0 will always decay via the $K_1{}^0$ mode and the other will decay via the $K_2{}^0$ mode. The observation of this effect serves then as a check on the assumption of S-state capture.

The reaction $\bar{p}+p \to K^0+\bar{K}^{0\prime}$ or $K^{0\prime}+\bar{K}^0$, in the event that the $K^{0\prime}$ has spin zero. In this case, the outgoing state must be an S state (since the relative parity of the K and K' is odd). Hence the initial state must be the singlet S state. Therefore it is even under charge conjugation. Hence the final state must be of the form $K^0\bar{K}^{0\prime} + K^{0\prime}\bar{K}^0$. The $K^{0\prime}$ (or $\bar{K}^{0\prime}$) decays via the mode

$$K^{0\prime} \to (\tfrac{1}{3})^{1/2}K^0\pi^0 - (\tfrac{2}{3})^{1/2}K^+\pi^-,$$
$$(\bar{K}^{0\prime} \to (\tfrac{1}{3})^{1/2}\bar{K}^0\pi^0 - (\tfrac{2}{3})^{1/2}K^-\pi^+).$$

If we now adopt the notation that subscript a refers to the primary K^0 or $\bar{K}^0$ and b refers to the other, we can rewrite our outgoing state as

$$\psi = \psi_1 + \psi_2 = (\tfrac{1}{3})^{1/2}\left\{\frac{K_a{}^0\bar{K}_b{}^0\pi^0 + \bar{K}_a{}^0K_b{}^0\pi^0}{\sqrt{2}}\right\} - (\tfrac{2}{3})^{1/2}\left\{\frac{K_a{}^0K_b{}^-\pi^+ + \bar{K}_a{}^0K^+\pi^-}{\sqrt{2}}\right\}.$$

We shall deal now only with the first part of this state. Let us substitute

$$K^0 = (K_1{}^0+K_2{}^0)/\sqrt{2}, \quad \bar{K}^0 = (K_1{}^0-K_2{}^0)/\sqrt{2}.$$

We then have

$$\psi_1 = (K_{1a}{}^0K_{1b}{}^0 - K_{2a}{}^0K_{2b}{}^0)/\sqrt{2}.$$

Hence we will observe either a two-$K_1{}^0$ type of decay or a two-$K_2{}^0$ type of decay, but no events in which we have both a $K_1{}^0$ and a $K_2{}^0$.

The reaction $\bar{p}+p \to K^0+\bar{K}^{0\prime}$ or $K^{0\prime}+\bar{K}^0$, in the event that the spin of the K' is 1. In this case the outgoing state must be a p state. Hence we can have either $J=0$ or $J=1$. $J=2$ is forbidden

since there is no $J=2$ initial state. The $J=0$ part is even under charge conjugation and the $J=1$ part is odd. Hence we have

$$\psi_1 = A_0\left(\frac{K_{1a}{}^0K_{1b}{}^0 - K_{2a}{}^0K_{2b}{}^0}{\sqrt{2}}\right) + A_1\left(\frac{K_{1a}{}^0K_{2b}{}^0 - K_{2a}{}^0K_{1b}{}^0}{\sqrt{2}}\right),$$

where A_0 refers to the $J=0$ part and A_1 refers to the $J=1$ part.

Turning to the problem of determining the spin of the K', let us first select that group of $\bar{p}$ stoppings which show a $K_1{}^0$ decay with a momentum such that the other outgoing particle is a K' (or $\bar{K}'$) meson. This can be done above background to the extent that the K' mass is well defined. Then we can deduce the following points:

1. If the spin of the K' is zero, then another $K_1{}^0$ decay must also occur.

2. If the spin of the K' is 1, then the other K^0 can decay via the $K_2{}^0$ mode some of the time, unless A_1 happens to be zero.

3. In addition, we can unambiguously determine the spin by considering those cases where both decays are observed to be of the $K_1{}^0$ type. Let us consider the z axis along the direction in which the K' was moving before decay. Events of the above sort must have $J=0$ regardless of the spin of the K'. The orbital angular momentum of the $K\bar{K}'$ (or $K'\bar{K}$) system must have z component equal to zero. Hence the K' must have its spin in the $m=0$ state. If we now consider its decay into π^0+K^0 in its own center-of-mass system, the outgoing particles will have the following distributions about the z direction:

(a) If spin $K'=0$, the distribution is obviously isotropic.

(b) If spin $K'=1$, the distribution must have the form $\cos^2\theta$, where θ is the polar angle between π^0 and K'.

In the event that there is a nonresonant $K_1{}^0K_1{}^0\pi^0$ background, as there most certainly will be, then the distribution which one will obtain as a result of the above procedure will have the form $|\sum\alpha_i P_i{}^0(\cos\theta)|^2$. In principle, one can then determine the coefficients α_i from the distribution and observe whether α_0 or α_1 varies significantly in passing through the resonance. If α_0 varies, then the spin of the K' is zero. If α_1 varies, the spin is 1.

The author would like to express his gratitude for valuable discussions with Dr. M. Nauenberg, Dr. G. Feinberg, and Dr. J. Steinberger.

*Alfred P. Sloan Research Fellow.

[1]M. Alston et al., Phys. Rev. Letters 6, 300 (1961).

[2]T. B. Day, G. A. Snow, and J. Sucher, Phys. Rev. Letters 3, 61 (1959).

PION-LAMBDA RESONANCE $(Y_1{}^*)^*$

J. P. Berge, P. Bastien, O. Dahl, M. Ferro-Luzzi,† J. Kirz, D. H. Miller, J. J. Murray, A. H. Rosenfeld, R. D. Tripp, and M. B. Watson

Lawrence Radiation Laboratory and Department of Physics, University of California, Berkeley, California

(Received April 27, 1961)

Alston et al.[1] have discovered an $I=1$ π-Λ resonance with a mass of 1380 Mev and a half-width $\Gamma/2$ consistent with 32 Mev. They reported on 141 $\Lambda\pi^+\pi^-$ events made by 1150-Mev/c K^- mesons incident on the 15-in. Lawrence Radiation Laboratory hydrogen bubble chamber which produced the sequence

$$K^- + p \rightarrow Y_1{}^{*\pm} + \pi^{\mp}, \qquad (1)$$

followed by a strong decay,

$$Y_1{}^{*\pm} \rightarrow \Lambda + \pi^{\pm} + 130 \text{ Mev}. \qquad (2)$$

In the course of a continuing study of K^-p interactions, we have now explored the same reactions from $Y_1{}^*$ threshold [P_K(lab) = 405 Mev/c] through $P_K = 850$ Mev/c. We report on ~500 $\Lambda\pi^+\pi^-$ and find $m(Y_1{}^*) = 1385$ Mev and $\Gamma/2$ closer to 20 Mev;

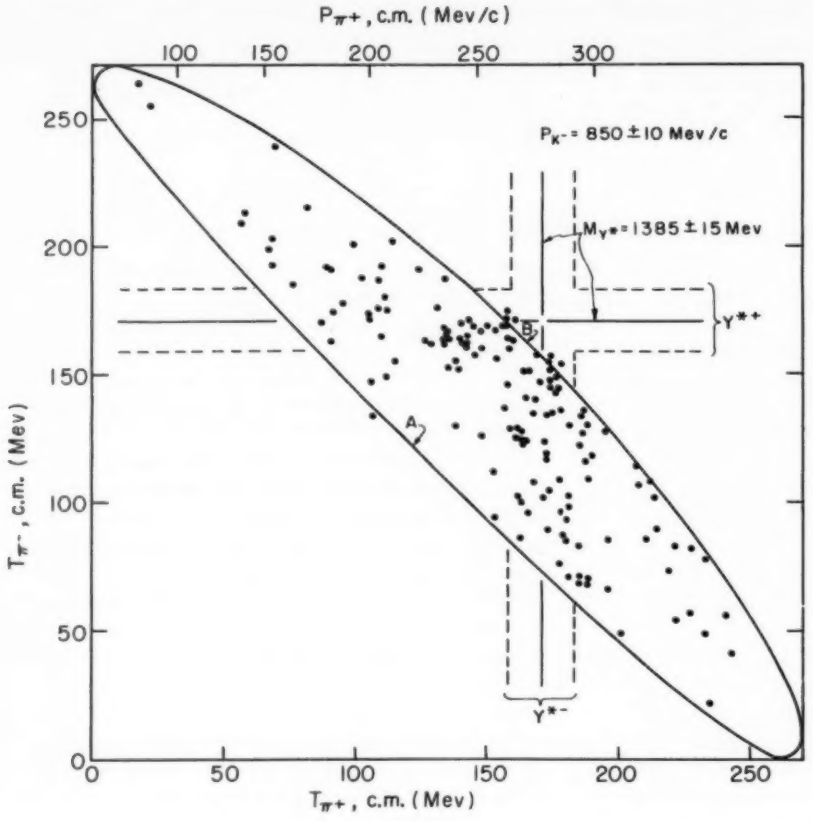

FIG. 1. Dalitz plot of $K^- + p \rightarrow \Lambda + \pi^+ + \pi^-$ for 185 events at P_K(lab) = 850 Mev/c. Note that within the Y_1^{*-} band, for example (i.e., for constant T_{π^+}), T_{π^-} is linear in $(\vec{\Lambda}\cdot\vec{Y}^{*-})$, where $\vec{\Lambda}$ is the unit vector along the Λ momentum in the Y^* rest frame ($\vec{\pi}^- = -\vec{\Lambda}$). Thus Λ's which are produced forward by the strong decay of the Y^{*-} ($Y^{*-} \rightarrow \pi^- + \Lambda$) fall at the lower edge of the ellipse, and vice versa. Point A corresponds to maximum, and point B to zero, Λ kinetic energy.

however, we are still unable to distinguish between spins $J = 1/2$ and $J = 3/2$.

It is conventional to discuss Y^* data in terms of a simplified model in which they are produced and decay "isolated," that is, one neglects the interferences: (a) between Y_1^*'s and background $\Lambda\pi^+\pi^-$ produced in nonresonant partial waves, as well as (b) the influence of Bose statistics and final-state interactions on the $\pi\pi$ system.

Isolated Y_1^*'s will be produced in association with a pion of fixed center-of-mass (c.m.) kinetic energy (spread, of course, by $\pm\Gamma/2$). Thus in Fig. 1, which is Dalitz' representation of the $\Lambda\pi^+\pi^-$ data at P_K(lab) = 850 Mev/c, Y_1^{*+} will fall in a horizontal band and Y_1^{*-} in a vertical band. That this model is poor is shown by the fact that conservation of parity requires that our isolated Y_1^* show no fore-aft asymmetry on strong decay, i.e., in the strong-decay distribution in the Y^* c.m. frame,

$$dn/d\Omega = 1 + a_1(\vec{\Lambda}\cdot\vec{Y}_1^*) + a_2(\vec{\Lambda}\cdot\vec{Y}_1^*)^2 + \cdots, \qquad (3)$$

the odd coefficients must be zero. However, our data show a concentration of backwards Λ. The asymmetry coefficients a_1 (assuming $a_2 = 0$) in Table I show that the "isolated" model is far from realistic, both for our new data and the older events at 1150 Mev/c.[1] A major purpose of this Letter is to point out this difficulty.

In the following Letter,[2] Dalitz and Miller treat the reaction as a symmetrized three-body state which permits nonzero a_1. However, some of the features of the isolated model are still discernible, for example the extra population of the Y_1^* bands on the Dalitz plots. Therefore, in order

Table I. Coefficient a_1 (%) in Y_1^* strong-decay angular distribution.

P_K(lab) (Mev/c)	Y_1^{*+}	Y_1^{*-}
760	−24 ± 20	−16 ± 20
850	−92 ± 26	−24 ± 24
1150	−70 ± 26	− 2 ± 20

to simplify the discussion, in our Letter we still refer to this "isolated" model.

The data to which the model may be most meaningfully applied are those at $P_K = 850$ Mev/c, where the Y_1^* bands do not overlap badly (see Fig. 1). (They cross in the middle of the Dalitz plot at about 700 Mev/c.) Figure 2 is an experimental histogram of the Y_1^* mass. The individual uncertainty in each mass measurements is typically ±(3 to 5) Mev. If we fit the histogram with an s-wave resonance curve of the form $dn/dm \propto [(m - 1385)^2 + (\Gamma/2)^2]^{-1}$ as indicated in Fig. 2, we find $\Gamma/2 = 15$ to 20 Mev (depending upon whether or not some background is subtracted). This experimental value is an agreement with the "$\bar{K}N$ bound state" prediction of $\Gamma/2 = 18$ Mev,[3] but it is also not too far from global symmetry's $\Gamma/2 = 25$ Mev (see below).

Figure 3 displays the excitation data for Y_1^{*+} and Y_1^{*-} and total $\Lambda\pi^+\pi^-$. Data at 1150 Mev/c are from Alston et al.[1] and at 300 and 400 Mev/c are combined from the present experiment and from Nordin.[4] The Y_1^* cross sections at 850 Mev/c can be obtained fairly unambiguously in the sense that the $\Lambda\pi^+\pi^-$ events of Fig. 1 can be interpreted as a flat background plus an extra population of Y_1^*'s at the bands. A background subtraction is also possible at 760 Mev/c. However, at 620 Mev/c, the bands cover almost the whole ellipse, making it impossible to distinguish Y_1^* events from background. At 510 Mev/c, the bands no longer cover the middle of the ellipse, and we might expect any appreciable Y_1^* population to show up in the bands above background. In the Dalitz plot of the data for $P_K = 510$ Mev/c, we actually find, however, a concentration of events near the center of the diagram, not in the bands. This result could be consistent with essentially no Y_1^* production (as suggested in Fig. 3) plus a nonresonant background of $\Lambda\pi^+\pi^-$ events tending to favor equal pion momenta (for reasons unknown); it is also conceivable and quantitatively sensible that there is indeed appreciable Y_1^* production with the Y_1^* and the production pion predominantly in a relative p state (or higher). This would tend to depopulate the ends of the ellipse where the production pion momenta would be low and produce the observed distribution of events. Therefore, one cannot determine unambiguously from these data the cross section for Y_1^* production at $P_K = 510$ Mev/c.

Table II illustrates the apportioning of events between the various possible reactions.

The Y_1^* production angular distributions are isotropic within statistics for all our beam momenta. This would suggest that Y_1 production proceeds dominantly through a single $J = 1/2$ wave. However, the $\Lambda\pi^+\pi^-$ cross section alone comes very close to $\pi\lambda^2/2$, and so other partial waves are probably present.

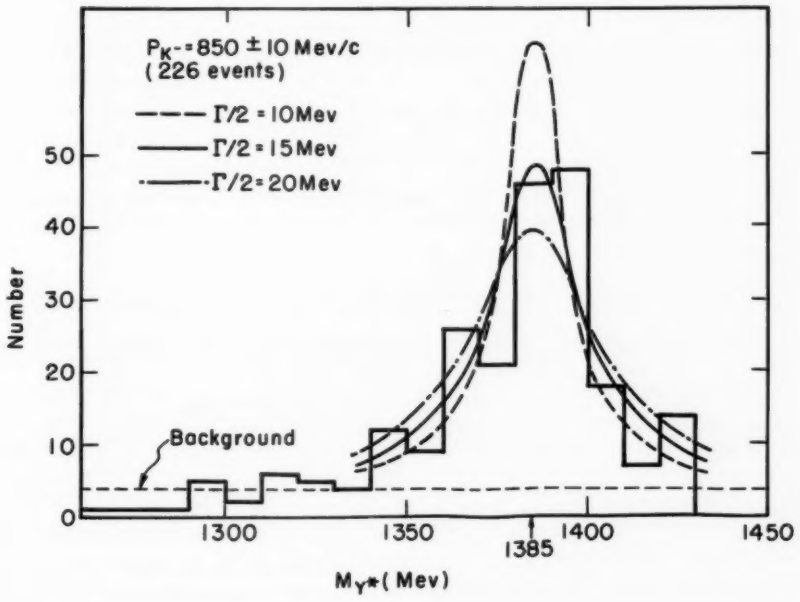

FIG. 2. Experimental histogram of the Y_1^* mass, $m(Y_1^*)$, at P_K(lab) = 850 Mev/c. To each event plotted in Fig. 1 there correspond two effective Y_1^* masses, $m(Y_1^{*+})$ and $m(Y_1^{*-})$; we choose as $m(Y_1^*)$ that which is closer to 1385 Mev. S-wave resonance curves of the form $dn/dm \propto [(m - 1385)^2 + (\Gamma/2)^2]^{-1}$ have been fitted to the data as indicated, with $\Gamma/2 = 10$, 15, and 20 Mev.

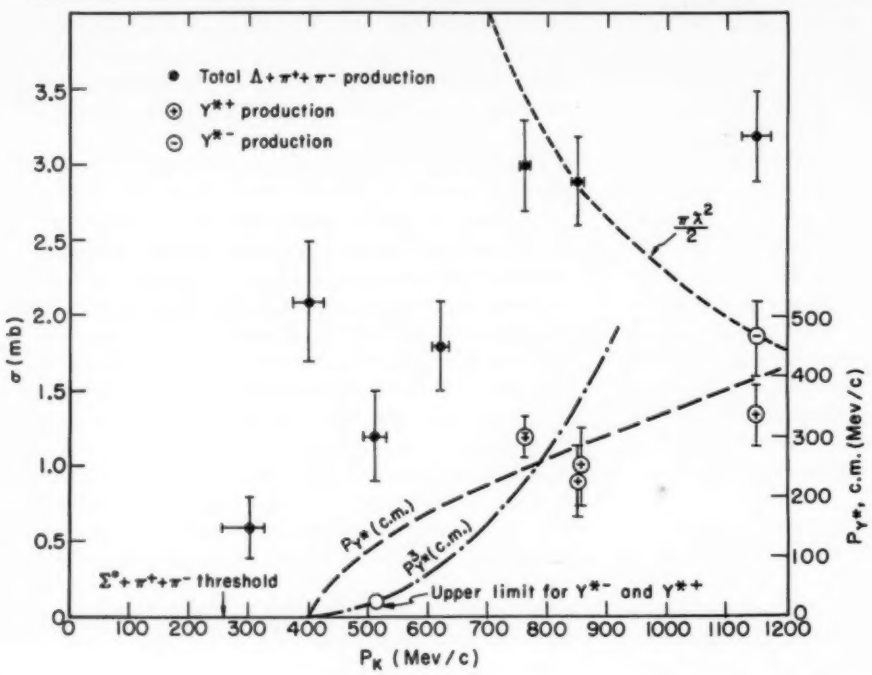

FIG. 3. Excitation data for total $\Lambda\pi^+\pi^-$ production and its apportioning to Y^{*++} and Y^{*-}. The dashed curves show P_{Y^*}(c.m.) and $P_{Y^*}{}^3$(c.m.) as a function of P_K(lab) and are included for reference only. The line labeled $\pi\lambda^2/2$ is the maximum reaction cross section for a single isotopic-spin partial wave with $J=1/2$. The point plotted at P_K(lab) = 510 Mev/c represents an estimate of the cross section based on the assumption that the number of events actually within the "bands" is the total number of $Y_1{}^*$'s produced and does not represent a unique interpretation of the data.

Next we discuss the $Y_1{}^*$ spin. Global symmetry predicts a $\Lambda\pi$ resonance with spin $J=3/2$.[5] On the other hand, the Dalitz-Tuan s-wave resonance in the K^-p system corresponds to a $Y_1{}^*$ with $J=1/2$, and a strong decay via $S_{1/2}$ if the $K\Lambda$ parity is odd.[6] If our model of an isolated Y^* were correct, the strong decay angular distribution of Eq. (3) should be fore-aft symmetric ($a_1=0$), and the presence of any polar-equatorial anisotropy ($a_2\neq 0$) would be evidence for $J>1/2$. We find instead that $a_1\neq 0$ but within statistics $a_2=0$ at all production angles. After looking for evidence for $a_2\neq 0$ at any (or all) angles of Y^* production, we have confined our analysis to polar-produced Y^*'s where, as Adair has pointed out,[7] an isolated $J=3/2$ particle must decay according to $1+3(\vec{\Lambda}\cdot\vec{K})^2$ (the unit vector $\vec{K}$ is along the K^- beam direction) while $J=1/2$ must decay isotropically. The decay distribution for polar-produced Y^*'s ($|\vec{Y}^*\cdot\vec{K}|\geq 0.80$) is given in Fig. 4. We have used $\vec{\Lambda}\cdot\vec{Y}^*$ as a measure of the decay angle instead of $\vec{\Lambda}\cdot\vec{K}$ in order to display the fact that the Y^* are not isolated but tend to undergo strong decay with the Λ going backwards. (Essentially the same result is achieved for these polar events by choosing $+\vec{\Lambda}\cdot\vec{K}$ for forward-produced Y^*, and $-\vec{\Lambda}\cdot\vec{K}$ for backwards Y^*.) These Adair events of Fig. 4 again fail to show any evidence for $1+3(\vec{\Lambda}\cdot\vec{Y}^*)^2$ superimposed on the asymmetry, which is linear in $(\vec{\Lambda}\cdot\vec{Y}^*)$. This statement applies individually to both charges

Table II. Numbers and cross sections for V and two-prong events. Numbers in parentheses are cross sections in millibarns.

P_K (Mev/c)	$Y_1{}^{*-}$	$Y_1{}^{*++}$ $\Lambda\pi^+\pi^-$	Three-body	$\Sigma^0\pi^+\pi^-$	$\Lambda\pi^+\pi^-\pi^0$	$K^0p\pi^-$	Total
510	←	31 (1.2±0.3)	→	4 (0.2±0.1)	0	0	35
620	←	54 (1.8±0.3)	→	10 (0.3±0.1)	0 (0)	0 (0)	64
760	121 (1.2±0.14)	122 (1.2±0.14)	56 (0.6±0.1)	55 (0.6±0.1)	20 (0.2±0.05)	2 (0.03±0.02)	376
850	56 (0.9±0.25)	62 (1.0±0.25)	67 (1.0±0.15)	39 (0.6±0.1)	7 (0.1±0.04)	3 (0.03±0.02)	234

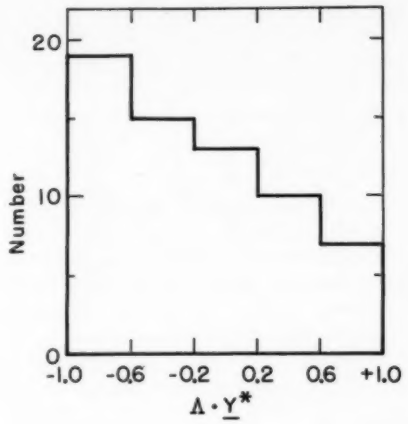

FIG. 4. Adair analysis of 62 $Y^{*\pm}$ events at $P_K = 760$ and 850 Mev/c; $|\vec{Y}^* \cdot \vec{K}| \geq 0.80$.

of Y^* at each momentum and to the sum of all events. However, as is shown in the next Letter, one cannot conclude that $J = 1/2$ since examples are given where Bose statistics can cause a Y^* with $J = 3/2$ to have a relatively isotropic angular distribution in the Adair analysis.

Next we discuss the branching ratio $Y_1^* \to \Sigma$ vs Λ. Global symmetry predicts definite ratios between the decay rate $\Gamma(N)$ of the 3/2, 3/2 pion-nucleon isobar ($N^* \to N + \pi$) and the equivalent rates of, for example, the three decay modes of Y_1^{*-}. These are $\Gamma(N):\Gamma(\Sigma^0):\Gamma(\Sigma^-):\Gamma(\Lambda) = p_N^3 : (1/6)p_{\Sigma^0}^3 : (1/6)p_{\Sigma^-}^3 : (4/6)p_\Lambda^3$. For $p_N = 230$ Mev/c, $p_\Sigma = 127$, $p_\Lambda = 207$, $(p_\Lambda/p_\Sigma)^3 = 1/4$, the relative rates are predicted to be 1.37:(1/24):(1/24):(2/3). The half-width $\Gamma/2(N)$ is known to be 45 Mev; so global symmetry predicts a Y_1^* half-width $\Gamma/2 = \frac{1}{2}[\Gamma(\Sigma^0) + \Gamma(\Sigma^-) + \Gamma(\Lambda)]$ of 24.7 Mev, and a branching ratio $\Gamma(\Sigma^0)/\Gamma(\Lambda) = 1/16$. (As already mentioned, our observed $\Gamma/2$ is 15 to 20 Mev, but the statistics are sufficiently poor and the effects of Bose statistics sufficiently great that $\Gamma/2 = 25$ Mev cannot be ruled out.) The Dalitz-Tuan resonance is expected to give values of $\Gamma(\Sigma^0)/\Gamma(\Lambda)$ ranging from $\geq 12\%$ (if the $K\Lambda$ and $K\Sigma$ parities are both odd) down to 6% (if $K\Lambda$ odd but $K\Sigma$ even).[3] We obtain $\Gamma(\Sigma^0)/\Gamma(\Lambda) < 3\%$ at 760 Mev/c and $< 5\%$ at 850 Mev/c; these values are obtained by making a background subtraction and represent "realistic" upper limits. "Maximum possible" upper limits come from counting every $\Sigma^0\pi^+\pi^-$ event with an effective $\Sigma^0\pi$ mass falling within 30 Mev of the Y_1^* mass of 1385; these are $< 20\%$ at 760 Mev/c and $< 10\%$ at 850 Mev/c. The observed limits on the branching ratios are consistent with the predictions of global symmetry and not necessarily inconsistent with those of the Dalitz-Tuan resonance.

The average Y^* polarization ($\bar{P}_{Y^*}$) has been measured from the asymmetry of the Λ-decay proton assuming $\alpha = +1$ and $\vec{Y}^* \times \vec{K} \equiv$ up; only events with $|\vec{Y}^* \cdot \vec{K}| \leq 0.85$ have been used, giving $\bar{P}_{Y^{*-}} = (+11 \pm 21)\%$ and $\bar{P}_{Y^{*+}} = (-16 \pm 21)\%$ at 760 Mev/c; $\bar{P}_{Y^{*-}} = (-56 \pm 20)\%$ and $\bar{P}_{Y^{*+}} = (+12 \pm 28)\%$ at 850 Mev/c. The fact that the Y^{*-} polarization seems to be large at 850 Mev/c and, by comparison, surprisingly small at 760 Mev/c could be a statistical fluctuation or may be connected with the fact that the Σ-production channels also show a rapid variation with energy in this region.[8]

Since no strong evidence for Y^* spin $J = 3/2$ has yet been found either at Berkeley or elsewhere,[9,10] it is intriguing to assume $J = 1/2$ and to try to distinguish between $S_{1/2}$ and $P_{1/2}$ Y^* strong decay.

We use about 60 polarized Y^{*-} at 850 Mev/c (assuming that the polarization is not a statistical fluctuation). In addition to the normal $\vec{n}$ to the production plane, it is convenient to define another unit vector $\vec{m} = 2(\vec{n} \cdot \vec{\Lambda})\vec{\Lambda} - \vec{n}$. This vector $\vec{m}$ lies in the plane of $\vec{n}$ and $\vec{\Lambda}$ (the direction of flight of the Λ), and if $\vec{\Lambda}$ makes an angle θ with $\vec{n}$, $\vec{m}$ makes an angle 2θ.[9] We write P_n for the measured Λ polarization along $\vec{n}$ and, similarly, P_m along $\vec{m}$. If the Y^* polarization is $\bar{P}$, then for strong decay via $S_{1/2}$, one can show

$$P_n = \bar{P}, \quad P_m = -\bar{P}/3, \quad P_m/P_n = -1/3. \tag{5a}$$

For $P_{1/2}$ decay the roles of $\vec{n}$ and $\vec{m}$ are interchanged; i.e., the Λ has its maximum polarization along $\vec{m}$, and we have

$$P_n = -\bar{P}/3, \quad P_m = \bar{P}, \quad P_m/P_n = -3. \tag{5b}$$

We find $P_n = (-56 \pm 20)\%$, $P_m = (+33 \pm 25)\%$, and $P_m/P_n = 0.6$. It is not meaningful to state statistical errors on a calculated ratio like P_m/P_n when the fractional standard deviations are large. Instead we apply the χ^2 test; the average value of χ^2 should be 1.0. For the $S_{1/2}$ hypothesis, we find $\chi_S^2 = 0.3$ (high probability), but for $P_{1/2}$, $\chi_P^2 = 4.5$ (probability $\simeq 3\%$). Martin et al.[9] also report $P_n = -0.38 \pm 0.25$ and $P_m = 0.19 \pm 0.25$, which yield $\chi_S^2 = 0$, $\chi_P^2 = 1$. Thus if it were established (a) that Y^* is the Dalitz-Tuan resonance of a $K + p$ in an $S_{1/2}$ bound state and (b) that Eqs. (5) are not badly perturbed by interference phenomena, then our

data would strongly suggest odd $K\Lambda$ parity.

It is a pleasure to acknowledge the help and support of Professor L. W. Alvarez and many members of the Alvarez and Gow groups. We thank R. H. Dalitz and A. Pais for their interest and suggestions.

---

*Work supported by the U. S. Atomic Energy Commission.

†National Academy of Sciences Fellow.

[1]M. Alston, L. W. Alvarez, P. Eberhard, M. L. Good, W. Graziano, H. K. Ticho, and S. G. Wojcicki, Phys. Rev. Letters 5, 520 (1960).

[2]R. H. Dalitz and D. H. Miller, following Letter [Phys. Rev. Letters 6, 562 (1961)].

[3]R. H. Dalitz, Phys. Rev. Letters 6, 239 (1961).

[4]Paul Nordin, Jr., Lawrence Radiation Laboratory Report UCRL-9489 Rev., 1961 (unpublished).

[5]M. Gell-Mann, Phys. Rev. 106, 1296 (1957).

[6]R. H. Dalitz and S. F. Tuan, Phys. Rev. Letters 5, 425 (1959); Ann. Phys. 8, 100 (1959); and Ann. Phys. 10, 307 (1960). The resonance is a consequence of the (a_-) solution to the s-wave data on the K^-+p interaction. It is not yet known whether (a_-) is the correct solution. See R. H. Dalitz, Revs. Modern Phys. (to be published).

[7]R. K. Adair, Phys. Rev. 100, 1540 (1955).

[8]Alvarez Group Memorandum No. 252, January, 1961 (unpublished). For additional experimental data see also M. H. Alston and M. Ferro-Luzzi, Revs. Modern Phys. (to be published); and University of California Radiation Laboratory Report UCRL-9587 (unpublished).

[9]H. J. Martin, L. B. Leipuner, W. Chinowsky, F. T. Shively, and R. K. Adair, Phys. Rev. Letters 6, 283 (1961). See also: R. K. Adair, in Proceedings of the 1960 Conference on Strong Interactions, Berkeley, December, 1960 [Revs. Modern Phys. (to be published)].

[10]M. M. Block et al., Nuovo cimento (to be published).

BOSE STATISTICS AND Y^* PRODUCTION AND DECAY IN K^--p COLLISIONS*

R. H. Dalitz† and Donald H. Miller

Lawrence Radiation Laboratory and Department of Physics, University of California, Berkeley, California

(Received April 27, 1961)

Experimental evidence for the occurrence of an $I=1$, Λ-π resonant state (Y^*) as an intermediate step in the reaction

$$K^-+p \rightarrow \begin{Bmatrix} Y^{*-}+\pi^+ \\ Y^{*+}+\pi^- \end{Bmatrix} \rightarrow \Lambda+\pi^++\pi^- \qquad (1)$$

has been presented by Alston et al.[1] for K^-(lab) momentum 1150 Mev/c. The same reaction has also been studied recently by Berge et al.,[2] and the related K_2^0-p reactions have been analyzed by Martin et al.[3] for K_2^0 momentum 975 Mev/c. The interpretation of these data in terms of the mass (M^*), half-width ($\Gamma/2$), spin (J), and parity of the Y^* state has been confused by the evidence that the Y^* decay in these reaction sequences (1) cannot be regarded as the decay of a free particle. In this Letter, we show that this evidence can be largely understood as due to interference effects arising from the requirement of Bose statistics for the final pions, and we discuss the extent to which these Y^* parameters may ultimately be determined from data in this momentum range.

From the reported estimates (10 to 30 Mev) for $\Gamma/2$, the mean distance traveled by the primary pion in one Y^* mean lifetime is more than 4 fermis. It is therefore a plausible assumption that the successive pion-emission processes do not interfere dynamically to any marked degree. In this case we are led to an amplitude $M(1,2)$ for the reaction sequence $\bar{K}+N \rightarrow Y^*+\pi_1$, $Y^* \rightarrow \Lambda+\pi_2$, of the general form[4]

$$M(1,2)=\Phi(\vec{\sigma},\vec{q},\vec{p}_1,\vec{P}_2)A(P_2), \qquad (2)$$

where $\vec{q}$ and $\vec{p}_1$ denote the c.m. momenta of the K^- meson and the primary pion, and $\vec{P}_2$ denotes the momentum of the secondary pion in the π_2-Λ rest frame. The final configuration $\Lambda+\pi_2+\pi_1$ may also be specified by giving l, the orbital angular momentum of π_1, and L, the orbital angular momentum in the π_2-Λ system which corresponds to the Y^* spin and parity; the form of Φ is then determined for total angular momentum j by the angular momentum coupling and the $(K\Lambda)$ parity and by centrifugal barrier considerations. The role of the resonant state is represented by the second factor,

$$A(P)=\exp[i\delta(P)]\sin\delta(P)/P^{2L+1}. \qquad (3)$$

The amplitudes for the two sequences (1) must be added coherently, and their sum must correspond to a final state with correct symmetry for interchange of the two pions. Thus, for total isotopic spin $I=0$ and 1, the amplitudes M_0 and

M_1 are given by

$$M_0 = M'(1,2) + M'(2,1), \quad (4a)$$

$$M_1 = M''(1,2) - M''(2,1). \quad (4b)$$

For comparison with experiment, it is convenient to consider the probability distribution $P(E_+,E_-)$ on the (E_+,E_-) phase-space diagram. Since the distribution $P(E_+,E_-)$ sums over all orientations of the $\Lambda\pi^+\pi^-$ plane, the contributions to $P(E_+,E_-)$ from initial states of different angular momentum and parity add incoherently. Since $P(E_+,E_-) = \frac{1}{2}|M_0+M_1|^2$ and $P(E_-,E_+) = \frac{1}{2}|M_0-M_1|^2$, the symmetrized probability distribution $\{P(E_+,E_-)+P(E_-,E_+)\}$ is simply a superposition of the separate $I=0$ and $I=1$ distributions, without interference between them. The observation that the experimental distributions $P(E_+,E_-)$ and $P(E_-,E_+)$ do not differ markedly from each other at 760 and 850 Mev/c suggests that, for these two momenta, the reaction may be dominated by a single isotopic-spin channel.

Two $\Lambda\pi^+\pi^-$ configurations are of particular interest:

(A) $E_+ = E_-$, and maximum Λ recoil energy. For this configuration, the two pions have the same c.m. momentum, and $M(1,2)$ and $M(2,1)$ are necessarily equal. For 850 Mev/c and below, the Y^{*+} and Y^{*-} bands overlap strongly, and marked interference between these two terms is to be expected at A (see Fig. 1 of preceding Letter[2])—constructive for $I=0$, destructive for $I=1$. The experimental distributions at 760 and 850 Mev/c show an especially low density of events in the region near A, which suggests that it is the $I=1$ channel which is dominant at these momenta.[5] The density of events expected in this region for the models discussed below is compared with the data in Table I.

(B) $E_+ = E_-$, and the Λ hyperon at rest. For this configuration, the two pions have equal and opposite momenta in the c.m. system. With $I=1$ ($I=0$), $M(1,2)$ and $M(2,1)$ interfere constructively or destructively according as $l+L$ is odd (even) or even (odd). The observed distributions at 760 and 850 Mev/c indicate strong constructive interference in the region near B, leading to the conclusion that, with $I=1$, $l+L$ is odd.[6] An $S_{1/2}$ Λ-π resonance therefore requires a p-wave primary pion at these production energies, a $P_{1/2}$ or $P_{3/2}$ Λ-π resonance requires an s- (or d-) wave primary pion.

We now discuss in detail the calculations of the symmetrized (E_+,E_-) distributions for some cases of particular interest, to illustrate the nature of the interference effects resulting from Bose statistics. These cases represent only the simplest possibilities for fitting the available data, and are neither unique nor exhaustive examples.

$S_{1/2}$ Λ-π resonance. With the assumption of p-wave excitation, we have

$$M(1,2) = (a\vec{q}\cdot\vec{p}_1 + ib\vec{\sigma}\cdot\vec{q}\times\vec{p}_1)(M_2 - M^* + i\Gamma/2)^{-1}, \quad (5)$$

where M_2 denotes the total energy in the Λ-π_2 rest frame. Figure 1(a) compares the calculated distribution of $M(\Lambda$-$\pi)$ for $M^* = 1385$ Mev and several values of $\Gamma/2$ with the 850-Mev/c data (obtained by projecting the symmetrized (E_+,E_-) plot onto one axis). These curves display an insensitivity to $\Gamma/2$, for an adequate fit[7] to the data is obtained with any value of $\Gamma/2$ between 20 and 30 Mev. As shown in Table I, the destructive interference obtained for the $I=1$ $pS_{1/2}$ case is in reasonable accord with the data; $I=0$ $sS_{1/2}$ production, on the other hand, gives too high a density of events near A, as well as a poor fit to the mass distribution.[8]

The mass distribution calculated for $I=1$ $pS_{1/2}$ production also gives an adequate fit to the experimental data[1] at 1150 Mev/c, for the same

Table I. The number of $\Lambda+\pi^++\pi^-$ events expected in the region near A, with both E_+ and E_- less than the limit E_m stated, for the K^--p interaction data presently available.[a]

		Configuration $(lL_J)_j^I$					
		$(sS_{1/2})_{1/2}^0$	$(pP_{3/2})_{1/2}^0$	$(pP_{3/2})_{3/2}^0$	$(pS_{1/2})_{1/2}^1$	$(sP_{3/2})_{3/2}^1$	Events observed
850 Mev/c;	$E_m = 150$ Mev	35.8	26.0	8.5	12.3	11.0	11/262
760 Mev/c;	$E_m = 125$ Mev	29.8	32.8	8.6	9.7	10.5	18/252
	$E_m = 120$ Mev	17.4	21.1	4.2	3.1	2.2	8/252

[a]From references 2.

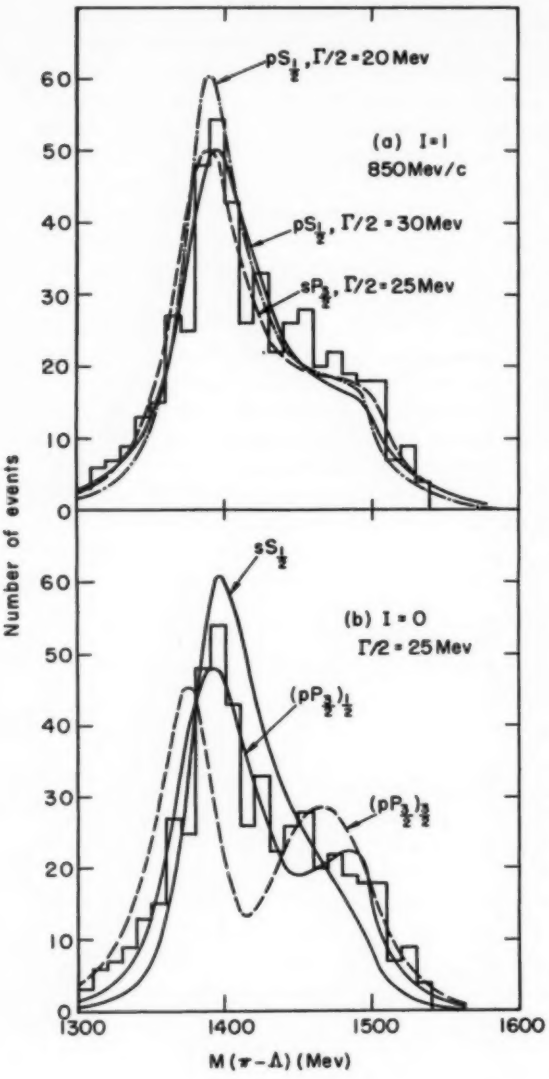

FIG. 1. The $M(\pi\text{-}\Lambda)$ distribution observed at 850 Mev/c is compared with (a) the calculated distributions for the $I=1$ $(pS_{1/2})$ and $I=1$ $(sP_{3/2})$ configurations with $M^*=1385$ Mev and various values of $\Gamma/2$, and (b) the calculated distributions for the $I=0$ configurations $sS_{1/2}$, $(pP_{3/2})_{1/2}$, and $(pP_{3/2})_{3/2}$ with $\Gamma/2=25$ Mev.

M^* and $\Gamma/2=25$ Mev. $I=0$ $pS_{1/2}$ production can also fit these data but, the interference at B being destructive, only with a larger width $\Gamma/2$. Since this K^- energy lies just above the strong $I=0$ $\bar{K}$-N resonance [at 1100-Mev/c K^- (lab) momentum], there is, of course, little reason to believe that this Y^* production should necessarily involve the same states as are effective at 850 Mev/c. In fact, these data show appreciable asymmetry between Y^{*+} and Y^{*-} production, an indication that both $I=0$ and $I=1$ production must be occurring from the same angular-momentum states.

$P_{3/2}$ Λ-π resonance. For $I=1$ production, we consider s-wave excitation,

$$M(1,2)=(2\vec{q}\cdot\vec{P}_2-i\vec{\sigma}\cdot\vec{q}\times\vec{P}_2)A(P_2), \qquad (6)$$

where the phase shift $\delta(P_2)$ has been taken to have the form known for the (3,3) resonance,[9] with suitable parameters M^* and Γ. The fit to the 850-Mev/c mass distribution is quite adequate with $\Gamma/2=25$ Mev, as shown in Fig. 1(a); the same parameters again give an adequate fit to 1150-Mev/c distribution. Figure 1(b) shows the calculated distributions for $I=0$ production in the $j=1/2$ and $3/2$ states $(pP_{3/2})$. Neither of these configurations reproduces the data. Table I shows that for $(pP_{3/2})_{1/2}$, the constructive interference near A is too strong; $(pP_{3/2})_{3/2}$ does give small intensity in this region because the Y^*-decay distribution (relative to production direction) happens to have approximately $(7\text{-}6\cos^2\theta)$ form for this case, but this angular distribution is incompatible with the data (see Fig. 2). Although a rough fit may be obtained by superposing these two configurations, it is clear that this comparison adds support to our assignment of $I=1$ production.

$P_{1/2}$ Λ-π resonance. For s-wave excitation, we have

$$M(1,2)=\vec{\sigma}\cdot\vec{P}_2A(P_2), \qquad (7)$$

where $A(P_2)$ is taken to have the form appropriate to a P-wave resonance, that used already with Expression (6). The symmetries required for fitting the (E_+,E_-) plots are similar to those for the $P_{3/2}$ possibility just discussed.

The highly anisotropic distribution observed for Y^* decay relative to its direction of motion may also be understood in terms of Bose statistics. For $I=1$ and $l+L=$ odd, the configuration with the secondary pion emitted forwards gives constructive interference, so that the angular distribution for Λ emission in the Y^* decay is peaked backwards. The decay angular distributions (averaged over all production directions), calculated for $(sP_{3/2})$ and $(pS_{1/2})_j$ for 850 Mev/c, are shown in Fig. 2 and compared with the experimental data.

The decay angular distribution for Y^* production at 0 and 180 deg is of particular inter-

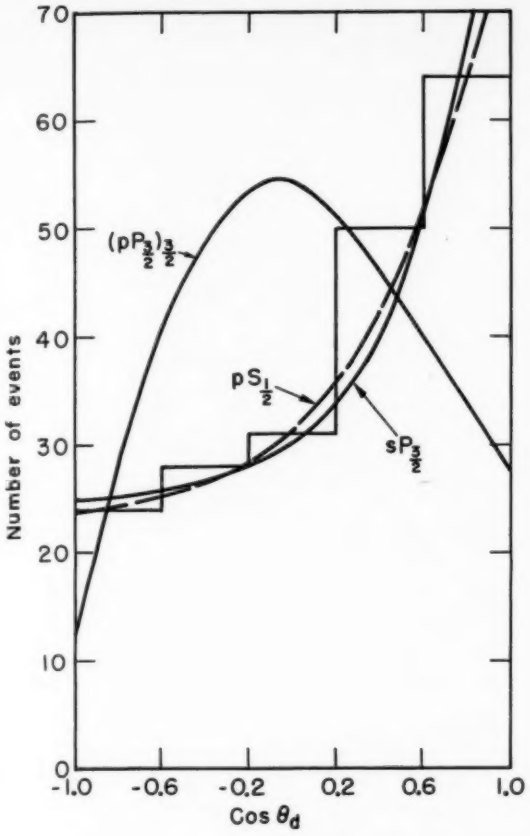

FIG. 2. The angular distribution of the pion from Y^* decay, relative to the Y^* direction of motion, for all events at 850 Mev/c with $M(\pi$-$\Lambda)$ between 1360 and 1410 Mev. The calculated curves for $I=1$ $sP_{3/2}$ and $I=1$ $pS_{1/2}$ production reproduce the general trend rather well. The curve for $I=0$ $(pP_{3/2})_{3/2}$ production is plotted to show that the data strongly exclude the possibility that this is the dominant production state.

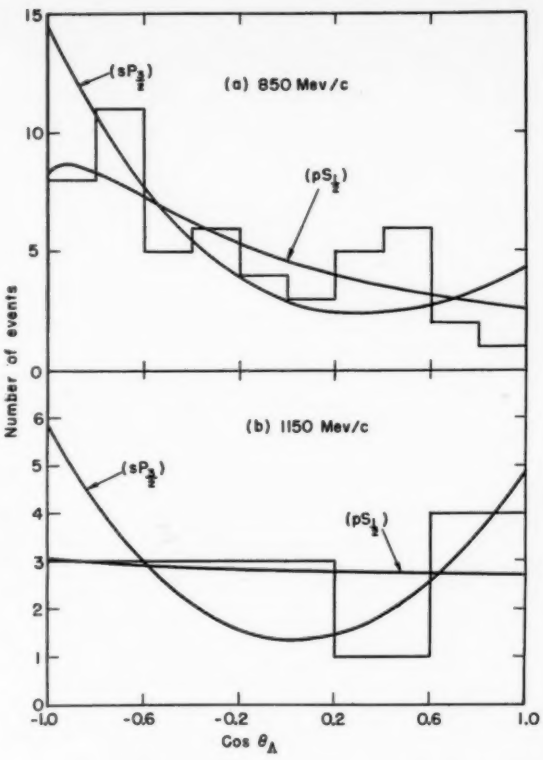

FIG. 3. Adair distributions are shown for forward- and backward-produced Y^* decay (integrated over the mass range $1360 \leq M(\Lambda$-$\pi) \leq 1410$ Mev) at K^- momenta 850 Mev/c and 1150 Mev/c, where the angle θ_Λ of the Λ particle in the Y^* rest frame is measured from the direction of motion of the Y^*. The distortion from the expected $(1+3\cos^2\theta_\Lambda)$ distribution for $J=\frac{3}{2}$ is much weaker at 1150 Mev/c than at 850 Mev/c. However, the present statistics at 1150 Mev/c do not yet allow the cases $J=\frac{1}{2}$ and $J=\frac{3}{2}$ to be distinguished.

est, in view of Adair's general result for its dependence on J. Again, the angular distributions characteristic of isolated decay are strongly modified by the requirements of Bose statistics. The distortion of the idealized $(1+3\cos^2\theta)$ distribution for $J=3/2$ is shown in Fig. 3(a). The difficulty in distinguishing conclusively between the cases $J=1/2$ and $J=3/2$ at 850 Mev/c is apparent.[10] The character of these distortions is closely linked with the requirement of constructive interference at B.

As the K^- momentum is increased further, the primary pion energy will exceed the energy of the secondary pion and Bose interference effects will become less and less important. In the calculations for 1150 Mev/c, this is already apparent.[11] As shown in Fig. 3(b), the distortion of the Adair distribution for $J=3/2$ is much less severe; unfortunately the paucity of data at this momentum does not yet allow a decision on the Y^* spin. It is clear that, in further experiments at higher K^- momenta, the effects of Bose statistics will be sufficiently reduced to allow the possibility of a clear-cut distinction between $J=1/2$ and $J=3/2$ for the Y^* state.

For Y^* production from a K^--p state of angular momentum j and isotopic spin I, it is important to note that the geometric limit on the absorption

cross section is $(2j+1)\pi\lambda^2/4$, which takes the value $2.85(j+\frac{1}{2})$ mb at 850 Mev/c. At this momentum, the cross section observed for Reaction (1) is 3.2 ± 0.3 mb, comparable with the geometric limit for $j=1/2$. This limitation provides a severe condition[12] which must be satisfied by any simple model of the production process. For $I=1$, this condition is satisfied by $(sP_{3/2})$ production, but not by $(sP_{1/2})$ production. The possibility $(pS_{1/2})_{3/2}$ [together, perhaps, with some $(pS_{1/2})_{1/2}$ production] also satisfies this condition. At this point we note that the angular distributions for Y^* production are isotropic at 760 and 850 Mev/c. This is consistent with $(sP_{3/2})$ production, of course. For the $(pS_{1/2})_{3/2}$ case,[13] a calculation of the angular distribution (including Bose effects) shows that a strong $\cos^2\theta$ term is to be expected at these energies; this discrepancy could be reduced by a large admixture of $(pS_{1/2})_{1/2}$ excitation of suitable phase. The large value observed for the $(\Lambda+\pi^++\pi^-)$ production cross section is most probably an indication that the distribution receives contributions from a number of partial waves and configurations, of which only the dominant terms have the symmetry specified in our discussion.

In conclusion, we are glad to express our deep indebtedness to Mr. Joseph Schwartz for his enthusiastic computational assistance in this work.

*Work done under the auspices of the U. S. Atomic Energy Commission.

†Permanent Address: Enrico Fermi Institute for Nuclear Studies, University of Chicago, Chicago, Illinois.

[1]M. H. Alston, L. W. Alvarez, P. Eberhard, M. L. Good, N. Graziano, H. K. Ticho, and S. G. Wojcicki, Phys. Rev. Letters 5, 557 (1960).

[2]J. Berge, P. Bastien, O. Dahl, M. Ferro-Luzzi, J. Kirz, D. Miller, J. Murray, A. Rosenfeld, R. Tripp, and M. Watson, preceding Letter [Phys. Rev. Letters 6, (1961)]. See also M. H. Alston and M. Ferro-Luzzi, Revs. Modern Phys. (to be published).

[3]H. J. Martin, L. B. Leipuner, W. Chinowsky, F. T. Shively, and R. K. Adair, Phys. Rev. Letters 6, 283 (1961).

[4]A matrix element of this form has also been used by B. Sakita, Nuovo cimento (to be published), in a discussion of some Λ polarization effects which can occur in this process in consequence of the effect of Bose-statistics interference.

[5]This conclusion may be checked directly by measurement of the Y^* production cross section in K^--n or K_2^0-p collisions, where only the $I=1$ interaction can be effective. If Y^* production is dominantly from the $I=1$ channel, then we expect $\sigma(K^-+n\rightarrow Y^*+\pi)=2\sigma(K_2^0+p\rightarrow Y^*+\pi)\approx2\sigma(K^-+p\rightarrow Y^*+\pi)$. It is of interest that Martin et al. (reference 3) have reported strong Y^* production in 975-Mev/c K_2^0-p collisions, although a precise value for the cross section is not yet available.

[6]That this evidence is significant for $I=1$ is shown by calculations based on specific models with $l+L$ even. The case $l=L=0$ is strongly excluded, as it requires the density to vanish along the line $E_+=E_-$. If $I=0$ held, this evidence would require $l+L$ even for the dominant production states. The simplest possibilities ($sS_{1/2}$, $pP_{1/2}$, or $pP_{3/2}$) can be excluded by the argument given above (see also Table I), or by the comparison in Fig. 2. An exceptional situation which could be consistent with $I=0$ production is mentioned in reference 8. It is possible, of course, that at these energies both $I=0$ and $I=1$ production occurs dominantly in the states with the symmetry specified here; it should be emphasized that these come from initial states of opposite parity and that, since they do not interfere, they would contribute no asymmetry to the $P(E_+, E_-)$ plot.

[7]In this fitting, no question arises concerning the identification of "background" to be subtracted: All events are included. As explained above, the weakly contributing states do not interfere with the resonant contributions, and their influence is thereby minimized.

[8]The assumption of $I=0$ production in the $sS_{1/2}$ configuration gives too high a density of events in the region near A (see Table I). However, it should be remarked here that an s-wave Λ-π resonance associated with a $\bar{K}$-N bound state is not necessarily well-fitted by a Breit-Wigner amplitude, but may be long-tailed on the low-energy side [see R. H. Dalitz, Revs. Modern Phys. (to be published)]. An asymmetric resonance amplitude of reasonable total width, which falls rapidly on the high-energy side, would be small in the region of A for K^- momenta 760 and 850 Mev/c; and the density of events would be low in this region, despite the constructive interference.

[9]M. Gell-Mann and K. M. Watson, Ann. Rev. Nuclear Sci. 4, 219 (1954).

[10]We note here that, in the Adair distributions, there is generally interference between amplitudes from different initial angular momentum states, so that these distributions are more sensitive to small admixtures of configurations of different symmetry.

[11]Note that the interference effects are model-dependent in that they depend on the form assumed for the function $A(P_2)$ at energies well above the π-Λ resonance energy. Somewhat stronger interference terms could be obtained by modifying the phase shift $\delta(P_2)$ in this region, or by including additional momentum-dependent factors.

[12]For $I=0$ absorption, we would have $\sigma(\Lambda+\pi^0+\pi^0)=\frac{1}{2}\sigma(\Lambda+\pi^++\pi^-)$, so that the Y^* production cross section must be increased to 4.8 ± 0.5 mb to allow for these unobserved events.

[13]R. H. Dalitz [Phys. Rev. Letters 6, 239 (1961)] has suggested that enhanced $I=1$ production would be ex-

pected as a consequence of the (3, 3) resonant interaction between the primary pion and the nucleon of a $J=\frac{1}{2}$ $\bar{K}$-N bound state. This interpretation suggests naturally that the primary pion be emitted in the p wave with $j=\frac{3}{2}$. Although the configuration $(pS_{1/2})_{3/2}$ fits the decay angular correlations and the (E_+, E_-) plot rather well, it appears excluded by the production angular distributions observed.

PION-NUCLEON INTERACTIONS IN THE REGION OF THE HIGHER RESONANCES

P. Carruthers

Laboratory of Atomic and Solid-State Physics, Cornell University, Ithaca, New York

(Received April 17, 1961)

In this note we attempt to clarify certain features of pion-nucleon interactions in the region of the "higher" resonances. We give most attention to the process of single-pion production.[1] Data are most complete for the following reactions:

$$\pi^- + p \rightarrow \pi^- + \pi^+ + n, \quad (1)$$

$$\pi^- + p \rightarrow \pi^- + \pi^0 + p. \quad (2)$$

Recent experiments[2-6] near a Bev have revealed the following interesting features of reactions (1) and (2). While the qualitative features of the usual π-N "isobar" model[7] are displayed by reaction (1), reaction (2) behaves quite differently. For the latter process the number of protons with small recoil energy is in excess of the phase-space value. Moreover, at least at 960 Mev, the distribution of events for (2) has a prominent peak at a π-π total center-of-mass energy squared, s, of about 22, in units of pion rest mass squared.[3,5,6] Neither of these features are displayed by reaction (1).

The principal subjects to be discussed are as follows: 1. Present data for reaction (2) cannot be explained by the one-pion exchange (OPE) process [Fig. 1(a)]. 2. Consideration of the rescattering by the nucleon of one of the pions resulting from a π-π collision [Fig. 1(b)] cannot explain the behavior of reaction (2). 3. The origin of the third resonance and the behavior of reactions (1) and (2) are discussed. 4. The relevance of the present remarks to the structure of the abrupt rise in the π^+-p cross section at 800-Mev pion lab kinetic energy[9-11] are explained.

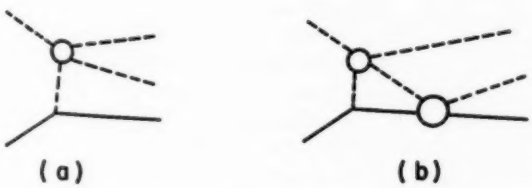

FIG. 1. (a) Pion production by the one-pion exchange process. (b) The rescattering of one of the pions in the 3-3 resonance.

1. The most damaging evidence against the explanation of the behavior of reaction (2) by OPE production [Fig. 1(a)] is the fact[5] that those events which contribute to the peak in the $Q_{\pi\pi}$ spectrum do not occur primarily at the small values of the proton invariant momentum transfer squared, Δ^2, expected from the calculations of Chew and Low[12] and Goebel.[13] Instead, the Δ^2 distribution of the π-π peak is nearly flat over a wide range of Δ^2, up to $\Delta^2 \approx 35$. Moreover, $\frac{3}{4}$ of those events with $\Delta^2 < 10$ occur for s values less than 20, the peak occurring for $20 < s < 25$. Thus the excess of events at low Δ^2 seems to have little to do with the peak in the $Q_{\pi\pi}$ spectrum.[14]

The second argument against the OPE explanation of the 960-Mev phenomena is that (for $\pi\pi$ isospin $t=1$) the π-π effect should be stronger in reaction (1) than in reaction (2). As is well known, for Fig. 1(a) the ratio $r=\sigma(-+)/\sigma(-0)$ is 2/1 for an isospin 1 interaction. Although this ratio is not far from that observed[15] near a Bev, OPE cannot possibly explain the 3-3 isobar behavior in reaction (1). Even if one supposes that the over-all process is initiated by OPE, the succeeding events in reactions (1) and (2) are so different that the survival of the ratio r is not to be expected a priori.

At this point it is convenient to introduce the isospin decomposition of the production amplitude.[1,16] Clearly there are four independent amplitudes corresponding to the reaction $\pi + N \rightarrow 2\pi + N$. We specify the total isospin T and the π-π isospin t to define the coupling scheme. The isospin amplitudes are written as $A(Tt)$. The

four amplitudes are $A(\frac{1}{2}0)$, $A(\frac{1}{2}1)$, $A(\frac{3}{2}1)$, and $A(\frac{3}{2}2)$. For even (odd) t these amplitudes are symmetric (antisymmetric) under interchange of the momenta of the outgoing pions. The implications of this important symmetry property have been discussed in reference 16. Denoting the observed reactions by the charge of the outgoing pions, we have[1,16]

$$A(-+) = -\tfrac{1}{3}\sqrt{2}A(\tfrac{1}{2}0) + \tfrac{1}{3}[A(\tfrac{1}{2}1) - A(\tfrac{3}{2}1)] + (1/3\sqrt{5})A(\tfrac{3}{2}2), \quad (3)$$

$$A(-0) = -\tfrac{1}{3}\sqrt{2}[A(\tfrac{1}{2}1) + \tfrac{1}{2}A(\tfrac{3}{2}1)] - (1/\sqrt{10})A(\tfrac{3}{2}2). \quad (4)$$

In terms of these amplitudes the $t=1$ OPE process gives $A(\frac{1}{2}1) = -2A(\frac{3}{2}1)$, $A(\frac{1}{2}0) = A(\frac{3}{2}2) = 0$. [This result is most simply derived by comparing (3), (4), and the ratio 2/1 for $\sigma(-+)/\sigma(-0)$ quoted above.] It was first suggested by Peierls[17] that the data under discussion are suggestive of the relation $A(\frac{1}{2}1) \approx A(\frac{3}{2}1)$. This allows the formation of a $t=1$ π-π isobar in the final state of reaction (2), but not in reaction (1). This view, that the final state of reaction (2) is reached by some process more complicated than OPE, is certainly not in conflict with the Δ^2 distribution of the events in the π-π peak of reference 5.

The possibility of a $t=2$ "di-pion" in the final state seems to be excluded by the predominance of the cross section for $\pi^+ + p \to \pi^+ + \pi^0 + p$ over $\pi^+ + p \to 2\pi^+ + n$ in the energy range 900-1300 Mev. The experimental ratio[18] is $\sigma(+0)/\sigma(++) \approx 4$. [In terms of the pure isospin cross sections,[16] $\sigma(+0) = \frac{1}{2}\sigma(\frac{3}{2}1) + \frac{1}{10}\sigma(\frac{3}{2}2)$; $\sigma(++) = \frac{2}{5}\sigma(\frac{3}{2}2)$.]

The fact that in the crucial range of the π-π energy the Δ^2 distribution of reaction (2) is qualitatively not at all like that of OPE clearly makes any extrapolation procedure unreliable at 960 Mev. In our opinion the minimum requirement for extrapolation is that the cross section in the physical region from which the extrapolation is made have the qualitative features of OPE. It is difficult to tell whether the data of Anderson et al.[19] (at 890-Mev π^- energy) satisfy this requirement. While the π-π cross section may well behave as indicated in reference 19, the procedure from which this result is derived is open to serious objection.

We suggest that the following use of "extrapolation" data may be more informative. First, we consider the results of references 3-5 as good evidence for an isospin one π-π resonance. The position and width are determined from these experiments. Using this information one can extrapolate from the pole in the unphysical region to the data in the physical region (rather than the other way around). The difference between this curve and that arising from OPE depends on the magnitude and phase of the non-OPE part of the production amplitude in a simple manner. The resulting information should be very useful in unraveling what seems to be a rather intricate situation.

2. About a year ago a number of people[20-22] suggested that the 3-3 isobar state was reached predominantly through the π-π channel [Fig. 1(b)]. "Quantitative" calculations have been made[1] taking into account essentially[23] the processes of Figs. 1(a) and 1(b), the nucleon being considered infinitely heavy. Let $\phi_\alpha(\omega_1, \omega_2)$ denote the appropriate partial-wave projection of the production amplitude, α denoting the relevant set of quantum numbers. ω_1 and ω_2 are the energies of the final pions; other variables are suppressed. Denoting the partial-wave projection of the OPE amplitude by $\phi_{\pi\alpha}(\omega_1, \omega_2)$, the solution for which pion 1 is in the 3-3 state is[1]

$$\phi_\alpha(\omega_1, \omega_2) = e^{i\delta_1}\cos\delta_1 \phi_{\pi\alpha}(\omega_1, \omega_2) + \frac{\omega_1 e^{i\delta_1}\sin\delta_1}{p_1^3 v^2(p_1)} \times \frac{P}{\pi}\int_\mu^\infty d\omega \frac{p^3 v^2(p)\phi_{\pi\alpha}(\omega, \omega_2)}{\omega(\omega - \omega_1)}. \quad (5)$$

δ is the 3-3 phase shift; $v(p)$ is the usual cutoff function of the static-nucleon meson theory. It is easy to see the significance of the various terms in (5). Write $e^{i\delta}\cos\delta = 1 + ie^{i\delta}\sin\delta$. The 1 corresponds to the OPE term; $ie^{i\delta}\sin\delta\phi_{\pi\alpha}$ corresponds to π-π scattering followed by real excitation of the 3-3 isobar.[24] It is curious to note that these contributions interfere in a destructive way. The integral term, proportional to the 3-3 scattering amplitude for meson 1, is due to off-the-shell scattering. This term receives large contributions from large p; since it depends critically on the cutoff, its value is numerically unreliable. Numerical calculations for the $D_{3/2}$ incident channel [leading to an s-wave and a p-wave (3-3 state) meson] indicate that the second term of (5) is about 3 times as large as the first. There seems no reason to doubt this feature for other channels, in view of the experimental evidence for the isobar model.[25]

When Eq. (5) is supplemented by the relevant charge state information, one finds the very interesting result[1] that for a $t=1$ π-π interaction, the 3-3 rescattering terms practically cancel

out for reaction (2), but not for (1). This can also be seen by considering the various ways in which Fig. 1(b) can contribute to the reaction (2) in a purely phenomenological way. Thus, were it not for the Δ^2 distribution at 960 Mev, the evidence would support the notions of a $t=1$ π-π resonance, the model of reference 1, and the extrapolation procedure for reaction (2).

Neither the integral term nor the partial-wave projection of the OPE amplitude seems capable of producing such a sharp peak in the $Q_{\pi\pi}$ spectrum as is found.[3-5] Moreover, the π-N correlations introduced by symmetrization of (5) cannot reproduce this phenomenon. If we abandon the $t=1$ channels to some unknown process leading to a final-state π-π isobar, such that $A(\frac{3}{2}1)\approx A(\frac{1}{2}1)$, then some interesting speculations can be made on the origin of the third resonance.

3. Near the third (900-Mev) resonance one is naturally led to consider those final-state 2π-N configurations in which both pions are in p states relative to the nucleon,[26] one state having π-N angular momentum 3/2. Of these states, those reached from the $F_{5/2}$ channel have the special property that the orbital momenta of both pions are parallel to the nucleon spin. As a consequence, the angular part of the production amplitude for this channel is symmetric in the two pions, so that symmetrization affects only the energy part, Eq. (5). Consider reaction (1), and suppose the isospin 1 amplitudes in Eq. (3) cancel as discussed above. Then since the integral term in (5) is supposed to dominate, and since the integral is a slowly varying function of ω_1 and ω_2 for moderate ω, the $\frac{1}{2}0$ and $\frac{3}{2}2$ contributions to reaction (1) are approximately proportional to

$$\omega_1 e^{i\delta_1}\sin\delta_1/p_1^3+\omega_2 e^{i\delta_2}\sin\delta_2/p_2^3, \qquad (6)$$

for all angles. [For $\omega_1=\omega_2$ the integral is the same for both terms in (6).] Thus the Bose symmetry, which requires that either pion have a chance to scatter off the nucleon, leads to a large constructive interference for ω_1 and ω_2 both near the 3-3 resonance energy. From this argument one expects a peak in reaction (1) at the third resonance. Whether a peak occurs in (2) depends on the sensitivity of the unknown intermediate state to the initial energy. If this state is not sensitive, $\sigma(-0)$ should rise abruptly above the threshold for production of the di-pion (740 Mev for $s=22$) and remain constant thereafter. Below the third resonance both $\sigma(-+)$ and $\sigma(-0)$ will be rising as the resonance is approached.[27] [$\sigma(-+)$ is already large.] If $\sigma(-0)$ levels off and $\sigma(-+)$ decreases above the third resonance, then the ratio r should drop. This picture is not incompatible with experiment; unfortunately, the ratio at 960 Mev is not yet certain.[15] It should be emphasized that in the present picture only one pion interacts with the nucleon rather than both, as in the theories of Peierls,[26] and Wong and Ross.[28]

4. It is of interest to ask whether the abrupt rise in the π^+-p cross section above 700 Mev has something to do with the 740-Mev threshold for producing an $s=22$ "particle" in the final state. First we give a simple argument that such a process leads to a strong $D_{3/2}$ state, as suggested by phenomenological analysis.[29] According to this picture, one is producing a spin-one, odd-parity di-pion. Shortly above threshold the orbital momentum of the di-pion relative to the nucleon is primarily s-wave. Thus we have $J=1/2$ or $3/2$, odd parity, i.e., $S_{1/2}$ and $D_{3/2}$ for the initial state.[30] The other possibility giving $D_{3/2}$ is the mechanism of the second resonance: an s-wave pion accompanying the 3-3 isobar.[1,22]

A measurement of the Q values for the various pairs of particles in the final state of the reaction $\pi^++p\rightarrow\pi^++\pi^0+p$ at about 800 Mev would be very useful. Should this reaction behave as does reaction (2), one could verify the p-wave character of the π-π resonance by measuring the angular distribution of the decay pions in their own center-of-mass system.[31] Let θ be the decay angle relative to the beam direction. For the $D_{3/2}$ case the distribution is $1+3\cos^2\theta$. This does not interfere with the isotropic $S_{1/2}$ component. A similar measurement could be made for reaction (2). Preliminary data[10] at 910, 1090, and 1260 Mev indicate the presence of the 3-3 π^+-p state in the reaction $\pi^++p\rightarrow\pi^++\pi^0+p$.

In conclusion we wish to emphasize once more the importance of measuring the various charge-state ratios throughout the resonance region.

The author would like to thank Professor H. A. Bethe and T. Truong for stimulating discussions.

---

[1]P. Carruthers, Ann. Phys. (to be published).
[2]I. Derado and N. Schmitz, Phys. Rev. 118, 309 (1960).
[3]E. Pickup, F. Ayer, and E. O. Salant, Phys. Rev. Letters 5, 161 (1960).
[4]E. Pickup, D. K. Robinson, and E. O. Salant, Proceedings of the 1960 Annual International Conference

on High-Energy Physics at Rochester (Interscience Publishers, Inc., New York, 1960), p. 72.

[5]J. G. Rushbrooke and D. Radojičić, Phys. Rev. Letters 5, 567 (1960).

[6]I. Derado, Nuovo cimento 15, 853 (1960).

[7]S. J. Lindenbaum and R. M. Sternheimer, Phys. Rev. 109, 1723 (1958).

[8]The momentum spectra of the final pions of reaction (2) vary in a complicated way as the lab energy is changed.[2-4] We do not want to discuss this here.

[9]B. C. Barish, W. N. Hess, V. Perez-Mendez, and J. Solomon, Phys. Rev. Letters 4, 242 (1960).

[10]J. C. Brisson, J. F. Detoeuf, P. Falk-Vairant, L. Van Rossum, and G. Valladas, Nuovo cimento 19, 210 (1961).

[11]P. Falk-Vairant and G. Valladas, Proceedings of the 1960 Annual International Conference on High-Energy Physics at Rochester (Interscience Publishers, Inc., New York, 1960), p. 38.

[12]G. F. Chew and F. E. Low, Phys. Rev. 113, 1640 (1959).

[13]C. J. Goebel, Phys. Rev. Letters 1, 337 (1958).

[14]Nearly half the "peak" events reported in reference 5 have $\Delta^2 > 20$. A simple kinematical calculation for a lab energy of 960 Mev for $s = 22$ shows that events with $\Delta^2 > 20$ correspond to "forward" protons (in the c.m. system). On the other hand, Pickup, Ayer, and Salant[3] find the π-π peak only for "backward" protons. The ratio of forward to backward protons in the relevant region is only about 1 to 3 in the latter experiment. The behavior of the Δ^2 distribution of the events in the π-π peak seems sufficiently important to require more statistically conclusive data.

[15]B. A. Munir, E. Pickup, D. K. Robinson, and E. O. Salant, Phys. Rev. Letters 6, 192 (1961).

[16]P. Carruthers, Phys. Rev. (to be published).

[17]R. F. Peierls, Phys. Rev. Letters 5, 166 (1960). There seems to be a numerical error in this paper; for OPE $t = 1$ production, the relation $A(\frac{1}{2}1) = -\sqrt{2}A(\frac{3}{2}1)$ is given (our notation). It seems doubtful to us that the interference between Peierls' amplitudes a and b can be safely neglected.

[18]C. Baltay, H. Courant, W. Fickinger, E. Fowler, H. Kraybill, D. Stonehill, J. Sandweiss, J. Sanford, and H. Taft (to be published).

[19]J. A. Anderson, V. X. Bang, P. G. Burke, D. D. Carmony, and N. Schmitz, Phys. Rev. Letters 6, 365 (1961).

[20]F. Selleri, Nuovo cimento 16, 775 (1960).

[21]L. Landovitz and L. Marshall, Phys. Rev. Letters 4, 474 (1960).

[22]P. Carruthers and H. A. Bethe, Phys. Rev. Letters 4, 536 (1960).

[23]Actually, the theory[1] is somewhat more elaborate in that one derives an integral equation for the production amplitude. Figures 1(a) and 1(b) correspond to the inhomogeneous term and the first iteration, respectively.

[24]This may be seen by noting that $ie^{i\delta}\sin\delta\varphi_{\pi\alpha}$ plus the integral term is equal to the same integral term in which the P symbol is removed and $-i\epsilon$ added to ω in the denominator.

[25]Note that the largeness of the second term of (5) arises from the fact that the 3-3 resonance is a p-wave resonance. For an s-wave isobar the integral term is probably negligible. Hence, pion production via $\pi + \Lambda \rightarrow Y^* + \pi$ will be very different from the process $\pi + N \rightarrow N^* + \pi$ (N^* is the 3-3 isobar) if the Y^* resonance is s-wave. Similar remarks apply to the 2π state produced in $\bar{K} + N \rightarrow Y^* + \pi$. The influence of the peculiar interference term $e^{i\delta}\cos\delta$, and the effect of Bose symmetry should be important in these reactions.

[26]R. F. Peierls, Phys. Rev. 118, 325 (1960).

[27]See reference 1 for a discussion of the second (600-Mev) resonance.

[28]W. N. Wong and M. Ross, Phys. Rev. Letters 3, 298 (1959).

[29]P. Carruthers, Phys. Rev. Letters 4, 303 (1960).

[30]Arguments against Peierls' suggestion[17] of $F_{5/2}$ for the π^+-p 800-Mev shoulder are given in footnote 1 of reference 1.

[31]This was suggested to the author by H. A. Bethe.

I-SPACE PARITY CONNECTION IN NONLEPTONIC WEAK INTERACTIONS

W. B. Zeleny
School of Physics, University of Sydney, Sydney, N. S. W., Australia
(Received April 3, 1961)

In a recent paper by Pais,[1] it was shown that the parity properties of nonleptonic hyperon decays suggest a doublet approximation for both strong and weak interactions and the existence of two isotopic spins, the doublet spin, $\vec{I}$, and the K spin, $\vec{K}$, with the usual isotopic spin, $\vec{T}$, given by $\vec{T} = \vec{I} + \vec{K}$. The nonleptonic weak interaction Hamiltonian, H, is assumed to consist of two parts,

$$H = H^{(0)} + H^{(1)}, \qquad (1)$$

where $H^{(0)}$ is a scalar and $H^{(1)}$ a vector in I space. $H^{(0)}$ and $H^{(1)}$ are to be separately parity conserving, but their sum is to be parity nonconserving. Thus, there exists a connection between rotations in I space and parity. It is the purpose of this note to suggest a possible basis for this connection.

Any connection between I space and parity immediately brings to mind the π meson, which is pseudoscalar and isovector. Clearly, the ad-

dition or removal of a π-meson field to an interaction will change both its parity and its I-space transformation properties. In particular, if ω^0 is a scalar and isoscalar neutral meson, then the interaction

$$H = W^0(\omega^0 + \pi^0) + W^+\pi^+ + \text{Herm. conj.}, \qquad (2)$$

where $W^{0,+}$ is either scalar or pseudoscalar and is a scalar in I space, has precisely the desired properties of (1). This is accomplished without the artificiality of introducing γ^5 and τ matrices ad hoc in some terms of H and not in others. These γ^5 and τ matrices appear instead in the strong interaction, where their positions are determined by the requirements of parity and isotopic spin conservation. The connection between I space and parity in nonleptonic weak interactions would appear simply as a result of the I-space and parity properties of the ω^0 and π mesons.

Now, experimental evidence for the existence of the isoscalar neutral meson is meager. Abashian, Booth, and Crowe[2] have found evidence for either a new neutral meson or a two-pion resonant state of total energy about 310 Mev in the reaction

$$p + d \to \mathrm{He}^3 + \omega^0.$$

Berkelman, Cortellessa, and Reale,[3] on the other hand, failed to observe an ω^0 of this energy in a search for the reaction

$$\gamma + p \to p + \omega^0.$$

Sachs and Sakita[4] have argued against a spinless ω^0 of this energy on the grounds that it would be expected to yield too large a ratio for $W(K^+ \to \omega^0 + \pi^+)/W(K_1^0 \to \pi^+ + \pi^-)$. However, if ω^0 is scalar, they are comparing reaction of opposite parities, and the decay $K^+ \to \omega^0 + \pi^+$ might be expected to proceed at a rate comparable to that of direct τ decay. These arguments, of course, would not rule out a spinless ω^0 of mass greater than the K-π mass difference.

In any event, should the scalar ω^0 exist, the following realization of (2) immediately suggests itself:

$$H = g[(\bar{N}_1\gamma^5 N_2 + \bar{N}_3\gamma^5 N_4)(\omega^0 + \pi^0) - \sqrt{2}(\bar{N}_1\gamma^5 N_3 - \bar{N}_2\gamma^5 N_4)\pi^+] + \text{Herm. conj.}, \qquad (3)$$

where the notation is as in reference 1. From (1) and (3) we have

$$H^{(0)} = g(\bar{N}_1\gamma^5 N_2 + \bar{N}_3\gamma^5 N_4)\omega^0 + \text{H.c.},$$

$$H^{(1)} = g[(\bar{N}_1\gamma^5 N_2 + \bar{N}_3\gamma^5 N_4)\pi^0 - \sqrt{2}(\bar{N}_1\gamma^5 N_3 - \bar{N}_2\gamma^5 N_4)\pi^+] + \text{H.c.}$$

The Hamiltonian (3) has the following important properties:

I. H has the same renormalizable Yukawa structure as the strong interactions.

II. $H^{(1)}$ contains both $\Delta S = 2\Delta K_3$ and $\Delta S = -2\Delta K_3$ terms. This is absolutely essential since $H^{(1)}$ must contribute to both $\Sigma^- \to n + \pi^-$ and $\Sigma^+ \to p + \pi^0$. $H^{(0)}$ contains only $\Delta S = -2\Delta K_3$ terms, which is sufficient since it need only contribute to $\Sigma^+ \to n + \pi^+$, $\Sigma^+ \to p + \pi^0$, and $Y^0 \to p + \pi^-$.

III. Since τ^+ decays have $\Delta S = 2\Delta K_3$, they may proceed only through $H^{(1)}$. On the other hand, a pseudoscalar interaction cannot contribute to τ decays. Thus $H^{(1)}$ must be scalar, and the possibility ($H^{(0)}$ scalar, $H^{(1)}$ pseudoscalar) is ruled out. Hence, $\Sigma^+ \to n + \pi^+$ and $\Sigma^- \to n + \pi^-$ are S-wave and P-wave, respectively, and should it turn out that the parities are the other way around, this model must be discarded.

IV. $H^{(1)}$ is of the "allowed form"[1]; that is, the $\Delta I_3 = 0$ part of $H^{(1)}$ shares with the strong π interaction invariance under

$$N_1 \to i\epsilon_2\tau_2 N_2, \quad \pi^\pm \to -\epsilon\pi^\mp,$$

$$N_2 \to i\epsilon_1\tau_2 N_1, \quad \pi^0 \to -\epsilon\pi^0,$$

$$N_3 \to i\epsilon_2\tau_2 N_4, \quad \omega^0 \to \epsilon\omega^0,$$

$$N_4 \to i\epsilon_1\tau_2 N_3,$$

where the ϵ's equal ± 1, and $\epsilon\epsilon_1\epsilon_2 = -1$. Hence, in the approximation where we neglect the N_1-N_2 mass difference, and provided the K interactions do not violate this symmetry appreciably, $H^{(1)}$ does not contribute to $\Sigma^+ \to n + \pi^+$,[1] and in this approximation, $\Sigma^+ \to n + \pi^+$ is parity conserving, as required by experiment.

The author is indebted to A. Pais for a preprint of his work.

[1] A. Pais, Phys. Rev. 122, 317 (1961).
[2] A. Abashian, N. E. Booth, and K. M. Crowe, Phys. Rev. Letters 5, 258 (1960).
[3] K. Berkelman, G. Cortellessa, and A. Reale, Phys. Rev. Letters 6, 234 (1961).
[4] R. G. Sachs and B. Sakita, Phys. Rev. Letters 6, 306 (1961).

ERRATUM

MICROWAVE EMISSION FROM AN OPTICALLY PUMPED ATOMIC SYSTEM. V. E. Derr, J. J. Gallagher, R. E. Johnson, and A. P. Sheppard [Phys. Rev. Letters 5, 316 (1960)].

The calculation giving an estimate of the linewidth is incorrect, and the paragraph beginning at the bottom of page 316, "Second, an estimate of the linewidth may be made...," should be deleted from the article. On the basis of this experiment alone, no estimate of the linewidth can be made.

ABSTRACTS

In this section are printed the abstracts of Articles that have been forwarded to The American Institute of Physics for publication in THE PHYSICAL REVIEW. In quoting information obtained from this section before the appearance of the corresponding Article, reference should be made to "Physical Review (to be published)" rather than to this Journal.

DIFFUSION OF NEON, HT, AND DEUTERIUM IN LIQUID HYDROGEN. G. Cini-Castagnoli,* Istituto di Fisica dell'Universita di Roma, Italy and Istituto Nazionale di Fisica Nucleare, Sezione di Roma, Italy, A. Giardini-Guidoni, Laboratorio di Chimica delle Radiazioni e Chimica Nucleare del Comitato Nazionale Energia Nucleare, Roma, Italy, and F. P. Ricci, Comitato Nazionale Energia Nucleare, Roma, Italy (Received February 10, 1961; revised manuscript received March 22, 1961).

Experimental results on diffusion of Ne, HT, and D_2 in liquid H_2 are reported and analyzed with the corresponding-states principle. The features of the quantum deviations are indicated.

*Now at: c/o Consiglio Nazionale delle Ricerche, Istituto di Metrologia-Sezione Termometrica, Torino, Italy.

COMPARISON OF TWO THEORETICAL APPROACHES TO ELECTRON BEHAVIOR IN Ar-CO_2, Ar-N_2, Ar-H_2, AND Ar-CO GAS MIXTURES. Martin A. Uman, The University of Arizona, Tucson, Arizona (Received March 7, 1961).

The electron drift velocity and electron average energy for low-energy electrons in binary gas mixtures of Ar-CO_2, Ar-N_2, Ar-H_2, and Ar-CO are determined using two theoretical methods of approach: (1) a "distribution function" or "Boltzmann equation" approach; and (2) an "average electron" approach. The results of the two theoretical methods of approach are compared and discussed.

OPTICAL ABSORPTION AND FLUORESCENCE OF OXYGEN IN ALKALI HALIDE CRYSTALS. J. Rolfe, F. R. Lipsett, and W. J. King,* Radio and Electrical Engineering Division, National Research Council, Ottawa, Canada (Received March 10, 1961; revised manuscript received April 17, 1961).

Single crystals of NaCl, KCl, and KBr were grown from the melt in an oxygen atmosphere, and their optical absorption, fluorescence excitation, and fluorescence emission spectra were measured at 300°K, 77°K, and 4.2°K. The weak absorption band caused by oxygen was the same in all three cyrstals, and did not vary with temperature. The band had maximum absorption at 5.0 ev and a half-width of 1.0 ev. All fluorescence excitation spectra contained a component identical to this absorption band. The fluorescence emission spectra consisted of a series of peaks in the wavelength range 4000-10 000 A, with an approximately equal energy separation of 1000 cm^{-1}. At 300°K, 12 to 15 peaks were resolved, and at 4.2°K each of these peaks split into 4 to 6 components. From these optical results and from paramagnetic resonance experiments, it is concluded that O_2^- molecule ions located in anion sites in the crystal are responsible for the absorption and fluorescence.

*Present address: Goodrich High Voltage Astronautics, Inc., Burlington, Massachusetts.

CURRENT-CARRIER TRANSPORT WITH SPACE CHARGE IN SEMICONDUCTORS. W. van Roosbroeck, Bell Telephone Laboratories, Murray Hill, New Jersey (Received March 9, 1961).

Differential equations are given for a general formulation that includes space charge. Arbitrary dependences of diffusivities and magnitudes of drift velocities on electrostatic field are considered, and extension is made for applied magnetic field. Though excess electron and hole concentrations are not equal, the small-signal recombination rate depends on a single lifetime, the "diffusion-length lifetime," τ_0. The formulation is applied to one-dimensional drift with recombination for an injected pulse of electron-hole pairs. The exact electron and hole distributions are obtained in closed form for the linear small-signal case. The condition is given for linearity or substantially unperturbed applied field, E_0. There are two principal types of solutions, essentially according to whether τ_0 is larger or smaller than the dielectric relaxation time, τ_d. For $\tau_0 > \tau_d$, the electron and hole dis-

tributions in not too strongly extrinsic material are ultimately similar Gaussian distributions displaced by the "polarization distance," x_P, the distance electrons and holes drift apart in time $(\tau_d^{-1} - \tau_0^{-1})^{-1}$. These distributions drift at a velocity that differs from the ambipolar velocity by an amount which, besides being small for small τ_d/τ_0, vanishes for equal mobilities. They spread, exhibiting an apparent diffusion. A "pseudodiffusivity," D_v, is defined. For $\tau_0 \gg \tau_d$ and constant mobilities, D_v is proportional to $\tau_d E_0^2/\sigma_0^2$, with σ_0 the conductivity. The ambipolar diffusivity and D_v are additive. They are equal in intrinsic material for E_0 equal to kT/e divided by the Debye length $(kT\epsilon/8\pi n_i e^2)^{1/2}$, or 10 volt/cm for silicon at 300°K. An extension to a nonlinear case involving high-level injection is given; concentration-dependent D_v and velocity function are defined. For sufficiently strongly extrinsic material and $\tau_0 > \tau_d$, the minority carriers drift in a delta pulse that leads the majority carriers distributed in an exponential tail of characteristic length x_P, which may be quite large. For nonconstant mobilities and $\tau_0 > \tau_d$, ambipolar velocity in the majority-carrier or "reverse" direction may occur. For $\tau_d > \tau_0$, the other principal type of solution gives distributions that in general (and for constant mobilities) drift in the reverse direction. Involving also regions of local carrier depletion and thus generation as well as recombination, they may persist for times long compared with τ_0, being attenuated then with time constant τ_d.

SPECIFIC HEATS OF DELTA-PHASE Zr-H AND Zr-D. Walter J. Tomasch, Atomics International Division of North American Aviation, Canoga Park, California (Received March 6, 1961).

The specific heats of fcc $ZrH_{1.58}$ and $ZrD_{1.58}$ have been measured in the temperature interval 30-500°C. The data are interpreted in terms of a harmonic oscillator model for the hydrogen and deuterium specific heat contributions. This model is in accord with recent inelastic neutron scattering studies and predicts an isotopic depression of the deuteride Einstein temperature by a factor of $1/\sqrt{2}$ relative to the hydride value. Over the interval 30-200°C, the data and model are quantitatively consistent. At higher temperatures, the deuteride specific heat is somewhat smaller than anticipated. Quantities of noncubic γ-phase material are known to be present in the samples used, particularly in the deuteride, and this is thought to be a likely cause for the deviations. The hydride Einstein temperature calculated from the difference between deuteride and hydride specific heats at 150°C is 1500 ± 300°K, as compared with the inelastic neutron scattering value of 1500 ± 60°K.

GYROMAGNETIC RATIO OF NICKEL FERRITE. G. G. Scott, Research Laboratories, General Motors Corporation, Warren, Michigan (Received March 10, 1961).

The gyromagnetic ratio of the ferrite $NiOFe_2O_3$ was determined by measurements of the Einstein–de Haas effect. The g' value of 1.849 ± 0.002 indicates that the magnetization is largely due to the Ni^{++} ions as in the Néel model. Comparison with values of g determined by ferromagnetic resonance investigations furnishes evidence as to the validity of the Kittel–Van Vleck relation for ferrites.

ANTIFERROMAGNETIC RESONANCE IN FeF_2 AT FAR-INFRARED FREQUENCIES. R. C. Ohlmann* and M. Tinkham, Department of Physics, University of California, Berkeley, California (Received March 14, 1961).

Antiferromagnetic resonance in single crystals of FeF_2 was observed between 1.5°K and 66°K ($T_N = 78.4$°K) in the far-infrared region. The resonance frequency at $T \approx 0$ was found to be $\tilde{\nu}(0) = 52.7 \pm 0.2$ cm^{-1}. Using the antiferromagnetic resonance relation derived by Kittel, Nagamiya, Keffer, and others, and using the experimental value for the static susceptibility, the uniaxial anisotropy constant at absolute zero, $K(0)$, was inferred to be 1.1×10^8 ergs/cm^3 (40 cm^{-1}/atom). Measurements of the splitting of the line caused by an external magnetic field gave $g_{\|} = 2.25 \pm 0.05$. The anisotropy energy in FeF_2, being primarily due to the crystalline field-spin-orbit interaction, may be described by a term $\sum_i DS_{zi}^2$ in the Hamiltonian. By including this interaction in the molecular-field treatment, we have determined $D = -9 \pm 2$ cm^{-1}, and have calculated the temperature dependences of the sublattice magnetization, the anisotropy constant, the resonance frequency, and the linewidth. The last two were compared with the experimental results and found to be in reasonable agreement. The linewidths were

found to follow a T^4 law above 15°K. The search over a frequency region of 13-70 cm^{-1} for the absorption lines expected in the paramagnetic region was unsuccessful, possibly indicating a relaxation time of less than 10^{-12} sec.

*Now at Westinghouse Research Laboratories, Pittsburgh, Pennsylvania.

SIZE EFFECTS IN THIN SUPERCONDUCTING INDIUM FILMS. A. M. Toxen, International Business Machines Research Center, Yorktown, New York (Received March 8, 1961; revised manuscript received April 27, 1961).

Measurements of residual resistivity, superconductive critical temperature, and critical magnetic field have been carried out on indium films ranging in thickness from 650 A to 126 000 A. The thickest films had the bulk critical field and critical temperature. The variation of residual resistivity with thickness is consistent with Fuchs' model if one assumes an intrinsic resistivity ρ_0 of 1.31×10^{-8} ohm cm and an intrinsic mean free path l_0 of 152 000 A. The value of $\rho_0 l_0$ so obtained was 2.0×10^{-11} ohm cm^2. The critical temperature was found to be a systematic function of film thickness, increasing with decreasing thickness. The magnitude of this change in critical temperature is in good agreement with a simple model relating critical temperature to elastic stresses in the films. The penetration depth, as calculated from the critical field by means of the London theory or the Ginzburg-Landau theory, was found to increase with decreasing film thickness. This result is consistent with a nonlocal model and implies a coherence-length of approximately 2600 A.

GALVANOMAGNETIC EFFECTS IN SEMICONDUCTORS AT HIGH ELECTRIC FIELDS. E. M. Conwell, General Telephone and Electronics Laboratories, Incorporated, Bayside, New York (Received March 13, 1961).

A treatment of magnetoconductivity is developed for high electric fields and general energy-band structure using a partial solution of the Boltzmann equation in a form similar to that set up by McClure for low electric fields. The present treatment is valid when the scattering processes are such that the distribution function varies but a small amount over an entire constant-energy surface, or, in the case of the many-valley band structure, over the part of a constant-energy surface within each valley. In the latter case different distribution functions must be used for the different valleys. The elements of the magnetoconductivity matrix that results are expressed in terms of carrier concentration, total or within each valley, and averages over the carriers of a quantity involving the momentum relaxation time and the $\tilde{S}$ tensor defined by McClure. This tensor, which depends on the shape of the constant-energy surfaces and on the magnetic field strength, is evaluated for the individual valleys in a nondegenerate many-valley semiconductor. The magnetoconductivity matrix is then in a form convenient for calculation of conductivity and galvomagnetic effects for either low or high electric fields. It is used to obtain expressions for anisotropy voltage and Hall coefficient in high electric fields involving the number of carriers in each valley, orientation of the valleys, and valley averages over quantities involving relaxation time and energy.

DIFFERENTIAL PARAMAGNETIC EFFECT IN SUPERCONDUCTORS. Robert A. Hein and Raymond L. Falge, Jr., U. S. Naval Research Laboratory, Washington, D. C. (Received February 2, 1961; revised manuscript received April 20, 1961).

The magnetic moment and the differential magnetic susceptibility of two spherical samples of tin and tantalum have been measured as a function of magnetic field and temperature. The differential paramagnetic effect (DPE) is observed in both ac and dc mutual inductance measurements provided the sample exhibits a good Meissner effect. For a superconducting sample in which the infinite conductivity behavior dominates the Meissner effect, the DPE will not appear in the ac measurements but will, under certain conditions, show up in dc measurements. The results of the dc mutual inductance measurements are used to classify the DPE as reproducible or nonreproducible. The former is characteristic of ideal Meissner-type superconductors while the latter is more characteristic of superconductors whose macroscopic magnetic properties are dominated by the classical infinite electrical conductivity behavior. The superconducting to normal transitions obtained by the three techniques are

compared and the data discussed in view of (a) occurrence of the DPE; (b) magnitude of the DPE; (c) ability of these data to give information about the volume participation of the sample; and (d) relation of the "characteristic magnetic fields" determined by these transitions and the bulk critical field of the sample.

STUDY OF THE SUPERCONDUCTING TRANSITION TEMPERATURE IN DILUTE THALLIUM SOLID SOLUTIONS. D. J. Quinn and J. I. Budnick,* International Business Machines Research Laboratory, Poughkeepsie, New York (Received March 6, 1961).

The superconducting transition temperature, T_c, has been measured for dilute solid solutions of indium, bismuth, and lead in thallium. The transition temperature is found to increase in all cases, thus exhibiting a behavior opposite to that observed by Serin, Lynton, and co-workers in their studies of solid solutions of tin, indium, and aluminum. Some loss in residual impurity scattering which occurs upon annealing suggests the migration of solute atoms to grain boundaries in the dilute alloys.

*Now at International Business Machines Watson Laboratory, Pougkeepsie, New York.

INTERSTITIAL DEFECTS IN LiH AND NaCl IRRADIATED AT LOW TEMPERATURES. F. E. Pretzel and R. L. Petty, Los Alamos Scientific Laboratory, Los Alamos, New Mexico (Received March 10, 1961).

Expansions of the lattice parameters of both LiH and NaCl exposed to β radiation at 77 and 245°K have been observed using a vacuum x-ray diffractometer stage operated at 77°K. The source of the β radiation was 5.56% LiT contained in a LiH crystal which was ground and mixed with NaCl in the samples. The LiH lattice parameter increased 0.0020 ± 0.0007 A in three samples. This result is consistent with density measurements and with the formation of interstitial He^3 atoms in the LiH lattice. The NaCl lattice parameter increased 0.0061 ± 0.0009 A even though the average β dose for the NaCl was less than 1% of that in the Li(H, T) and tritium β particles with maximum energy cannot produce direct displacements in NaCl. A mechanism is proposed for the production of Cl^- interstitials and vacancies (Frenkel defects) in NaCl which is similar to one proposed by Klick for the production of F and H centers. This mechanism is related to observations of the production of α centers in alkali halides irradiated at low temperatures.

KAPITZA RESISTANCE BETWEEN HELIUM AND METALS IN THE NORMAL AND SUPERCONDUCTING STATES. W. A. Little, Stanford University, Stanford, California (Received February 16, 1961).

The contribution of the conduction electrons of a metal to the heat flow across a helium-metal interface has been calculated. It is found that the "totally" reflected phonons from the fluid play an important role in the transfer mechanism as had been predicted previously. The dominant term in the heat flow is proportional to $T^3\Delta T$ in agreement with the experimentally observed value on lead. However, the numerical agreement is poor. The reasons for this are discussed. In the superconducting state it is shown why this heat transfer becomes inoperative. Several interesting consequences of this calculation are given. In particular, it is predicted that a phonon-drag effect may be observed between the conduction electrons in the metal and the phonons in the fluid and vice versa. Also, it is shown that the variation of the Kapitza resistance with applied magnetic field can help to distinguish between the various contributions to the heat flow.

GENERALIZED KOOPMANS' THEOREM. J. C. Phillips, Department of Physics and Institute for the Study of Metals, University of Chicago, Chicago, Illinois (Received February 24, 1961).

Koopmans' theorem states that if the wave function of a many-electron system is approximated by a Slater determinant of Hartree-Fock one-electron wave functions, with one-electron energies defined as the difference in energy of $(N+1)$- and N-particle systems, then these one-electron energies are given by the expectation value of the Hartree-Fock Hamiltonian with respect to the one-electron wave functions. Koopmans' theorem is here generalized to include

correlation effects by using Hubbard's expression for the total energy of a free electron gas. The resulting one-electron Hamiltonian contains, in first-order, screened exchange. Hubbard's lowest polarization diagram gives, in addition, part of the screened second-order Coulomb interactions, which is small for metallic densities. Collective terms are also obtained. Comparison with the Bohm-Pines Hamiltonian shows a one-to-one correspondence but with different cutoff functions in each term. Following Hubbard we extend the method to include the effects of a periodic potential to first order. The resulting one-electron Hamiltonian provides a convenient and accurate basis for self-consistent energy band calculations including exchange and correlation in metals and semiconductors.

INDIRECT EXCHANGE MODEL FOR FERROMAGNETIC METALS. S. H. Liu, Research Center, International Business Machines Corporation, Yorktown Heights, New York (Received March 13, 1961).

The ferromagnetic properties of rare earth metals and their alloys are discussed in terms of the indirect exchange model. It is shown by the molecular field approximation that in calculating the Curie temperatures of these metals the simple theory of Fröhlich and Nabarro and Zener is applicable. The second-order energy terms calculated by Ruderman and Kittel, Kasuya, and Yosida are important in discussing the low-temperature properties. Some numerical results are obtained which are in good agreement with the experiments.

CONTRIBUTION OF LATTICE SCATTERING BETWEEN NONEQUIVALENT VALLEYS TO FREE-CARRIER INFRARED ABSORPTION IN SEMICONDUCTORS. H. Risken, Deutsche Philips G.m.b.H., Zentrallaboratorium Aachen, Germany, and H. J. G. Meyer, Philips Research Laboratories, Eindhoven, Netherlands (Received March 13, 1961).

In a multivalley band-structure like that of the conduction band of germanium a contribution to the absorption of infrared radiation by free carriers is made by a scattering process which does not play a role in normal transport processes but which may be of importance for hot-electron phenomena; this is the scattering between nonequivalent valleys of the conduction band. The absorption induced by this extra scattering process results in a transfer of the electrons from the $\langle 111 \rangle$ valleys to the $\langle 100 \rangle$ valleys or the [000] valley. A quantum mechanical calculation was made of the partial absorption constant μ_i^* due to this scattering on the basis of a deformation-potential type theory. The final formula obtained for μ_i^* is similar to that derived previously for the partial absorption constant μ^{opt} due to optical intravalley scattering. The physical significance of some limiting forms of μ_i^* at low temperatures is discussed.

ULTRAVIOLET ABSORPTION SPECTRA IN RUBY. A. Linz, Jr., and R. E. Newnham, Massachusetts Institute of Technology, Cambridge, Massachusetts (Received March 6, 1961).

The optical properties of highly doped rubies have been investigated. Al_2O_3 and Cr_2O_3 form a complete solid-solution series; single crystals containing up to 5 mole % chromia were grown by the Verneuil technique. The optical absorption of a group of ultraviolet crystal-field bands near 3400 A was studied as a function of temperature, crystal orientation, and chemical composition. The intensity of these absorption bands varies with the square of the Cr concentration, perhaps indicating strong chromium-pair interactions.

LOW-TEMPERATURE SPECIFIC HEAT OF INDIUM AND TIN. C. A. Bryant* and P. H. Keesom,† Department of Physics, Purdue University, Lafayette, Indiana (Received March 9, 1961).

The heat capacities of indium and tin were measured between 0.4 and 4.2°K. In the normal state, the specific heat could be represented by $AT^{-2}+\gamma T+\alpha T^3+\beta T^5+\mu T^7$. For Sn, in molar millijoule units, $A=0$; γ, the coefficient in the electronic term, is 1.80; $\alpha=0.242$, corresponding to a Debye temperature, θ_0, of 200°K; $\beta=0.004$; and $\mu=0.00014$. For In, A, the coefficient of a nuclear electric quadrupole term, is calculated to be 8.97×10^{-4} from resonance data; $\gamma=1.61$ for one ingot and 1.59 for another; $\theta_0=109$ and 108°K; and $\beta=0.008$. In the superconducting state, the

specific heat of Sn could be expressed as the normal lattice term plus an electronic term of the form $a\gamma T_c \exp(-bT_c/T)$, with $T_c = 3.70°K$ (0.02 deg lower than found in a magnetic measurement), $a = 7.63$, and $b = 1.41$ when $2 < T_c/T < 7$; the value of b agrees with infrared measurements of the energy gap. This sort of analysis could not be applied to In, for below 0.8°K, the total superconducting specific heat was less than the normal lattice term. A possible interpretation is that θ_0 is 9% higher in the superconducting state than in the normal metal at 0.4°K; this is not supported, however, by the recent acoustic measurements of the elastic constants by Chandrasekhar and Rayne. The anomaly is not as yet understood, but a few plausible explanations are discussed.

*Present address: International Business Machines Corporation, Yorktown Heights, New York.

†On leave of absence at the Kamerlingh Onnes Laboratory, Leiden University, Leiden, The Netherlands.

THEORY OF RESONANCE ABSORPTION OF ENERGY BY A ROTATING SOLID. Joseph Dreitlein, University of Pennsylvania, Philadelphia, Pennsylvania, and Horst Kessemeier, Washington University, Saint Louis, Missouri (Received February 13, 1961).

The theory of both nuclear resonance energy absorption and the relaxation of a coherent magnetization transverse to an applied external magnetic field is developed for nuclei in a mechanically rotating solid. The consequences of the formalism in the simple case of a solid composed of effectively isolated nuclear pairs are presented. For the more general nuclear lattice, a procedure for isolating and experimentally measuring the "exchange" interaction between the nuclei in the solid is proposed. Finally, the moments of the energy absorption line shape for the rotating solid are investigated and the second and fourth moments are explicitly calculated.

PINCH EFFECT IN INDIUM ANTIMONIDE. A. G. Chynoweth and A. A. Murray, Bell Telephone Laboratories, Murray Hill, New Jersey (Received March 10, 1961).

The critical current at which pinching occurs in indium antimonide has been measured by three independent methods: (i) by noting the current at which the pinched current-voltage characteristic deviates from the unpinched characteristic that is obtained in the presence of a longitudinal magnetic field, H, using crystals of sufficiently high resistance for the avalanche breakdown current to be considerable before pinching sets in as the electric field is increased; (ii) by noting the current at which the magnetoresistance as a function of H shows a change in its behavior; and (iii) from a study of the critical current as a function of H. The three methods lead to a value for the critical pinching current of 4 to 5 amp. This current is the same for both single-crystal and polycrystalline samples and is insensitive to small changes in the donor concentration or cross-sectional area of the crystal. The value of the critical current leads to a mean carrier temperature of 0.04 ev in avalanche breakdown. An irregular form of noise is observed when the crystal is operated in the transition region between the pinched and unpinched conditions, and it is thought that this noise is caused by pinching-unpinching instabilities.

SINGLE-CRYSTAL AND POLYCRYSTAL RESISTIVITY RELATIONSHIPS FOR YTTRIUM. J. K. Alstad, R. V. Colvin,* and S. Legvold, Institute for Atomic Research and Department of Physics, Iowa State University, Ames, Iowa (Received February 20, 1961).

Different proposals for calculating polycrystal resistivities from single-crystal values are applied to yttrium metal. It is shown that a simple average, yielding $\rho_{poly} = \frac{1}{3}(2\rho_{\perp} + \rho_{\parallel})$, gives the best fit to experimental data.

*Presently at the Edgar C. Bain Laboratory of the United States Steel Corporation, Monroeville, Pennsylvania.

LOW-TEMPERATURE DISSIPATION PEAK IN NIOBIUM. P. G. Bordoni, M. Nuovo, and L. Verdini, Istituto Nazionale di Ultracustica, Rome, Italy (Received February 7, 1961).

The energy dissipation coefficient Q^{-1} and the resonant frequency of a circular plate of niobium have been measured as a function of temperature in the range 60-300°K. The measurements have been carried out at four different frequencies from 18 kc sec^{-1} and 174 kc sec^{-1} with strain amplitudes smaller than 10^{-7}. For each vibration

mode, a pronounced peak is found for the dissipation coefficient while the frequency-temperature curves show a corresponding inflection. The temperature T_m of the dissipation peak depends on the vibration frequency according to an Arrhenius equation which characterizes the thermally activated relaxation effects.

The activation energy $\overline{W}$ and the limiting relaxation time $\overline{\tau}_0$ of the process have been computed and these values [$\overline{W} = 0.265$ ev and $(\overline{\tau}_0)^{-1} = 61 \times 10^{11}$ sec^{-1}] are in agreement with the values previously found in some fcc metals for the relaxation effect due to the motion of dislocations.

The value of $\overline{W}$ found in niobium shows that the effect cannot be directly produced by the motion of interstitial atoms of hydrogen.

DECAY OF PHOSPHORESCENCE FROM A DISTRIBUTION OF TRAPPING LEVELS. W. L. Medlin, Field Research Laboratory, Socony Mobil Oil Company, Incorporated, Dallas, Texas (Received March 13, 1961).

In a previous paper it was shown that the usual model for second-order decay predicted the correct form for the decay in many thermoluminescent crystals but gave the wrong behavior for the parameters involved. Specifically, it was shown that b and m in the decay expression, $I = I_0[b/(b+t)]^m$, should behave differently as functions of the decay temperature and the degree of trap filling than is observed experimentally at temperatures near or below the glow peak. In the present paper it is shown that the discrepancies can be accounted for by assuming a first-order decay from a distribution of trapping levels. Most of the results are based on a Gaussian distribution but it is shown that other distributions can produce similar results. The first-order mechanism is justified by considering the relative magnitudes of the rate constants for trap emptying, retrapping, and recombination. At temperatures well above the glow peak this assumption is no longer justified, but in this range the second-order decay predicts the observed results for b and m. The effects of retrapping and of crystal dimensions are considered. Also, the effect on the glow peak of having a distribution of levels rather than a set of discrete levels is worked out and it is shown that the peak is broadened appreciably even for relatively narrow distributions.

STATISTICAL ELECTRON DENSITY DISTRIBUTIONS AND THOMAS-FERMI-DIRAC SCREENING FUNCTIONS FOR NEUTRAL ATOMS. Adolf A. Abrahamson, The City College of New York, New York, New York and Brookhaven National Laboratory, Upton, New York (Received March 3, 1961).

Statistical electron density distributions and Thomas-Fermi-Dirac (TFD) screening functions have been obtained for the 104 elements corresponding to integral atomic numbers $Z = 2$ to $Z = 105$, for 117 values of radial distance from the atomic center in each case. These results were calculated, in part, by using Thomas' solutions of the TFD equation in terms of the statistical electron distributions for nonintegral values of Z and Jensen's boundary conditions. Values for argon and copper are given here. The complete set of tables for all 104 elements has been deposited with the American Documentation Institute Auxiliary Publications Project.

TEMPERATURE VARIATION OF IONIC MOBILITIES IN HYDROGEN. Lorne M. Chanin, Honeywell Research Center, Hopkins, Minnesota (Received March 6, 1961).

Measurements have been made of the temperature variation of the mobilities of positive ions in hydrogen over the range 77-300°K. The zero-field mobility values are $\mu_0 = 12.3$ cm^2/volt-sec (300°K), 13.3 (195°K), and 13.0 (77°K). The present results at 300°K are in agreement with the data of Lauer, Bradbury, and Mitchell at low E/p_0 and at high E/p_0 they agree with Rose's measurements. Only a single ion species was observed in the present studies. Reasons are given which support the belief that the ion observed in these measurements was H_3^+.

ANALYTIC HARTREE-FOCK WAVE FUNCTIONS FOR THE $3p$ SHELL ATOMS. R. E. Watson, Avco Research and Advanced Development Division, Wilmington, Massachusetts, and A. J. Freeman, Materials Research Laboratory, Ordnance Materials Research Office, Watertown, Massachusetts (Received March 2, 1961).

Hartree-Fock wave functions have been obtained for the $3p$ row atoms, i.e., for neutral

Al, Si, P, S, Cl, and Ar, and for Cl^-. Solutions were determined in analytic form using a version of Nesbet's symmetry and equivalence restrictions to simplify the calculations for atoms with both closed and unclosed shells of the same l value. These restrictions, the reason for their use, and their relation to other open-shell methods are discussed and the calculated one-electron wave functions and their eigenvalues are presented.

ATOMIC BEAM RESONANCE EXPERIMENTS WITH STORED BEAMS. H. Mark Goldenberg, Daniel Kleppner, and Norman F. Ramsey, Harvard University, Cambridge, Massachusetts (Received March 13, 1961).

The atomic beam separated oscillatory field resonance technique has been used to study the hyperfine frequency of cesium, which is perturbed by collisions with storage box walls. With a wall coating of long, straight-chain saturated hydrocarbons, resonances are observed after as many as 200 wall collisions. A theory of the effect of wall collisions on the hyperfine frequency, which is in qualitative agreement with experimental results, is described. The shape of the resonance curve is analyzed by a detailed consideration of the statistical nature of the wall collision.

CESIUM TRANSITION PROBABILITIES FOR OPTICAL PUMPING. W. Bruce Hawkins, Department of Physics, Oberlin College, Oberlin, Ohio (Received March 6, 1961).

Optical transition probabilities are presented between the several magnetic sublevels of the Cs^{133} ground state via the first excited state, given separately for the two fine-structure components. Graphs of the populations of representative states are presented as a function of the time the atoms are illuminated, and a table is given of the populations of atoms absorbing integral numbers of photons from both D lines simultaneously, both polarized and unpolarized.

ANGULAR DISTRIBUTION OF THE GROUND-STATE NEUTRONS FROM THE $C^{13}(p,n)N^{13}$ AND $N^{15}(p,n)O^{15}$ REACTIONS. C. Wong, J. D. Anderson, S. D. Bloom, J. W. McClure, and B. D. Walker, Lawrence Radiation Laboratory, University of California, Livermore, California (Received March 1, 1961).

The angular distribution of the neutrons from the $C^{13}(p,n)N^{13}$ and $N^{15}(p,n)O^{15}$ ground-state reactions has been measured in 10° steps from 0° to 150° for incident proton (laboratory) energies of approximately 6.5, 6.9, 7.5, 8.1, 8.6, 8.9, 9.4, 10.6, 11.4, and 12.2 Mev. Additional measurements were made for C^{13} at 5.0, 10.2, 10.9, and 13.3 Mev, and for N^{15} at 5.5, 7.7, 7.8, and 13.6 Mev. A calibrated plastic or stilbene scintillator was used in order to obtain absolute differential cross sections. Time-of-flight techniques on the Livermore variable-energy cyclotron allowed positive identification of the ground-state neutrons. The targets [CO_2(58% C^{13}) and N_2(90% N^{15})] were sufficiently thick to average out the effects of possible compound-nucleus contributions. From preliminary fits to the C^{13} angular distributions, Glendenning and Bloom have inferred an effective neutron-proton interaction inside the nucleus.

MULTILEVEL ANALYSIS OF THE TOTAL NEUTRON CROSS SECTION OF Pu^{241} BELOW 12 ev. O. D. Simpson and M. S. Moore, Atomic Energy Division, Phillips Petroleum Company, Idaho Falls, Idaho (Received March 7, 1961).

Measurements of the total cross section of Pu^{241} have been analyzed with the use of a multilevel formula, under the assumption that the observed resonance asymmetries are due to interference in a small number of fission channels. As was the case for U^{233}, the analysis is interpreted as evidence that there are differences in the average fission widths of resonances belonging to the two possible spin states of the compound nucleus.

ANGULAR DISTRIBUTION AND RANGES OF N^{13} PARTICLES FROM N^{14} ON N^{14}. K. S. Toth, Oak Ridge National Laboratory, Oak Ridge, Tennessee (Received March 2, 1961).

The distribution of N^{13} particles from the neutron transfer reaction $N^{14}(N^{14}, N^{13})N^{15}$ was investigated from 3.5°-32° in the laboratory. Range curves for N^{13} particles were obtained from 16° to 32° (laboratory system). Transfers leaving both residual nuclei in their ground states were dis-

tinguished from those in which the products are left in excited states. It is found that (1) the ground-state transfer cross section decreases as the bombarding energy is lowered; (2) of the N^{15} excited states only the first and/or second contribute significantly to the transfer cross section; (3) for a given bombarding energy the excited state transfer distribution peaks at an angle larger than that at which the ground-state transfer distribution reaches its maximum; (4) from the ground-state transfer distribution an r_0 of 2.2 f can be determined, while the excited state transfer distribution yields an r_0 of about 1.65 f; and (5) the excited state distributions are more consistent with the tunneling mechanism of Breit and Ebel than are the ground-state distributions.

BETA-DECAY COUPLING CONSTANT AND THE *ft* VALUE OF O^{14}. R. J. Blin-Stoyle and J. Le Tourneux, Clarendon Laboratory, Oxford, England (Received March 1, 1961).

A calculation is made of the effect of a charge-dependent internucleon potential on the $O^{14}(0^+, T=1) \rightarrow N^{14}(0^+, T=1)$ β-decay matrix element. It is found that a not unreasonable strength and form for such a potential can lead to a reduction in the matrix element $\approx 1\%$ which is of the right order of magnitude to resolve the present discrepancy between the β- and μ-decay polar vector coupling constants.

PROTON SPECTRA FROM THE NITROGEN BOMBARDMENT OF FLUORINE. C. E. Hunting, Oak Ridge National Laboratory, Oak Ridge, Tennessee (Received March 13, 1961).

Energy spectra and absolute differential cross sections of protons from bombardment of F^{19} with 21.4-Mev and 27.4-Mev N^{14} were measured. The energy spectra were analyzed in terms of the statistical model with a level density $\exp(E^*/T)$, where E^* is the excitation energy in the residual nucleus of the assumed reaction $F^{19}(N^{14}, p)P^{32}$. The nuclear temperature T increased from about 1.9 Mev at 0 deg to about 2.5 Mev at 145 deg c.m., but did not vary with bombarding energy. The angular distributions show minima near 90 deg c.m., with anisotropy increasing as the bombarding energy and proton energy increase. At the lower bombarding energy there is approximate agreement with the Ericson-Strutinski theory of angular momentum effects in compound nucleus processes, over the entire observed ranges of angle and proton energy. The fit is consistent with $\sigma=3$ in the nuclear level spin distribution $(2j+1)\exp[-j(j+1)/(2\sigma^2)]$. At the higher bombarding energy a considerable excess of protons are emitted into the backward hemisphere, especially at high proton energies, suggesting a direct-interaction mechanism in which the observed proton comes from the F^{19}.

STUDY OF THE DIFFERENTIAL CROSS SECTIONS OF DEUTERON STRIPPING REACTIONS AS A FUNCTION OF THE INCIDENT ENERGY. E. W. Hamburger,* University of Pittsburgh, Pittsburgh, Pennsylvania and Universidade de São Paulo, São Paulo, Brasil (Received March 1, 1961).

Angular distributions for the reactions $C^{12}(d,p)$ and $O^{16}(d,p)$ to the ground and first excited states of C^{13} and O^{17} have been obtained at deuteron energies of 10.2, 12.4, and 14.8 Mev. These results and those of previous experiments at other energies between 3 and 19 Mev are compared with the predictions of the usual plane-wave Born approximation theory, due originally to Butler. The assumption of plane waves leads to the prediction that the differential cross section is a function of energy and scattering angle only through the transfer momentum q: Angular distributions at different energies should coincide when plotted vs q. It is found that this is only approximately true on the main stripping peak of the angular distribution; at larger angles the cross section is a more complicated function of energy and angle. Furthermore the stripping peak itself shifts as a function of q, principally in the deuteron energy range 10 to 19 Mev.

*Permanent address: Department de Física, Faculdade de Filosofia, Universidade de São Paulo, São Paulo, Brasil.

BETA-GAMMA DIRECTIONAL CORRELATION IN Eu^{154}. K. S. R. Sastry, R. F. Petry, and R. G. Wilkinson, Indiana University, Bloomington, Indiana (Received March 9, 1961).

The energy dependence of the beta-gamma angular correlation between the outer beta-ray

group of Eu^{154}, $W_0 = 1.86$ Mev, and the 123-kev gamma ray of the daughter Gd^{154} has been measured with a shaped magnetic field beta-gamma coincidence spectrometer. A negative correlation coefficient, accurate to about 5%, is obtained which ranges from -0.10 to -0.17 in the energy region 0.80 to 1.60 Mev. It is shown that the modified B_{ij} approximation must be relaxed to explain the data. The nuclear parameters (Kotani's notation) which result are: $x = -0.24 \pm 0.05$, $u = +0.05 \pm 0.03$, $Y = +0.76 \pm 0.08$. These values are compared with those which have been reported for Eu^{152}: $x = u = 0$, $Y = 0.69 \pm 0.06$.

LIFETIMES OF ENERGY LEVELS IN Al^{28}, Mn^{56}, Cu^{64}, Rh^{104}, AND I^{128} EXCITED BY SLOW-NEUTRON CAPTURE. S. J. du Toit* and L. M. Bollinger, Argonne National Laboratory, Argonne, Illinois (Received March 8, 1961).

Measurements of delayed coincidences between γ rays were used to determine the half-lives of states excited by slow-neutron capture in various nuclei. The half-lives found were: Mn^{56}, first excited level 11.4^{+2}_{-3} nsec, second excited level 5.1 ± 0.5 nsec; Rh^{104}, first excited level 2.6 ± 0.2 nsec, 96-kev transition ≤ 0.6 nsec; Cu^{64}, first excited level ≤ 0.3 nsec, second excited level ≤ 0.3 nsec; Al^{28}, first excited level 2.3 ± 0.2 nsec; I^{128}, 30-kev level 8.8 ± 1.0 nsec, 137-kev level 8.0 ± 0.6 nsec, 90-kev transition ≤ 0.7 nsec. Measurements of pulse-height spectra satisfying the condition of prompt and delayed coincidence and measurements at neutron resonances of iodine were used to establish the presence of excited states at 30 and 137 kev in I^{128}. A previously unreported neutron resonance was observed in I^{127} at a neutron energy of 10.7 ev.

*Permanent address: South African Atomic Energy Board, Pretoria, Union of South Africa.

DIRECTIONAL CORRELATION MEASUREMENTS IN Hf^{178}. U. Bertelsen, J. Borggren, and O. Nathan, Institute for Theoretical Physics, University of Copenhagen, Copenhagen, Denmark (Received March 10, 1961).

Measurements of the directional correlations of the 1335-93 kev, 1345-93 kev, and 1390-93 kev γ-γ cascades in Hf^{178} have been made, using a liquid source of 21-day W^{178} equilibrium with 9.3-min Ta^{178}. It is shown that the data support the tentative spin assignments of Gallagher et al. The 1390-kev γ ray is found to be almost pure quadrupole radiation. If the spin and parity of the 1430-kev level is 1+, as suggested by Gallagher et al., the multipolarity of the 1335-kev γ ray is determined by our measurements to be mainly $M1$. Using these results, the amount of $E0$ radiation in the 1390-kev transition has been estimated. It is found that approximately 70% of the 1390-kev K-conversion electrons are due to monopole transitions.

DETERMINATION OF $M1$-$E2$ MIXING AMPLITUDES IN Mg^{25}, Al^{27}, Si^{29}, AND P^{31}. G. J. McCallum,* Atomic Energy of Canada Limited, Chalk River, Ontario, Canada (Received March 13, 1961).

A method of analyzing gamma-ray angular distribution and direction-polarization data to yield values for the relative amplitudes of mixed multipole gamma-ray transitions is described. The analysis of the data does not demand a knowledge of the mechanism of formation of the gamma-emitting level. Measurements are reported on some mixed $M1$-$E2$ de-excitation gamma rays from low-lying levels in Mg^{25}, Al^{27}, Si^{29}, and P^{31}; these levels were excited by inelastic proton scattering. The following results were obtained:

Nucleus	Initial state Energy (Mev)	Initial state Spin & parity	Final state Energy (Mev)	Final state Spin & parity	$\frac{E2 \text{ amplitude}}{M1 \text{ amplitude}}$
Mg^{25}	0.98	3/2+	ground state	5/2+	0.30 ± 0.15
	0.98	3/2+	0.58 Mev	1/2+	0.15 ± 0.05
Al^{27}	1.01	3/2+	ground state	5/2+	-0.32 ± 0.14
Si^{29}	1.28	3/2+	ground state	1/2+	0.21 ± 0.03
P^{31}	1.27	3/2+	ground state	1/2+	-0.25 ± 0.15

CLUSTER MODEL CALCULATION ON THE ENERGY LEVELS OF THE LITHIUM ISOTOPES. Y. C. Tang and K. Wildermuth, Florida State University, Tallahassee, Florida, and L. D. Pearlstein, John Jay Hopkins Laboratory of Pure and Applied Physics, General Atomic, San Diego, California (Received February 24, 1961).

A variational procedure is adopted to determine the energies of the levels of the highest space-symmetry type in Li^6 and Li^7. The trial wave functions employed take into consideration the existence of cluster structures in those nuclei. With a simple two-body force, it is shown that the computed energies of the various states are in reasonable agreement with experiment. The $^2F_{5/2}$ level in Li^7, as yet undetermined experimentally, is found to have an excitation energy of about 5.6 Mev and a rather large level width. The calculation also indicates that to explain the splitting of levels in those nuclei, a constant two-body spin-orbit force of the pure neutral form is inadequate.

YIELD RATIOS FOR THE ISOMERIC PAIR $Sc^{44m,44}$ FORMED IN $(\alpha,\alpha n)$ AND (α,n) REACTIONS. Sylvia M. Bailey,* Lawrence Radiation Laboratory, University of California, Berkeley, California (Received January 23, 1961).

The yield ratio of Sc^{44m}/Sc^{44} was measured in $Sc^{45}(\alpha,\alpha n)Sc^{44}$ reactions with helium ions of energies between 20 and 43 Mev and at 320 Mev. The measured ratio was nearly constant at a value of 1.5 between 20 and 43 Mev and was 0.62 at 320 Mev. The Sc^{44m}/Sc^{44} ratio was measured in $K^{41}(\alpha,n)Sc^{44}$ reactions at 10 and 43 Mev with values of 0.3 and 0.9, respectively. The isomer ratio was calculated for the K^{41}(10-Mev α,n)Sc^{44} reaction by means of a compound-nucleus model and for the Sc^{45}(320-Mev $\alpha,\alpha n$)Sc^{44} reaction by means of a classical knock-on model. The calculated ratios were 0.32 and 0.51, respectively.

*Present address: National Bureau of Standards, Washington 25, D. C.

PION PRODUCTION IN ELECTRON-POSITRON COLLISIONS. Frank Chilton, Department of Physics, University of Washington, Seattle, Washington (Received March 13, 1961).

The properties due to the presence of symmetries in pion production processes in electron-positron collisions are discussed. Cross sections are calculated for the production reactions $e^+ + e^- \rightarrow \pi^0 + \gamma$, $e^+ + e^- \rightarrow e^+ + e^- + \pi^0$, and $e^+ + e^- \rightarrow \pi^+ + \pi^-$. The photon spectrum for the reaction $e^+ + e^- \rightarrow \pi^+ + \pi^- + \gamma$ is also calculated. The role of form factors and some of the possible effects of resonant strong interactions are discussed.

SPALLATION OF URANIUM AND THORIUM NUCLEI WITH Bev-ENERGY PROTONS. B. D. Pate* and A. M. Poskanzer, Chemistry Department, Brookhaven National Laboratory, Upton, New York (Received March 6, 1961).

Cross sections have been measured for the production of isotopes of uranium, protactinium, thorium, and actinium in the irradiation of U^{238}, U^{235}, and Th^{232} with 0.68- and 1.8-Bev protons. In addition, some yields were determined at other bombarding energies ranging up to 6.2 Bev. Calculations of the cross sections at 1.8-Bev bombarding energy were made, based on recent Monte Carlo calculations of the knock-on phase of the interaction, combined with published systematics of nuclear evaporation, and several assumptions as to fission-evaporation competition. Even without fission competition the calculated yields are considerably lower than the experimental ones, indicating a failure of the model for the knock-on phase of the reaction to predict sufficient probability for simple processes with low deposition energy. In view of the better agreement with experiment that previous workers have obtained with this type of calculation for 0.34-Bev protons on uranium, it is suggested that the present discrepancy may be due to an overemphasis of meson processes in the proliferation of the knock-on cascade in the calculation.

*Present address: Chemistry Department, Washington University, St. Louis, Missouri.

INTERACTION OF 1.0-, 2.0-, AND 3.0-Bev PROTONS WITH Ag AND Br IN NUCLEAR EMULSION. Elizabeth W. Baker and Seymour Katcoff, Chemistry Department, Brookhaven National Laboratory, Upton, New York (Received March 10, 1961).

Stars produced in insensitive nuclear emulsions by 1.0-3.0 Bev protons have been classified into

different groups depending on whether light fragments and/or fission fragments are emitted. Alpha-particle spectra and angular distributions are presented for each of the various groups. The probability for light-fragment emission increases rapidly with increasing beam energy up to 2.0 Bev. The angular distribution of the light fragments is peaked forward but also shows a preference for emission at 90° to the beam. Fission events increase from ~3% of the interactions with Ag and Br at 1.0 Bev to ~11% at 3.0 Bev. Ranges and angular distributions are also given for the recoil and fission fragments.

ANGULAR ASYMMETRY THEOREMS FOR DECAY PRODUCTS. Murray Peshkin, Argonne National Laboratory, Argonne, Illinois (Received February 1, 1961).

The method of Eberhard and Good, for using decay angular distributions to determine the spins of unstable systems, is developed. Their inequality, which expresses the impossibility of getting too symmetric a decay pattern from an asymmetric initial state, is tightened. The results are generalized to include spinning decay products. The Adair analysis is generalized in the same framework.

SEARCH FOR POSITIVE PARTICLES OF MASSES ABOUT $500m_e$ AND $1400m_e$. V. Cook, D. Keefe, L. T. Kerth, P. G. Murphy, W. A. Wenzel, and T. F. Zipf, Lawrence Radiation Laboratory, University of California, Berkeley, California (Received March 2, 1961).

The mass spectrum of positive particles in a secondary beam from the Bevatron has been measured at a distance of 90 feet from the internal target. At a confidence level of 93% the proportion of particles with mass between $420m_e$ and $630m_e$ in the 1-Bev/c beam is estimated to be $< 6\times10^{-8}$. An upper limit of about 3×10^{-6} is obtained for the proportion of particles of mass approximately $1400m_e$ in the 2.3-Bev/c beam.

TEST OF GLOBAL SYMMETRY IN PION-BARYON INTERACTIONS BY K^-+p REACTIONS. Jogesh C. Pati,* Department of Physics, University of Maryland, College Park, Maryland and Norman Bridge Laboratory of Physics, California Institute of Technology, Pasadena, California (Received March 8, 1961).

Under the hypothesis that the K-meson interactions do not mask the symmetries of the pion-baryon interactions appreciably, the branching ratios of the K^-+p reactions are studied to test the validity of global symmetry. The T^{-1}-matrix formalism of Matthews and Salam is adopted to calculate the branching ratios. The new Dalitz-Tuan solutions for $\bar{K}N$ scattering lengths, which incorporate the (K^+, K^0) mass difference and the new branching ratios of the various K^-+p reactions, presented at Kiev, are adopted in the analysis. The errors in the experimental branching ratios are so chosen as to satisfy the Amati-Vitale inequality. It is found that the a^- and b^+ (also a^+, though poorly) Dalitz-Tuan solutions can explain the branching ratios for K^- captured at rest. The extension of the analysis to 30-Mev incident K^- mesons under the zero-range approximation leads to very poor agreement with experiments.

*Now at the Norman Bridge Laboratory of Physics, California Institute of Technology, Pasadena, California.

SINGULARITIES OF SCATTERING AMPLITUDES ON UNPHYSICAL SHEETS AND THEIR INTERPRETATION. R. Blankenbecler, M. L. Goldberger, S. W. MacDowell,* and S. B. Treiman, Palmer Physical Laboratory, Princeton University, Princeton, New Jersey (Received March 1, 1961).

The analytic structure of two-particle scattering amplitudes on the unphysical sheet of the Riemann surface reached by crossing the two-particle cut is discussed. The singularities of the amplitudes there are shown to be poles, and their physical interpretation is studied. The way in which bound states appear on the physical sheet in the Mandelstam representation, both as isolated poles and as cuts, is traced in detail. The properties of partial-wave amplitudes and of the field amplitude as a function of energy and angle and of energy and momentum transfer are discussed. Finally, a few remarks are made in connection with unstable states.

*Present address: Centro Brasileiro de Pesquisas Fisicas, av. Venceslau Braz. 71, Estado da Guanabara, Brasil.

EXCITATION SPECTRUM IN MANY-BOSON SYSTEMS. Fumihiko Takano,* Metcalf Chemical Laboratories, Brown University, Providence, Rhode Island (Received March 14, 1961).

When only two-body correlations are fully taken into account, there appears an energy gap in the excitation spectrum for many-boson systems as shown by Girardeau and Arnowitt and as confirmed by Wentzel. This energy gap is shown to disappear and the spectrum to become phonon-like again and proportional to the momentum for small momentum, if we construct the eigenmodes of excitations (collective excitations) taking into consideration appropriate higher order terms.

*On leave of absence from Tokyo University of Education, Tokyo, Japan.

OPTIMAL MEASURING APPARATUS. Mutsuo M. Yanase, Palmer Physical Laboratory, Princeton University, Princeton, New Jersey (Received March 6, 1961).

An upper limit for the accuracy of the measurement of a simple quantity, which does not commute with a conserved quantity, is obtained in terms of the "size" of the apparatus. The "size" of the apparatus is defined as the mean square value, $\hbar^2M^2$, of the conserved quantity for the apparatus which is, in the example chosen, the z component of the angular momentum. The measured quantity is the projection of a spin in a perpendicular direction. It is found that the probability of an unsuccessful measurement is at least $1/8M^2$.

THEORY OF SINGLE PION PRODUCTION IN PROTON-PROTON COLLISIONS. J. Iizuka* and A. Klein, University of Pennsylvania, Philadelphia, Pennsylvania (Received March 9, 1961).

Single pion production in nucleon-nucleon collisions in the Bev energy region is studied by means of the picture due to Weizsäcker-Williams (peripheral interaction model) and in the (3/2, 3/2) resonance approximation for the final-state pion-nucleon interaction. The excitation curve for the reaction $p+p-p+n+\pi^+$, nucleon momentum distributions, and Q-value distributions in the center-of-mass system are calculated and compared with the published experimental data as well as with the work of Lindenbaum and Sternheimer. Agreement is reasonable with both, thus indicating that these particular distributions are insensitive to the isobar production mechanism (single pion exchange), though more recent experiments seem to have indicated clearly a preference for the theory developed here.

*Present address: Enrico Fermi Institute for Nuclear Studies, University of Chicago, Chicago, Illinois.

DOMAINS OF DEFINITION FOR FEYNMAN INTEGRALS OVER FEYNMAN PARAMETERS. Tai Tsun Wu, The Institute for Advanced Study, Princeton, New Jersey (Received March 1, 1961).

Given a Feynman diagram, the corresponding integral over real Feynman parameters is meaningful and analytic in a certain domain in the space of the Lorentz invariants formed from the external momenta, each of which is on the mass shell. In the case where all the masses are equal, the intersection of these domains for all proper convergent diagrams is studied. For the cases of four and five external lines, the real intersections are explicitly found; for the case of six, seven, and eight external lines, procedures for finding the real intersections are given. A knowledge of the real intersection makes it possible to construct geometrically a subset of the complex intersection. Generalization to unequal external masses is briefly considered.

PROPERTIES OF NORMAL THRESHOLDS IN PERTURBATION THEORY. Tai Tsun Wu, Institute for Advanced Study, Princeton, New Jersey (Received March 1, 1961).

Making use of the relation between a Feynman diagram and the corresponding electric circuit, several properties of the normal thresholds are established.